Montana Bureau of Mines and Geology

Miscellaneous Contribution 23

Technical Reports Completed by Montana Technological University's Geophysics Field Camp near Virginia City, Montana

July 2022

Compiled by Andrew L. Bobst

Conducted in Support of the Montana Bureau of Mines and Geology's Virginia City Groundwater Investigation

MBMG

Montana Bureau of Mines and Geology

Introduction

The Montana Bureau of Mines and Geology (MBMG) Ground Water Investigation Program (GWIP) conducted a study near Virginia City, Montana. The objectives for this study were: (1) to understand the source of the springs that Virginia City uses for their public water supply; (2) to evaluate the potential for residential and commercial development to impact these springs; and (3) to evaluate the potential for developing supplemental water supplies.

In support of the project objectives, the Montana Technological University's Geophysics Field Camp conducted geophysical surveys in the area in 2017 and 2018. In 2017 this included 2D electrical resistivity tomography (ERT) at Virginia City's springs, very low frequency electromagnetic (VLF-EM) surveys in the area above Virginia City's Spring 1, and a seismic survey following a road uphill from Spring 1. In 2018 seismic surveys were conducted for four transects along Alder Gulch to evaluate the thickness of the saturated unconsolidated sediments along this creek.

Note that the reports for these projects are provided in this document as they were supplied by the field camp classes so that these results are available to interested parties. They were not edited by the MBMG.

The ERT surveys showed that both springs occur at contacts between overlying lava flow deposits and underlying tuff. As such, they appear to be contact springs. The VLF-EM and seismic surveys in 2017 showed that fracture zones are present in the materials uphill from the springs, which match with the locations of presumed fracture plains due to landslide movement. The seismic surveys in 2018 showed that the saturated unconsolidated materials along Alder Gulch are up to 100 ft thick.

Files included in this publication are:

1. *2D electrical resistivity tomography and VLF-EM survey in Virginia City, Montana,* prepared by Carson Coleman, Constance Fenske, Ngoc Ha, Sierra Luoma, Kaitlyn O'Connell, Jonathan Rice, Jess Scanlan, Kyle Schuerg, Scott Schmitt, Nathan Simons, Jon Szarkowski, Maren Tanberg, and Tayler Todd, under the supervision of Dr. Mohamed Khalil; and

2. *A seismic survey in Virginia City, Montana, to investigate the origin of natural springs,* prepared by Carson Coleman, Constance Fenske, Ngoc Ha, Sierra Luoma, Kaitlyn O'Connell, Jonathan Rice, Jess Scanlan, Kyle Schuerg, Scott Schmitt, Nathan Simons, Jon Szarkowski, Maren Tanberg, and Tayler Todd, under the supervision of Brad Rutherford and Dr. Marvin Speece; and

3. *A seismic refraction survey in Virginia City, Montana, to investigate streambed hydrologic conditions along Alder Creek*, prepared by Rachel Basnaw, Jacob Clarke, Emelina Doucette, John Fitzgerald, Jay Hillygus, Kenton Hoshino, Eva Hover, Brayden Hungrige, Richard Lee, Mariah Mosdal, Shane Namie, Joseph Natale, Kabree Nichols, Christopher Smith, Brent Sordo, Zane White, Andrew Wilson, and TroyWolff, under the supervision of Dr. Martin Speece.

Other products associated with this GWIP project include:

Bobst, A., 2020, Virginia City aquifer tests: Montana Bureau of Mines and Geology Open-File Report 726, 17 p.

Bobst, A., Michalek, T., and Mosolf, J., 2022, An investigation of spring sources and potential alternative water supplies near Virginia City, Montana: Montana Bureau of Mines and Geology Report of Investigation 30, 71 p.

Khalil, M., Bobst, A., and Mosolf, J., 2018, Utilizing 2D electrical resistivity tomography and very low frequency electromagnetics to investigate the hydrogeology of natural cold springs near Virginia City, southwest Montana: Pure and Applied Geophysics, v. 175, no. 10, p. 3525–3538.

2D Electrical Resistivity Tomography and VLF-EM Survey in Virginia City, Montana

Prepared By:

Carson Coleman, Constance Fenske, Ngoc Ha, Sierra Luoma, Kaitlyn O'Connell, Jonathan Rice, Jess Scanlan, Kyle Schuerg, Scott Schmitt, Nathan Simons, Jon Szarkowski, Maren Tanberg, Tayler Todd

For:

Montana Bureau of Mines and Geology

Under the Supervision of:

Dr. Mohamed Khalil

Department of Geophysical Engineering
Montana Tech of the University of Montana
Butte, MT 59701

May 15th — 20th, 2017

Executive Summary

Geophysical methods can be useful when trying to identify the subsurface structures and geology. This survey has been conducted in order to determine subsurface structure near two natural springs and near an old landslide area located near Virginia City, Montana. Two geophysical methods were chosen to help with this survey. For determining the subsurface near two natural springs, we used the 2D Electric Resistivity Tomography method (ERT). To determine the structure of the old landslide area we used very low frequency electromagnetics (VLF-EM). The ERT method uses electrodes to send electric current through the ground and determine the resistivity behavior of the underlying material while VLF-EM uses radio frequencies of 15-30 kHz to interpret the subsurface.

We conducted this survey on May 15th and 16th, 2017. During these two days in the field both VLF-EM and ERT data were collected. On May 15th we conducted the resistivity survey at the first natural spring. This survey consisted of two profiles, each 200 meters in length with an electrode spacing of 10 meters. One profile ran north–south while the other ran east–west. On the same day, we conducted our first line of the VLF-EM survey. Each line of this survey was 500 meters in length and required readings to be taken every five meters. On May 16th, we conducted our second resistivity survey located at the second natural spring. This resistivity survey had the same layout as the previous survey. We also completed the second two lines of our VLF-EM survey. However, there were two more lines required for VLF-EM that could not be completed due to hazardous weather conditions.

To interpret the resistivity data collected in the field an inversion software, RES2DINV, was used to create resistivity cross sections of the subsurface. Using this program, we were able to find distinct characteristics in all four profiles. Two of the profiles showed strong evidence of resistivity discontinuities in the underlying material. Our first north–south profile, located at Spring 1, shows an abrupt change in resistivity values that indicates some sort of faulting. Another similar change in resistivity values is shown in the last profile that runs east–west located at Spring 2. We used the Fraser and Karous-Hjelt filters to interpret the VLF-EM data. From the interpretation, we can conclude that there are roughly three inferred faults in the area based on three zones of high current density detected.

From these models, we were able to make rough geologic interpretations of the area. The best interpretation we could make is based on the North–South profile at the first spring. From research and observation it was determined that this discontinuity is likely an oblique fault at a contact of high resistivity basaltic lava and low resistivity clay. Using the VLF-EM data, an accurate geologic interpretation could not be completed. However, we were able to infer that there is a series of detachment faults off a larger listric fault.

To complete this survey, the VLF-EM dataset needs more profiles to be collected. To enhance the quality of data and confirm our results, we recommend adding more north–south and east-west resistivity cross sections at both springs. By adding more cross sections, we can create a 3D resistivity model of the data.

Table of Contents

I. Introduction

On May 15th and 16th, 2017 a geophysical electrical survey was conducted in an area near Virginia City, Montana. Students from Montana Tech collected data via Global Positioning System (GPS) survey, 2D Electrical Resistivity Tomography (ERT) survey, and a Very Low Frequency Electromagnetics (VLF-EM) survey. The purpose of the 2D ERT survey was to collect data to allow for an interpretation of the subsurface faulting and the implications on two springs located in the survey area. The purpose of the VLF-EM survey was to map the displacement of the volcanic material in the area. The students were split into three groups to collect the appropriate data; one conducting the GPS survey, one conducting the ERT survey, and one conducting the VLF-EM survey.

From May 17th to 20th, the students were tasked with uploading and interpreting the collected data. The GPS data was uploaded and transferred to Google Earth to create accurate site maps. The ERT data taken at Springs 1 and 2 was processed using RES2DINV, a Geotomo software by Loke 1995, to create 2D resistivity sections. The VLF-EM data was run through the KHFfilt program by Pirttijarvi, M 2014, and both Karous-Hjelt and Fraser filtering was applied to create a 2D cross section showing the calculated electric current density at different depths. The methods used to gather data, results from field work, and interpretations are discussed in this report.

II. Site Description

Virginia City is located in Madison County in southwest Montana, roughly 100 kilometers (60 miles) southeast of Butte, Montana. Virginia City encompasses an area of 608 acres over Sections 22, 23, 24, 26, and 27. Virginia City lies in the vicinity of two mountain ranges: The Tobacco Root Mountains and the Gravelly Range. See Figure 1 to view a regional map. Figure 2 outlines the locations of each survey site near Virginia City.

Figure 1: Regional Map

Figure 2: Regional map with approximate site locations

II.I Site 1 – Spring 1

Located on the periphery of the landslide, Site 1 is located at the base of one of two springs within the study area. Site 1's coordinates are 45.29888287° N 111.9271716° W. The center of the site is a relatively flat area of roughly 50 square meters where infrastructure, such as pipes and a water containment tank, exists. At the base of the spring, there is a manmade trench filled with gravels and a pipe to control water flow out of the spring. The region beyond the center of the site is characterized by sloped terrains covered by landslide debris, largely composed of basalts. It was assumed prior to the survey that there was a fault within the area of Site 1.

II.II Site 2 – Spring 2

Site 2 was designated near Spring 2 along a stretch of north–south trending dirt road. The center of the survey at Site 2 was centered about 45.29925022° N 111.9191184° W. The terrain adjacent to the road was steeply inclined and rose to the East. From field observations, we were able to identify some geologic characteristics. The rock within the road-cut (Figure 3) appears to contain in-place basalts and a layer of breccia, indicating that Site 2 is located off the landslide. Many of the basalts were slightly weathered and exhibited scoriaceous or amygdaloidal textures. The amygdules within these basalts contained unidentified zeolite minerals and a variety of clay minerals, which were later identified by TerraSpec Halo infrared spectroscopy to include Fe-smectite, montmorillonite, and nontronite. It was assumed prior to the survey that there was a fault within the area of Site 2.

Figure 3: Road cut on Site 2, North - South line

II.III Site 3 – Very Low Frequency Electromagnetic (VLF-EM)

Site 3 was located in the center of the landslide (Figure 2), around the coordinates 45.30420674° N 111.923336° W. This site consists of grass-covered terrain with little infrastructure. There is a fence that ran through the western end of Line 2. Pressure ridges at this site are visible from satellite imagery. A pressure ridge forms during a landslide when the bottom of the slide buckles due to uneven terrain, or when the slip surface becomes gentler than the surface in the zone of accumulation. The sliding material can bulge as a whole, or as multiple pressure ridges as a result of compressional stress at the foot of the slide.

II.IV Geologic Setting

II.IV.a. Regional geology

The regional geology of Virginia City is dominated by Archean, metamorphic, crystalline basement rocks. These rocks are mainly gneisses of varying composition from quartzo-feldspathic gneisses to hornblende-plagioclase gneisses and amphibolite. These rocks are overlain by a thick sequence (≈ 550 meters) of Paleozoic clastic and chemical sediments associated with advancing and receding seas. Appendix (A) includes a stratigraphic column of Virginia City's regional geology as provided by Ruppel and Liu (2004). The area around Virginia City has been intruded by multiple igneous bodies, including granite pegmatites, mafic diabase dikes, and multiple iterations of basalt and ash flows.

The granite pegmatite dikes intruded the area in the late protopaleozoic, approximately 1.6 Ga. The dikes extend in a northwest-trending belt west of the head of Alder Gulch. These dikes are composed of coarse-grained quartz, biotite, microcline, and plagioclase (Despotovic, 2000).

Mafic diabase dikes intruded in the western extends of Virginia City. These fine-grained dikes intruded roughly 1.4 Ga parallel to the granite pegmatite dikes. These are composed of amphibole, chlorite, plagioclase, and minor quartz; however much of the plagioclase has been altered to albite, clinozoisite, and sericite. Accessory minerals of magnetite and ilmenite have been noted by Ruppel and Liu (2004).

The basalt and ash flows in the northeast region of Virginia City intruded approximately 33 Ma. The basalts are "partly vesicular or amygdaloidal," (Ruppel & Liu, 2004) and can be identified by its dark greenish-gray color. The basalts are composed of "plagioclase, sparse magnetite, and about 25 to 30 percent of olivine and augite phenocrysts in equal proportions (Hadley, 1980)" (Ruppel & Liu, 2004). These basalts are underlain by volcanic ash and tuffs, separated by gravel beds (Ruppel & Liu, 2004).

Glaciation and erosion during the Quaternary period produced two units of sediments: the Pleistocene moraine and Holocene alluvium. The Pleistocene moraine is exposed at the head of Bachelor Gulch. The unconsolidated glacial debris is weakly rounded and poorly sorted, consisting of blocks of Tertiary basalt, Paleozoic limestone, and Archean basement rock up to 3 meters in diameter (Despotovic, 2000). The Holocene alluvium consists of

moderately well-rounded pebbles to boulders of Archean basement rocks. The matrix is a sand or silt. Due to dredge tailings, this unit is largely disturbed (Despotovic, 2000).

II.IV.b. Regional Faults and Tectonics

The tectonics of the Virginia City region trend to the northwest, along the Virginia City fault zone. It has been observed by Ruppel and Liu that the older metamorphic rocks tend to be displaced by a left-lateral strike-slip fault. This fault could be the point where the lava field erupted because the basaltic lavas are centered on the fault zone and are not significantly displaced. There is also indication that the left-lateral displacement is echoed across the fault zones that affect the gold deposits of Virginia City. Figure 4 shows the faulting around the Virginia City area (Ruppel & Liu, 2004).

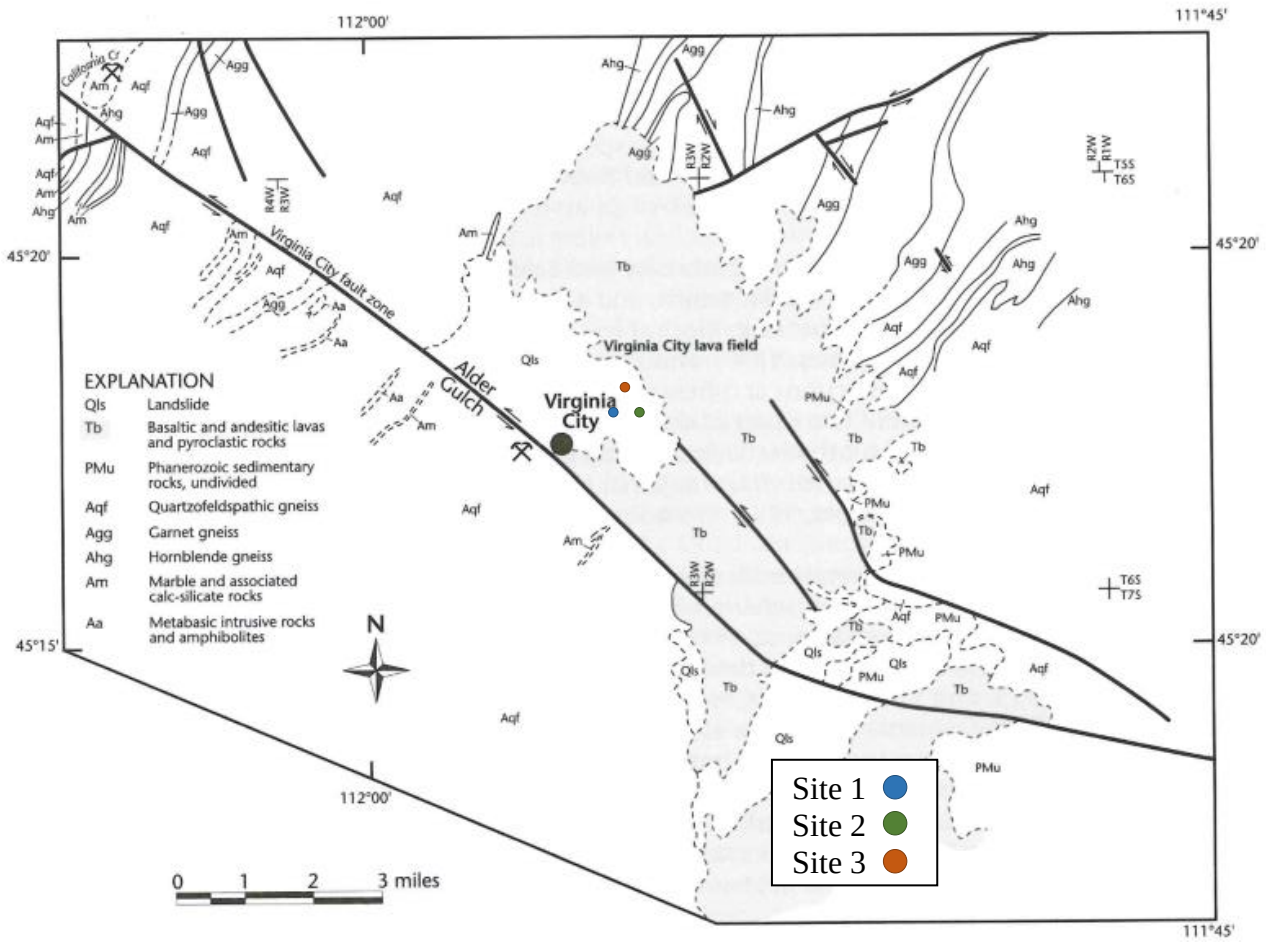

Figure 4: Apparent left-lateral displacements across the Virginia City fault zone. Geology modified from Vitaliano and Cordua, 1979; Weir, 1982; and Hadley, 1969. Geology partly remapped by Ruppel, 1985.

It is possible that the fault we detected in the field was the fault to the north of the largest fault of the Virginia City fault zone. The body intersecting the lava field is landslide material, and it is possible that the fault extends beyond the intersection, below the landslide material.

III. Field Methodology

We made use of three methods in this project: global positioning system (GPS); electrical resistivity tomography (ERT); and very low frequency electromagnetics (VLF-EM).

III.I GPS Survey

III.I.a. Leica GPS: ATX1230, GX1230, RTK Base & Rover 1200 Series

The Leica GPS system works by receiving signals from satellites and calculates the distance from the satellites to the receivers. Then the location of the receiver is determined by trilateration. Thus, the system must receive signals from at least four different satellites in order to pinpoint its location.

In this survey, a process called real-time kinematic (RTK) was used by using one stationary reference receiver (base station) and one moving receiver (rover). The base station received signals from the satellites and created a correction factor. This correction factor was sent via Bluetooth to the rover. The rover received signals from the satellites and correction factor from the base to calculate the coordinates of its positions. Figure 5 shows the positions of the survey lines determined by the GPS system.

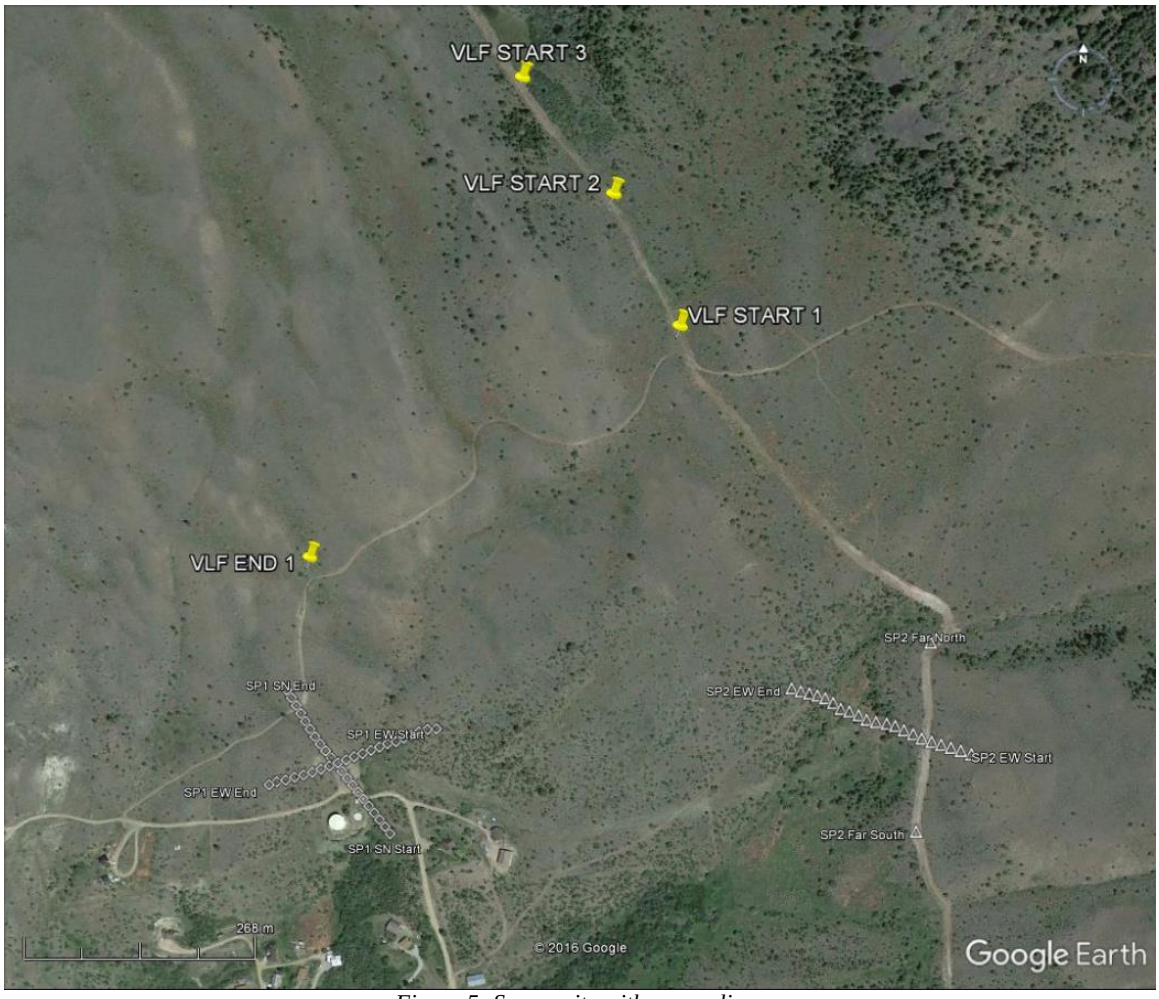

Figure 5: Survey site with survey lines

III.II Electrical Resistivity Tomography Survey

ERT methods are known for their versatility with the ability to function well in regions with irregular topography. In this project, we decided to use the Wenner array due to its high signal strength and sensitivity to resistivity variation.

III.II.a. General Theory of ERT

The ERT method is one of many methods used in geophysics. Although the ERT method can be time consuming, if employed properly, it provides accurate estimates of depths, thickness, and electrical resistivities of subsurface layers. Natural variations in resistivity within the earth's materials allows geophysicists to collect resistivity measurements by injecting electrical current to two current electrodes and measuring the potential difference between two potential electrodes (Figure 6). To take this simple principle and create a reliable, efficient method of taking resistivity measurements over a cross-section, geophysicists commonly use different arrays such as, Wenner, Schlumberger, or Dipole-Dipole. The Wenner array has the highest signal strength and sensitivity to the vertical resistivity changes. It is used when trying to determine ground water depth. An additional advantage to using this array is that the large potential electrode spacing requires less sensitivity from the equipment (Burger, Sheehan, & Jones, 2006).

Wenner arrays use equal spacing between electrodes positioned on a straight line. Typically, a series of electrodes are set-up and salt water is poured on them to decrease the contact resistance between the electrodes and the soil. To collect a cross-section of the subsurface, the current and potential electrode locations are varied. First, spacing between electrodes (distance "a" in Figure 6) is reduced to the distance between the set electrodes; no electrodes in the line are skipped. This "four-in-row" pattern is then shifted down the electrode line. For example, if the first electrode pattern is current electrodes [1,4] and potential electrodes [2,3], the second electrode pattern is current electrodes [2,5] and potential electrodes [3,4]. The shifting is continued until the last electrode is reached. This constitutes one section of data collection as it provides sub-surface information from ground-level to a depth equal to roughly $1/5^{th}$ of the distance between A and B (Bernard, 2003). In order to gather data at deeper depths, the spacing between A and B is increased. This is accomplished by using every other electrode in the electrode line. Instead of using electrodes [1,4,2,3] for the first reading, electrodes [1,7,3,5] are used. The same technique of shifting electrodes down-line is used; the second measurement in this section uses electrodes [2,8,4,6]. This general pattern of increasing the spacing between electrodes with each additional section continues as shown in Figure 7. Resistivity measurements are entered into a software package such as RES2DINV to create a 2D resistivity image.

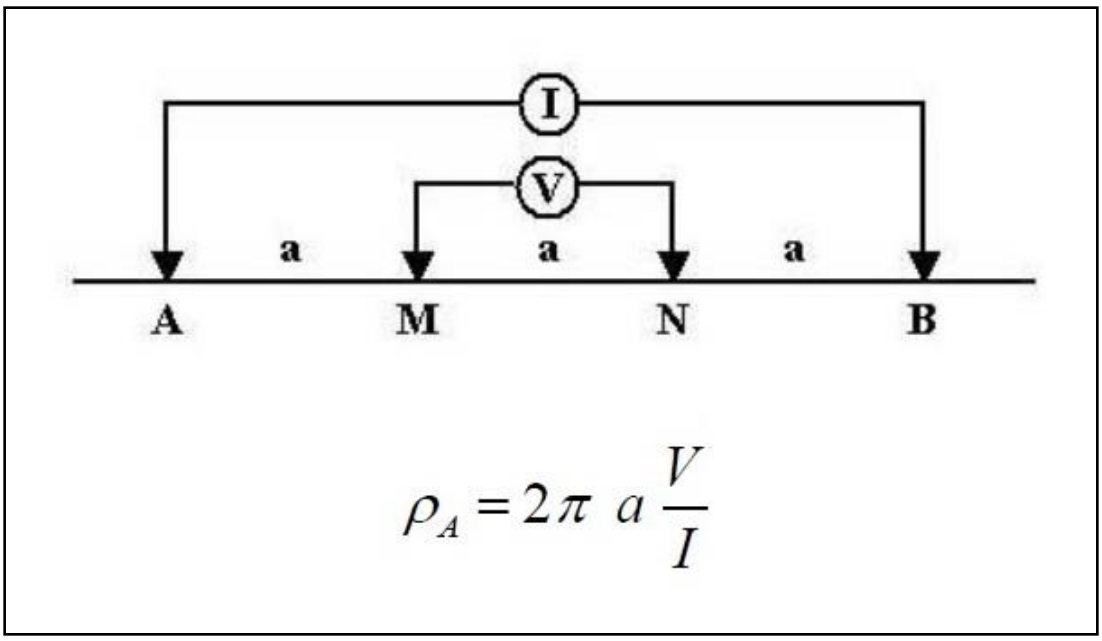

Figure 6: In the Wenner array, spacing between electrodes is constant and denoted by distance "a"

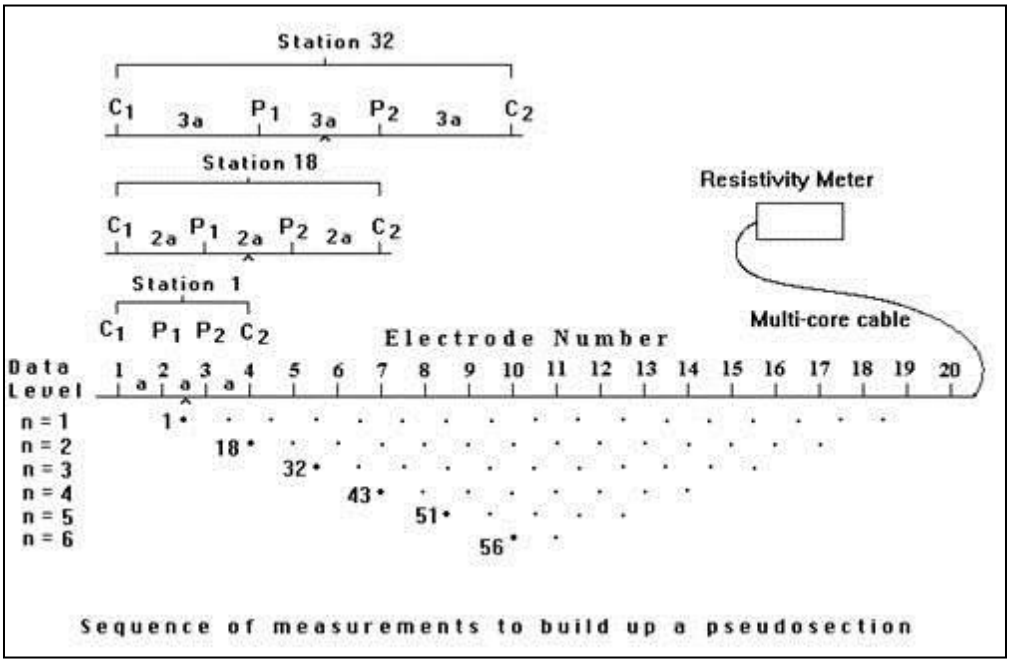

Figure 7: Wenner array spacing used for creating a 2D image. (Landvisor LLC, 2016)

RES2DINV uses an inversion routine based on the smoothness-constrained, least-squares method. The user is given the option of using the quasi-Newton method (fastest), Gauss-Newton method (slower but increased accuracy), and a moderately fast hybrid technique which incorporates the advantages of the quasi-Newton and Gauss-Newton methods (TerraPlus, 2013). The methods are all based on the equation presented in Figure 8. RES2DINV also provides optimized algorithms for areas that have smooth resistivity variation or sharply contrasting variation.

$$(\mathbf{J}^T\mathbf{J} + u\mathbf{F})\mathbf{d} = \mathbf{J}^T\mathbf{g}$$

where $\mathbf{F} = \mathbf{f_x}\mathbf{f_x}^T + \mathbf{f_z}\mathbf{f_z}^T$

$\mathbf{f_x}$ = horizontal flatness filter

$\mathbf{f_z}$ = vertical flatness filter

$\mathbf{J}$ = matrix of partial derivatives

u = damping factor

$\mathbf{d}$ = model perturbation vector

$\mathbf{g}$ = discrepancy vector

Figure 8: Equation used by RES2SINV to create a 2D cross section of the sub-surface (Geotomo Software, 2010).

III.II.b. Field Procedure

In this survey, the Wenner array for DC resistivity was used in order to determine the geologic structure of the subsurface near two different natural springs. Each survey consisted of a north-south profile and an east-west profile. Each of these profiles were 200 meters long with an electrode spacing of 10 meters. To take these readings, we used a resistivity meter by IRIS called the SYSCALR2. A 250-watt DC/DC converter was used for converting energy from a 12-volt battery to inject electrical current through the ground. The current is sent through the 21 electrodes spaced along the 200-meter profile. Electrode spacing is increased with each new line of data allowing us to look deeper into the subsurface. The first line of data started with a 10-meter electrode spacing. This spacing was increased by 10-meters until the electrode spacing reached 60-meters. This process was repeated for each profile located at the two springs.

III.III Very Low Frequency Electromagnetic Survey

The VLF-EM uses radio frequencies from military transmitters located around the world (Figure 10). The frequency range is between 15-30 kHz. There are around 40 of these transmitters that operate in the designated range for VLF-EM equipment operation. VLF-EM is primarily only used for finding subsurface conductive anomalies, such as water bearing fractures or linear conductive bodies.

III.III.a. Theory

Far from the source, the radio transmitter can be considered as a vertical electric dipole, the primary EM field of which has vertical electric dipole, possesses a vertical electric field component, and a horizontal magnetic field component (HPy), parallel to the ground and perpendicular to the propagation direction (Figure 9). At a distance greater than several free wavelengths from the transmitter, the primary EM field components can be assumed to be horizontally traveling waves. The primary HPy penetrates into the ground and induces eddy currents forming a secondary horizontal electric component in buried conductive structures. A secondary magnetic field is generated which is out of phase with the primary magnetic field. The intensity of the secondary magnetic field depends on the conductivity of the ground. The interface between the primary and the secondary magnetic fields produces a resultant magnetic field which is elliptically polarized. The orientation of this ellipse is arbitrary but is greatly extended along the direction of the primary field. This is referred to as the polarization ellipse. The parameters of interest are (a) the orientation of

the minor axis (tilt angle, α) and (b) the ratio of the minor to the major axis of the polarization (ellipticity, e). These two parameters are also called the real (in-phase) and imaginary (quadrature) components of the VLF-EM, respectively (McNeill JD, Labson VF ,1991).

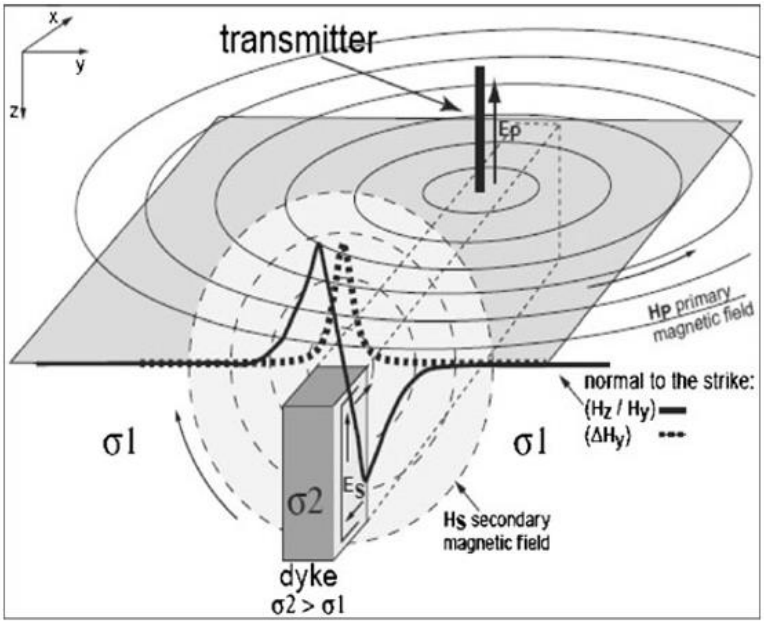

Figure 9: EM field distribution for the VLF method in E-polarization with theoretical signals over a vertical conductive dike

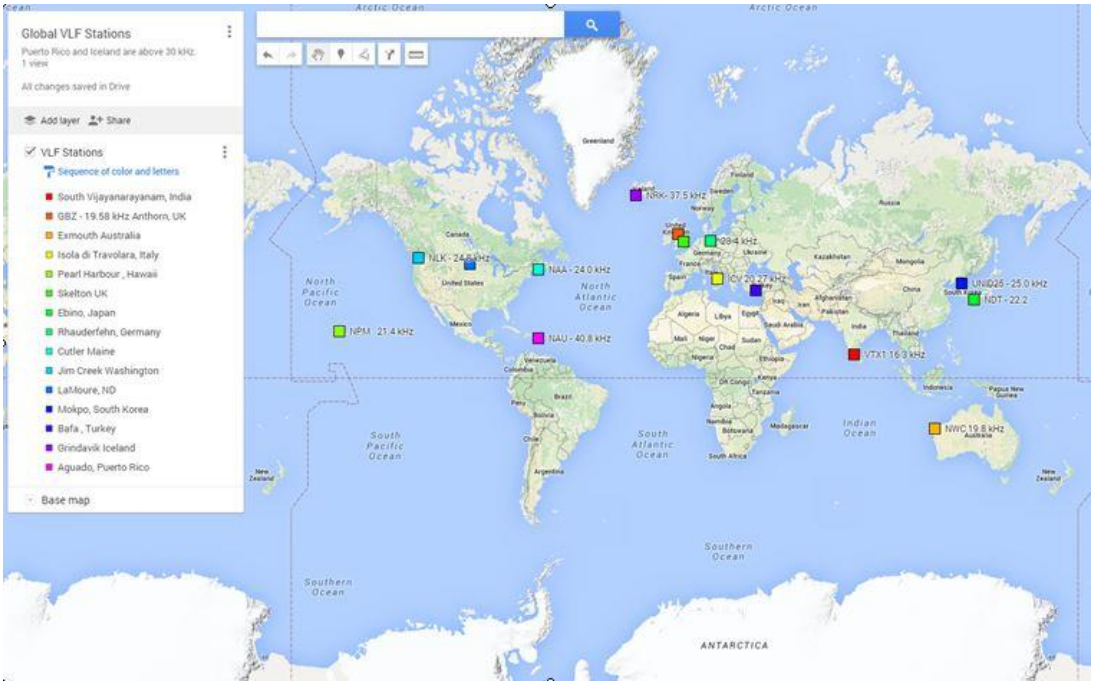

Figure 10: VLF-EM Worldwide Station Coverage

III.IV Procedure

The setup and procedure for the instrument is relatively simple, because the instrument is portable, and the user does not have to set up transmitters because they previously exist around the world.

Setup

1. Set up the line start points for the study and mark them with a flag. For this study, lines were set up 150 meters apart.
2. Unpack the VLF-EM instrument from the box. The necessary equipment includes a belt, power supply, antenna, and the measuring unit.
3. Put on the belt, and turn on the power supply and the instrument.
4. To search for a reasonable transmitter, turn the antenna until the strongest signal (longest bar) is reached. The signal is generally between 15 and 30 kHz. For this study, the signal used was 24.7 kHz.
5. Take the first reading at station zero.
6. Move to the next reading station. For this study, 500 meter lines were used and readings were taken every five meters.
7. Mark the end point of each line with a flag so that the GPS location can be picked up for each point. The VLF-EM survey lines can be seen below in Figure 20.

Data Analysis

The first step of data analysis is to input the data into an Excel spreadsheet. The columns needed are Distance, In-Phase (real), and Out-Of-Phase (imaginary). Once the data has been typed into Excel, a notepad file in the form of .DAT is created. This enables the data to be read by the program, KHFfilt. Below is an example of how the data should be put into the notepad file (Figure 11).

```
Synthetic VLF data

30 2

  20.000   2.349  -14.636  2222.633  37.753
  40.000   3.731  -16.339  2159.510  38.755
  60.000   5.763  -18.146  2079.178  39.902
  80.000   8.158  -20.152  1981.082  41.240
  ...
 580.000   1.003   10.426  2370.703  35.563
 600.000   1.490    9.340  2394.223  34.925
```

Figure 11: Example data of a .DAT format for VLF-EM interpretation

Row 1 of this format is the header text. Rows 2 and 4 can be used for notes, but are generally left blank. Row 3 has two important pieces of information for data analysis. The first number in the third line is the number of data points in the profile, and the second number is the column index for the data to be analyzed (in this case, we analyzed "Real" data in column 2). Copy and paste the data from Excel to Notepad.

Once the .DAT file has been created, the KHFfilt program can be opened. When the program is opened, it prompts the user to select a .DAT file. Select the file created from the Excel points in Notepad with the format from Figure 11. When that data is selected, the following view shows up in the program.

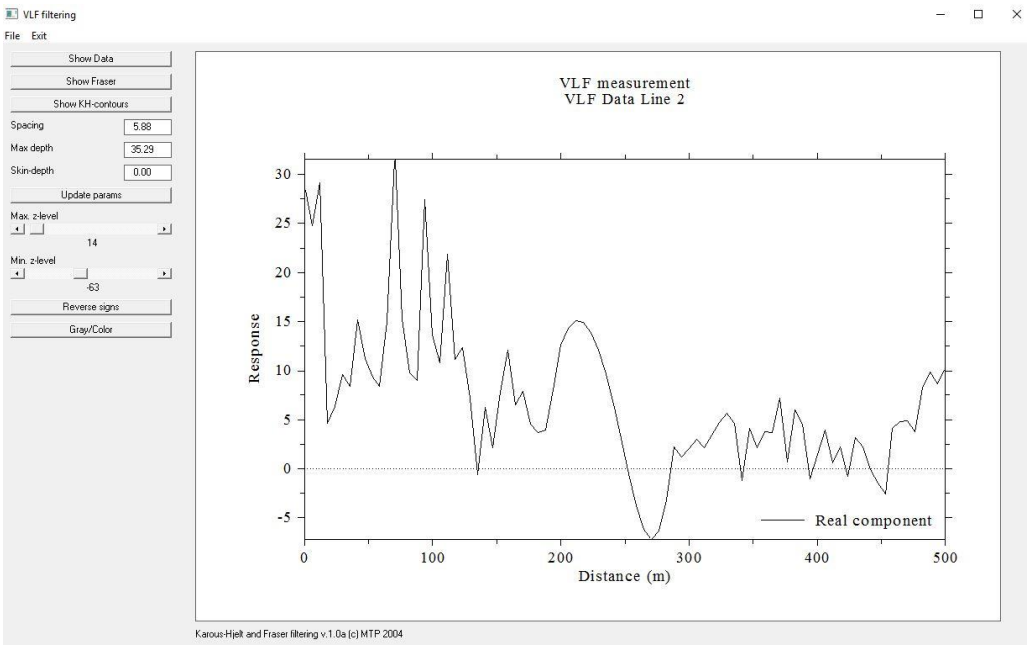

Figure 12: KHFfilt Program Screen

The graph in Figure 12 represents the data without any filtering. On the left hand side of the screen, the user can pick different filters and adjust parameters in order to clear up the data. The point that created the "spike" in the data was deleted. The data has been smoothed out before processing.

IV. Results

The following section presents our results from the two different surveys. First, the ERT is presented, then the VLF-EM data.

IV.I Electrical Resistivity Tomography Data

After data acquisition, a smoothness-constrained, least-squares inversion was performed, using RES2DINV software from Geotomo Software. We produced a 2D resistivity section that is free of distortions caused by the electrode array geometry used. During this process, a homogeneous earth model with multiple layers was used as the starting model for which the apparent resistivity partial derivative values can be calculated analytically. This initial model was modified in an iterative manner such that the root-mean-squared (RMS) error of the difference between the model response and the observed data values is minimized (Loke et al., 1995). However, minimizing the RMS error to its lowest possible value produces models that sometimes show large and unrealistic variations in resistivity and might not always be the best model from a geological perspective. A better approach is to choose the model at the iteration after which the RMS error does not change significantly.

IV.II Very Low Frequency Electromagnetics Data

First, the handwritten VLF-EM readings are typed into Microsoft Excel. This allows the user to be able to quickly plot the lines and see how smooth the data is. It also allows users to quickly edit or delete outlier points in order to create a better interpretation. Once the Excel file has been prepared, the VLF-EM data interpretation is processed with KHFfilt. In the program, two different filters are applied, Fraser and Karous-Hjelt.

IV.II.a. Fraser filter

Fraser filtering is effectively the first derivative of the data. The formula for Fraser filtering is Equation 1:

$$\frac{(f_1+f_2)-(f_3+f_4)}{4\Delta x} \qquad (1)$$

where f is the responses for the points, and Δx is the distance between two points. Because Δx is generally constant, it can usually be ignored. This results in Equation 2 below.

$$(f_1 + f_2) - (f_3 + f_4) \qquad (2)$$

In Figure 13 and Figure 14, the middle image is the Fraser filtering.

IV.II.b. Karous-Hjelt filter

Karous-Hjelt filtering is used in qualitatively interpreting VLF-EM data. It was derived from the concept that magnetic fields associated with subsurface current flow can result in a 2D cross section showing current density at different depths. The high current density (hot colors) refers to a saturated fracture zone (an inferred fault) whereas low current density (cold colors) refers to a resistive zone. In Figure 13 and Figure 14 the bottom image is the Karous-Hjelt filter for Lines 2 and 3, respectively.

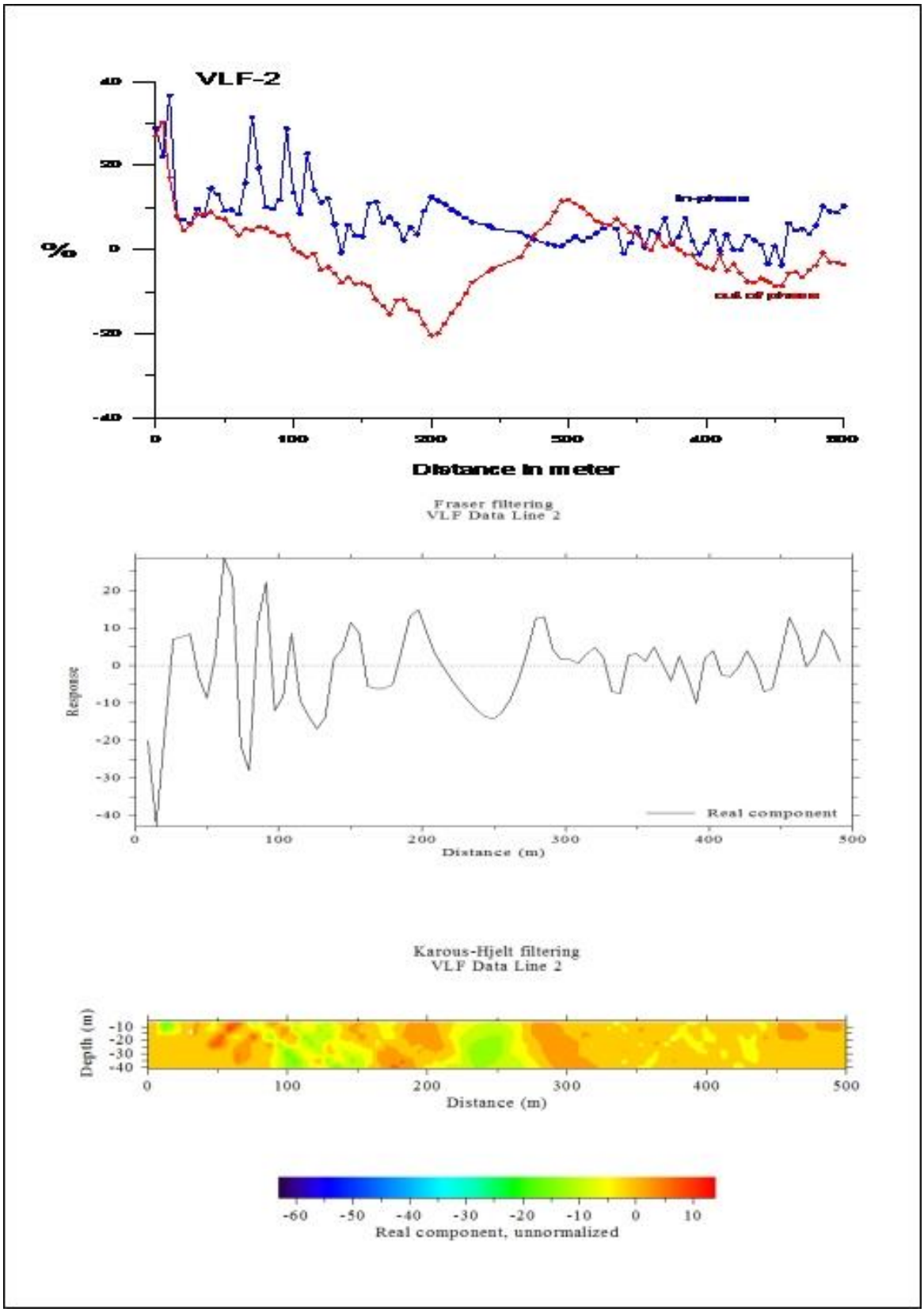

Figure 13: Line 2 KHFfilt Data

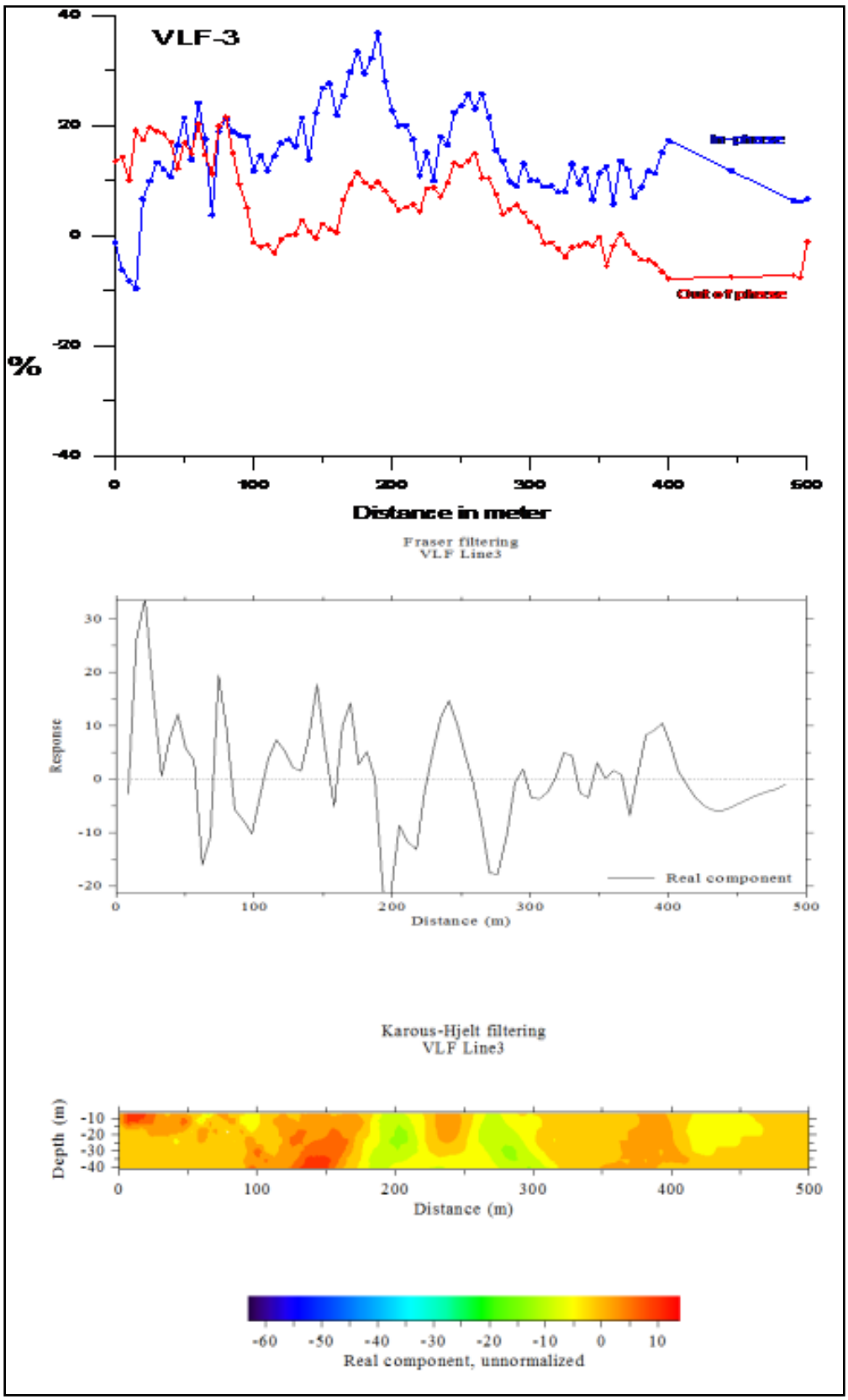

Figure 14: Line 3 KHFfilt Data

V. Interpretations

Below are our interpretations of the ERT and VLF-EM survey data. For each geophysical interpretation, we included a geological interpretation.

V.I Electrical Resistivity Tomography

V.I.a. Profile 1A

The first resistivity survey we conducted is located at Spring 1 and is a profile that ran north–south (Figure 15).

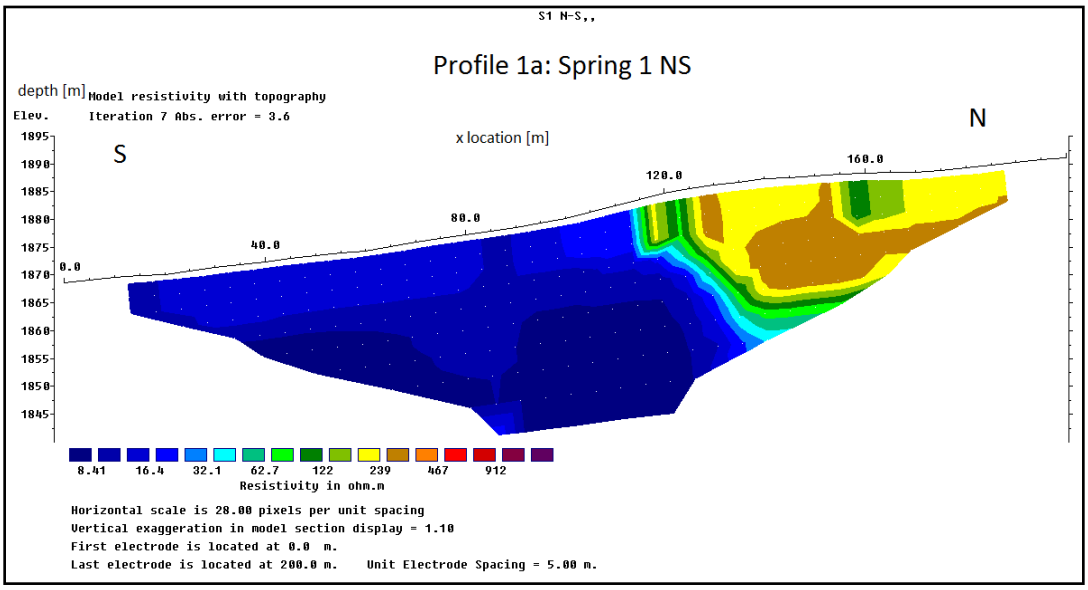

Figure 15: Profile 1A Spring 1 North - South

This profile shows two geoelectric zones. The first zone to the north is characterized by high resistivity values (about 400 Ω·m). The second zone to the south has an average low resistivity (about 15 Ω·m). From this profile, we can see there is a horizontal discontinuity located roughly 110 meters from the first electrode. This discontinuity is located at the approximate location of Spring 1. Based on the geologic information of the study area, this discontinuity could represent an inferred fault. The large variation in topography and the existence of a spring strongly support this result. From the resistivity values shown above, we determined this discontinuity could be the contact between a clay layer (low resistivity) and the bedrock (high resistivity).

V.I.b. Profile 1B

The second resistivity survey conducted was also located at Spring 1 (Figure 16). This profile consisted of the line running on the East-West plane. The RES2DINV interpretation is shown in Figure 16.

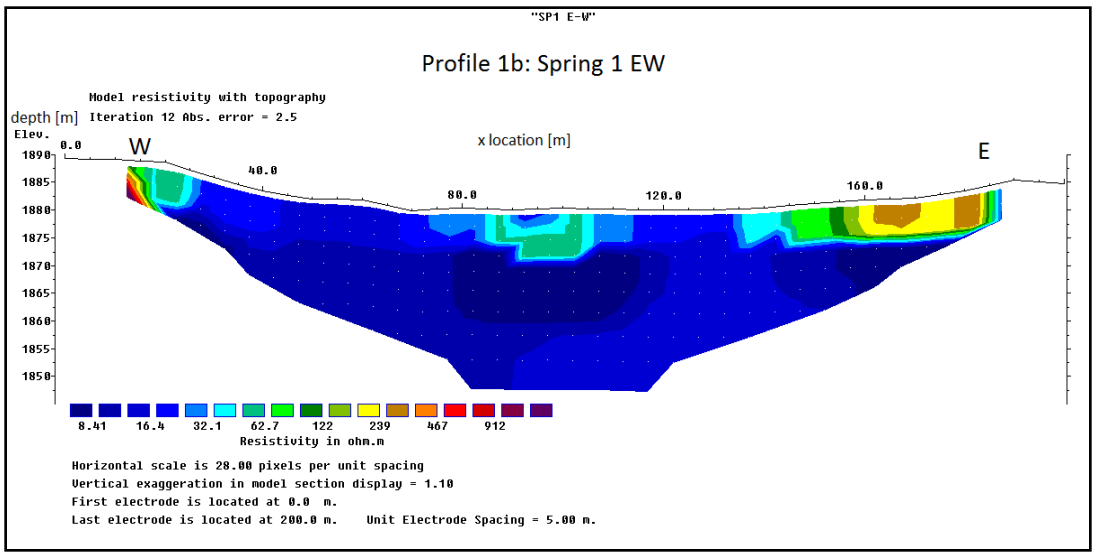

Figure 16: Profile 1B Spring 1 East-West

The resistivity is relatively low (about 15 Ω·m) and consistent throughout this profile. The material is generally the same with slight changes near the surface of the survey. We can conclude this profile is mostly clay or some low resistive material.

Profile 2A

The second two resistivity profiles were both completed at the second spring. The first profile ran north–south along the road, near the spring. The results of the RES2D modeling can be seen in Figure 17.

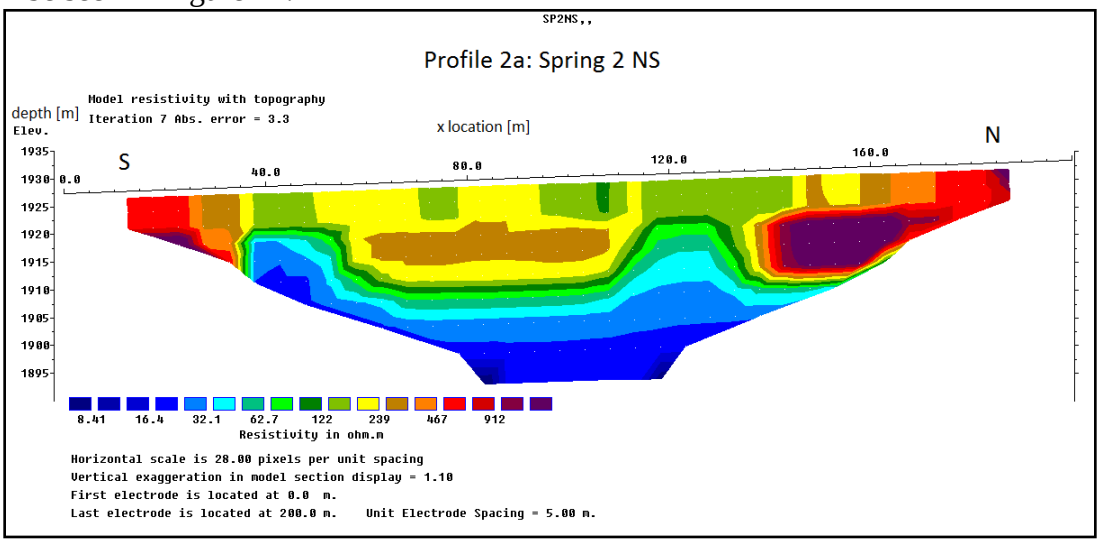

Figure 17: Profile 2A Spring 2 North–South

From Figure 17, we can see the overall resistivity for this profile decreases with depth. This could represent many material changes in the subsurface under the road. However, on the far north end, around 10 meters in depth, there is an area of high resistivity (more than 900 Ω·m). The obvious horizontal discontinuity in resistivity data refers to an inferred structural effect at 40m and 120m.

V.I.c. Profile 2B

The East–West cross section at Spring 2 (Figure 18) shows low to high resistivity values (between 15 Ω·m and 400 Ω·m). High resistivity values near the surface on the east side show an offset of 15 meters in the horizontal direction at a depth of 8 meters. There is also a marked change in resistivity values at roughly 120 meters (surface location) with an apparent dip of 45 degrees east. The contact between high and low resistivity zones refers to an inferred fault at 120m. It is worth mentioning that the resistivity values in this section, its spatial distribution, and its relation with topography is more or less the same as profile 1A at spring 1.

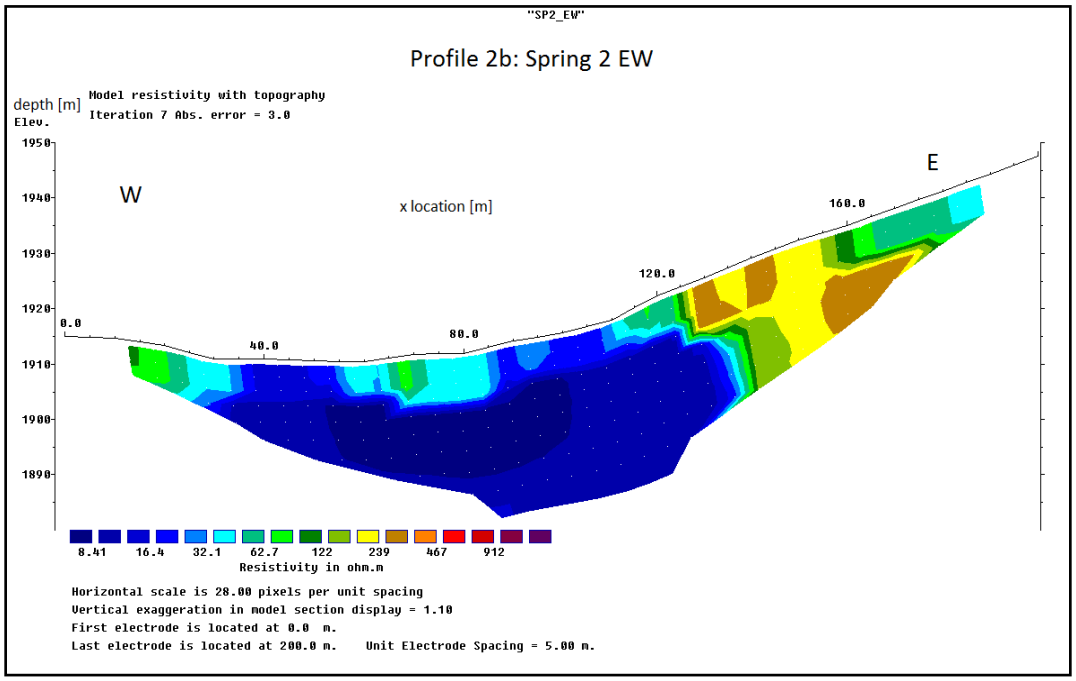

Figure 18: Profile 2B Spring 2 East-West.

V.I.d. Geologic Interpretations

The yellow unit of higher resistivity in Profiles 1a and 1b most likely represents basalt flows. The blue unit of low resistivity in both profiles is likely to be composed of weathered clay and ash beds, as indicated by Ruppel and Liu (2004) when they mention that, "[t]he eastern and northern borders of the mining district are concealed beneath basaltic volcanic rocks and underlying tuffs or volcanic ash beds". In addition, the authors further mention that, "[t]he tuff…was composed primarily of volcanic glass shards, much of it now altered to clay."

The North–South trending resistivity Profile 1a shows a distinct structure between the clay and ash unit (blue) and the basalt (yellow). The structure is projected to dip to the north, which indicates that the structure is a normal fault induced by regional tectonics. However, the previous works of Pero Despotovic (2000) suggests that the fault is a strike-slip fault. It is possible that the structure incorporates both elements of movement in the form of an oblique fault.

Profile 2b (Figure 18: Profile 2B Spring 2 East-West.), trending east-west shows a similar structure. The structure may be the same inferred fault detected in Profile 1a, but it may also be a separate fault—one of possibly several splay faults within the fault zone. In addition, another structure is shown by Profile 2b that is parallel to topography. This structure is most likely an interface where sliding occurred. Figure 19 shows the approximate location of the slide along the survey profile:

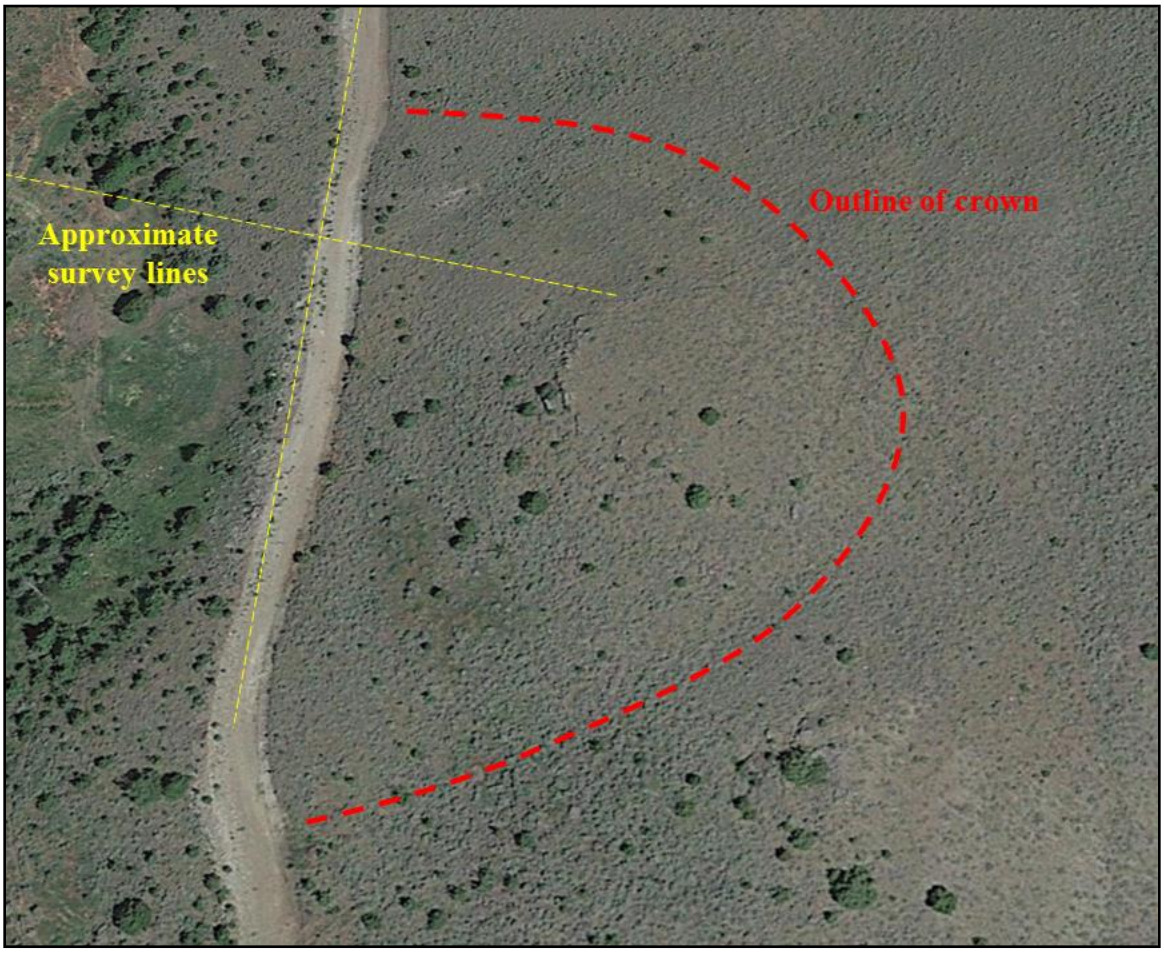

Figure 19: An approximate outline of the minor slide with respect to survey lines.

Profile 2b would indicate that the mass slid approximately 10 meters downslope to the west. In addition, the outline of the crown of the slide appears to coincide with two minor points of drainage along the road.

Profile 2a, oriented north–south at Spring 2, shows two anomalous bodies at the 40 meter mark and 120 meter mark. These bodies with low resistivity, as well as the material underlying it, are likely to be weathered beds of ash, tuff, and breccia. The lobes of relatively high resistivity adjacent to the bodies of low resistivity are most likely individual basalt flows. Basalt lavas are effusive and have low viscosity; they have a tendency to flow into narrow channels while producing brecciated material on the sides. This would explain the localized lobes of high resistivity along Profile 2a and the adjacent breccias described

previously. In addition, the contrast in high resistivities between the lobes are likely to represent a difference in lithology. The lobes of higher resistivity (red) are likely to be more intact, low porosity basalts, while the lobe of lesser resistivity (yellow) is likely to represent the vesicular and amygdaloidal basalts previously described. The zones of low resistivity adjacent to these inferred basalt flows are likely to represent high porosity, weathered breccias.

V.II Very Low Frequency Electromagnetics

Two VLF-EM profiles trending roughly southwest were measured in the area. The length of each profile is 500 meters. The Karous-Hjelt filter of the first profile shows high current density at about 180 meters and 300 meters from the beginning of the section. Based on the geology of the area, these two zones of high current density represent highly fractured saturated zones that could be interpreted as inferred faults (F1 and F2). The same high current density zones could be noticed also in VLF-EM profile No. 3 at distances of 150 meters, 250 meters, and 370 meters from the beginning of the section (F1, F2, and F3).

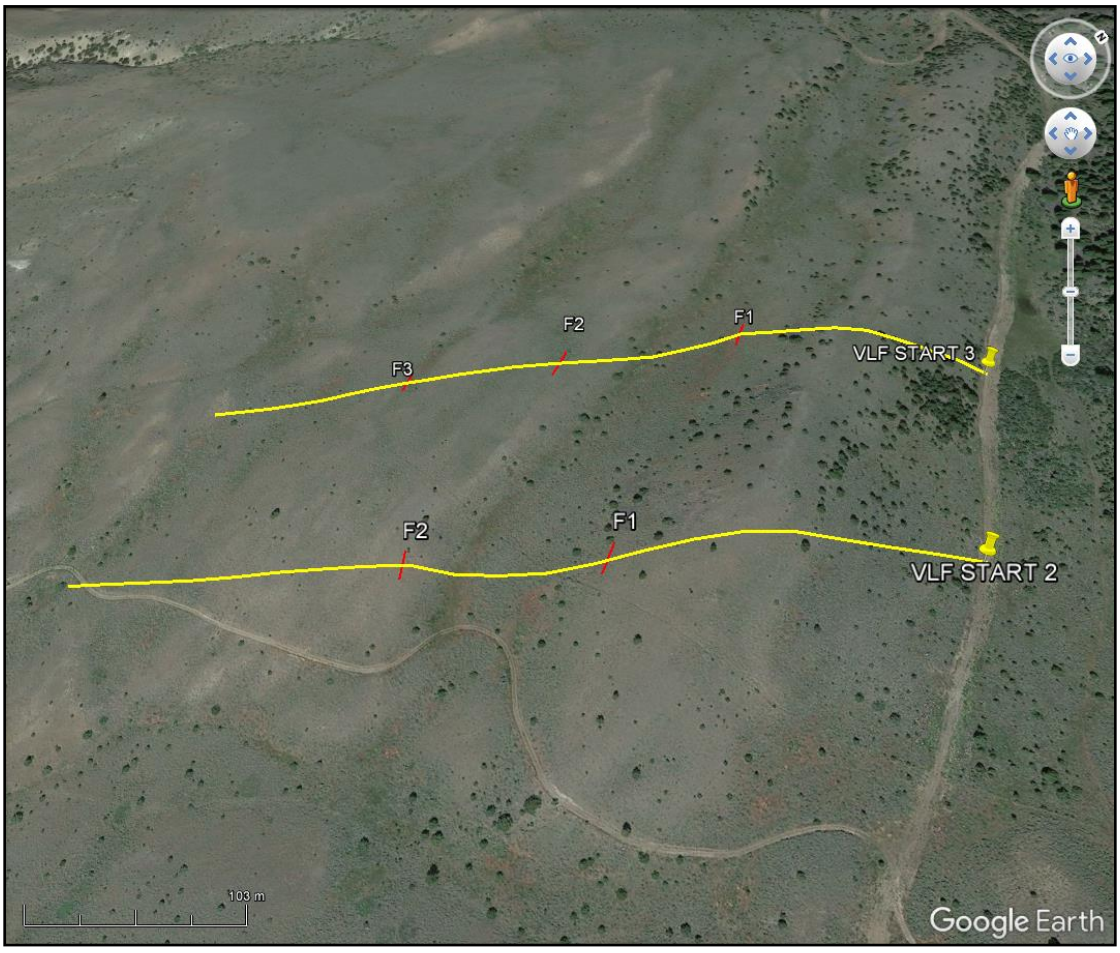

Figure 20: Mapped lines of VLF-EM lines 2&3 with fault interpretations

V.II.a. Geologic Interpretations

Anomalies in the Karous-Hjelt diagrams indicate that there are faults in the two lines. They are plotted as "F1, F2 and F3" in satellite view (Figure 20) to better show where they are estimated to be.

Comparing the data collected from the VLF-EM survey to an overhead image of Site 3 (Figure 20), it can be interpreted that there is a series of detachment faults (F1, F2, and F3) off a larger listric fault. These detachment faults begin forming on the western side of a plateau-like, uplifted area to the east of the site. Figure 22 shows a generic model of this type of structure. The half-grabens would represent the low points between the detachment faults seen in Figure 20. The whole structure appears to be slightly plunging northwest.

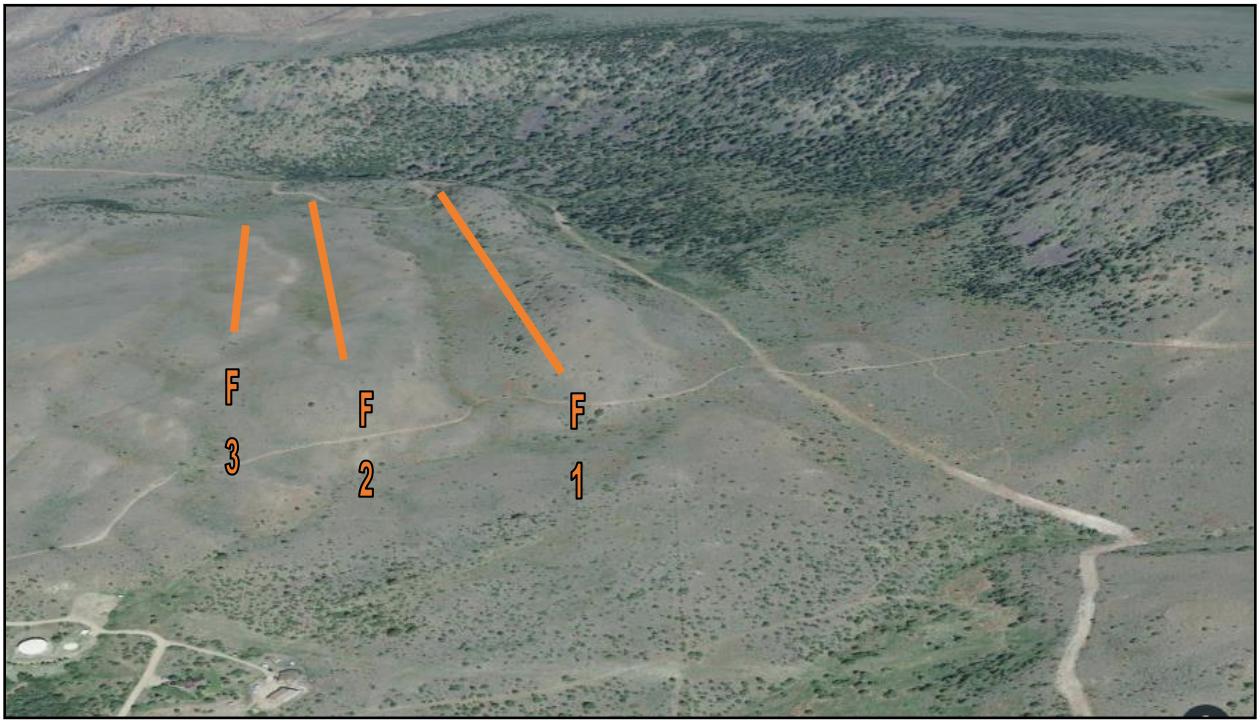

Figure 21: Overhead image of Site 3. Orange lines represent the proposed detachment faults. The low points in between these lines are referred to half-grabens in the proposed model.

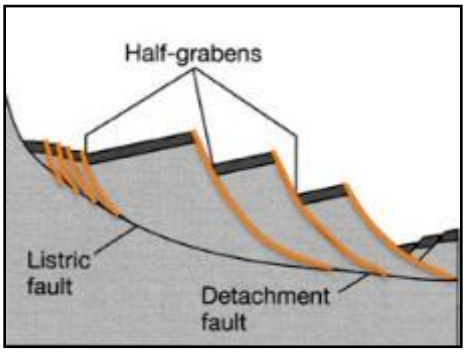

Figure 22: Generic model of detachment faults related to a listric fault (Simkat, 2017)

VI. Conclusions and Recommendations

The goal of this project was to aid in the interpretations of where Spring 1 and Spring 2 originated from. Two different types of surveys were done at three different sites: VLF-EM and ERT. We performed ERT surveys adjacent to the springs, and VLF-EM was performed north of both springs.

From the resistivity surveys, we interpreted a couple distinct features about the subsurface located at Spring 1 and Spring 2. Two of our profiles gave valuable data while the others gave data that could not be interpreted easily. For the North–South Profile 1a located at Spring 1, there is a distinct discontinuity that can be seen by an abrupt change in resistivity. Based on the geology in the area we can conclude this is most likely a normal or oblique fault, possibly part of a splay of faults located at the contact between a high resistivity basalt and a low resistivity, weathered clay and ash layer. This same type of discontinuity can be seen in the East-West Profile 2b located at Spring 2. The geology is most likely another splay fault located at the contact of multiple material types. The anomalous lobes in the North-South Profile 2a likely represent distinct flows of basalt with breccias in between. Differences in resistivity in the lobes are likely to represent different lithologies among the basalt flows.

The VLF-EM survey indicated that there is possibly a listric fault with three associated detachment faults in the region surveyed. We currently do not have enough data to produce adequate conclusions, but we believe the data and topography reveals listric faulting at Site 3.

We recommend collecting more data in the area, employing the same methods used in this study. For further study it would also be recommended to complete a 3D VLF-EM survey across Site 3, because there was not enough data to reach satisfying conclusions. We also recommend a 3D ERT survey on Sites 1 and 2. We will be going back to the site to perform a seismic survey in the center of our three sites. The seismic data will be compared to the VLF-EM data to get a clearer idea of what is happening at the northern end of our site.

VII. References

Bernard, J. (2003, July). *Parameters Controlling Depth of Investigation.* Retrieved from Heritage Geophyics: http://www.heritagegeophysics.com/papers/Depth_of_investigation.pdf

Burger, H. R., Sheehan, A. F., & Jones, C. H. (2006). *Introduction to Applied Geophysics.* New York: Norton.

Despotovic, P. (2000). *Geology and Geochemistry of Au-Ag-Mineralizations in the Virginia City Mining District (VCMD), Montana, U.S.A.* Berlin: Technische Universität Berlin.

Fraser Filter. (2017, April 2). Retrieved from https://en.wikipedia.org/wiki/Fraser_Filter

GEM Portable EM Instruments for Resistivity Mapping. (2017). Retrieved May 18, 2017, from http://www.gemsys.ca/very-low-frequency-electromagnetics/

Geotomo Software. (2010). *RES2DINV ver. 3.59 Rapid 2-D Resistivity & IP inversion using the least-squares method* . Penang, MALAYSIA .

Kellog, K. S., & Williams, V. S. (2006). *Geologic Map of Ennis 30' x 60' Quadrangle Madison and Gallatin Counties, Montana, and Park County, Wyoming.* Butte: Montana Bureau of Mines and Geology .

Landvisor LLC. (2016). *Electrical Profiling*. Retrieved from LandMapper ERM-02 - new handheld EC/ER/SP meter: http://landviser.net/sites/default/files/clip_image0025.jpg

Loke, M. H. (1995). Least-squares deconvolution of apparent resistivity pseudocetions. *Geophysics*, pp. 1682-1690.

McNeill JD, Labson VF (1991) Geological mapping using VLF radio fields. In: Nabighian, MN (ed) Electromagnetic methods in applied geophysics II. Soc Exp Geophys, pp 521–640.

Pirttijarvi, M. (2014). KHFFILTL Karous-Hjelt and Fraser filtering of VLF Measurements. Retrieved from https://wiki.oulu.fi/pages/viewpage.action?pageId=20677906.

Ruppel, E. T., & Liu, Y. (2004). *The Gold Mines of the Virginia City Mining District, Madison County, Montana.* Montana Bureau of Mines and Geology Bulletin 133.

Santos, M. M. (2014). On the Depth to Anomaly Estimation Using Karous and Hjelt Filter in VLF-EM Data. *Arabian Journal of Geosciences, 10*, pp. 4355-4359. Retrieved May 18, 2017, from https://link.spring.com/article/10.1007%2Fs12517-013-1110-3

Simkat, S. (2017, May 18). Imbricate Faults. Moscow, Idaho, United States of America.

Subsurface Surveys. (2017). *Geophysical Methods & Applications.* Retrieved from http://www.subsurfacesurveys.com/pdf/Methods.pdf

TerraPlus. (2013). *RES2DINV 2D Resistivity & IP Inversion Software*. Retrieved from TerraPlus -- Geophysical Equipment Supplier: http://terraplus.ca/products/resistivity/res2d.aspx

VLF Survey Methods. (2017). Retrieved May 18, 2017, from http://zonge.com/geophysical-methods/electrical-em/vlf-survey-methods/

Zhang, Z. (2015). *The Geophysical Very low Frequency Electromagnetic (VLF-EM) Method: Effects of Topography and Surface Water Investigated with Simulations and Field Measurements.* University of Saskatchewan. Retrieved May 18, 2017, from https://ecommons.usask.ca/bitstream/handle/10388/ETD-2015-03-2020/ZHANG-THESIS.pdf?sequence=6

VIII. Appendices

Appendix A: Stratigraphic Column

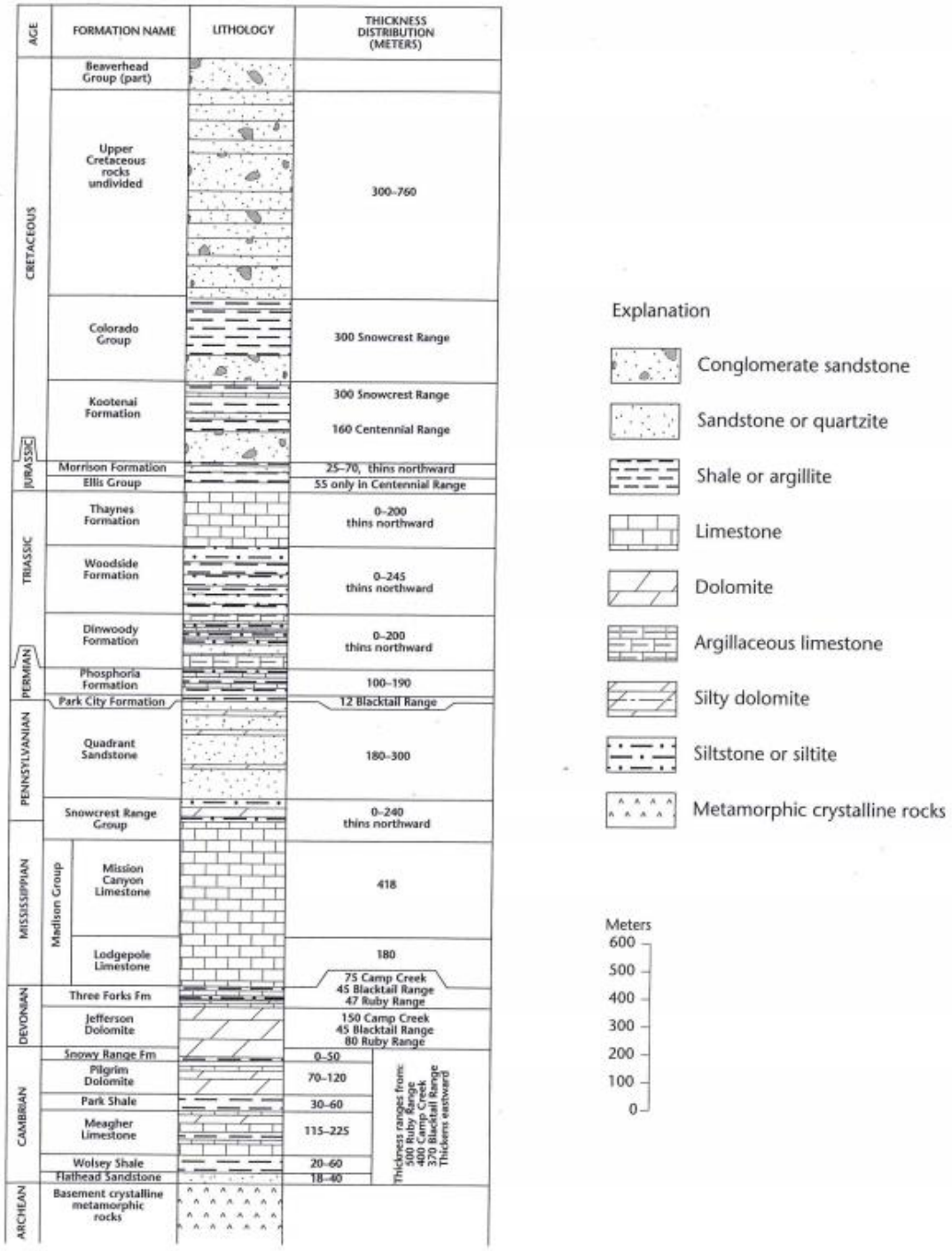

Appendix B: GPS Data

SP 1 EW Data	Lat. (Deg)	Long. (Deg)	Ele (m)
SP 1 POINT EW 1	45.29925184	-111.9257378	1889.402
SP 1 POINT EW 2	45.29924351	-111.925865	1889.238
SP 1 POINT EW 3	45.29921788	-111.9259849	1888.735
SP 1 POINT EW 4	45.29917979	-111.9260943	1885.941
SP 1 POINT EW 5	45.2991468	-111.9262074	1883.486
SP 1 POINT EW 6	45.29910929	-111.9263213	1882.101
SP 1 POINT EW 7	45.29908674	-111.9264433	1881.938
SP 1 POINT EW 8	45.29905182	-111.9265586	1879.987
SP 1 POINT EW 9	45.29902009	-111.9266776	1880.449
SP 1 POINT EW 10	45.29898734	-111.9267975	1880.182
SP 1 POINT EW 11	45.29895647	-111.9269167	1880.445
SP 1 POINT EW 12	45.29892489	-111.9270275	1880.257
SP 1 POINT EW 13	45.29889497	-111.9271473	1880.104
SP 1 POINT EW 14	45.29886271	-111.9272664	1880.196
SP 1 POINT EW 15	45.29883258	-111.9273861	1880.514
SP 1 POINT EW 16	45.29880218	-111.9275057	1881.311
SP 1 POINT EW 17	45.29877757	-111.9276277	1881.918
SP 1 POINT EW 18	45.29875773	-111.9277512	1882.175
SP 1 POINT EW 19	45.29873019	-111.9278749	1883.552
SP 1 POINT EW 20	45.29871498	-111.9279966	1885.57
SP 1 POINT EW 21	45.2986838	-111.928108	1884.767

SP 1 NS Data	Lat. (Deg)	Long. (Deg)	Ele (m)
SP 1 POINT SN 1	45.29815449	-111.9264374	1868.7
SP 1 POINT SN 2	45.29822775	-111.926508	1869.605
SP 1 POINT SN 3	45.29830123	-111.9265833	1870.172
SP 1 POINT SN 4	45.29837277	-111.9266577	1871.331
SP 1 POINT SN 5	45.29844439	-111.926732	1872.408
SP 1 POINT SN 6	45.29851723	-111.926805	1873.563
SP 1 POINT SN 7	45.2985904	-111.9268786	1874.399
SP 1 POINT SN 8	45.29866248	-111.9269516	1875.972
SP 1 POINT SN 9	45.29873525	-111.9270245	1877.326
SP 1 POINT SN 10	45.29880907	-111.9270959	1878.647
SP 1 POINT SN 11	45.29888287	-111.9271716	1880.114
SP 1 POINT SN 12	45.29895079	-111.9272379	1882.467
SP 1 POINT SN 13	45.29902248	-111.927308	1884.821
SP 1 POINT SN 14	45.2990948	-111.9273784	1886.208
SP 1 POINT SN 15	45.29917011	-111.9274471	1887.279
SP 1 POINT SN 16	45.29924664	-111.927513	1887.885
SP 1 POINT SN 17	45.29932354	-111.9275789	1888.408
SP 1 POINT SN 18	45.299401	-111.9276431	1888.426
SP 1 POINT SN 19	45.29947902	-111.9277052	1889.255
SP 1 POINT SN 20	45.29955589	-111.9277698	1890.333
SP 1 POINT SN 21	45.29963397	-111.9278316	1891.1

SP 2 EW Data	Lat. (Deg)	Long. (Deg)	Ele (m)
SP 2 POINT EW 1	45.29913638	-111.9185253	1947.66
SP 2 POINT EW 2	45.29916136	-111.9186498	1944.429
SP 2 POINT EW 3	45.29918347	-111.9187667	1941.309
SP 2 POINT EW 4	45.29920499	-111.9188844	1938.279
SP 2 POINT EW 5	45.29922669	-111.9190002	1935.197
SP 2 POINT EW 6	45.29925022	-111.9191184	1932.59
SP 2 POINT EW 7	45.29928479	-111.9192201	1929.317
SP 2 POINT EW 8	45.29931361	-111.9193311	1925.754
SP 2 POINT EW 9	45.29935001	-111.9194381	1922.455
SP 2 POINT EW 10	45.29936582	-111.9195416	1918.077
SP 2 POINT EW 11	45.29937252	-111.9196738	1915.724
SP 2 POINT EW 12	45.29939196	-111.9197962	1914.305
SP 2 POINT EW 13	45.29943425	-111.9199029	1912.085
SP 2 POINT EW 14	45.29946724	-111.9200253	1911.812
SP 2 POINT EW 15	45.29949057	-111.9201407	1910.519
SP 2 POINT EW 16	45.29954768	-111.9202444	1910.717
SP 2 POINT EW 17	45.29959457	-111.920355	1911.047
SP 2 POINT EW 18	45.29962161	-111.9204657	1910.986
SP 2 POINT EW 19	45.29964355	-111.9205805	1913.497
SP 2 POINT EW 20	45.29966591	-111.9207003	1914.817
SP 2 POINT EW 21	45.29969673	-111.9208289	1915.052

SP 2 NS Data	Lat. (Deg)	Long. (Deg)	Ele (m)
SP 2 POINT Far South	45.29835556	-111.9191758	1927.479
SP 2 POINT Far North	45.30016074	-111.9190043	1933.438

VLF Data	Lat. (Deg)	Long. (Deg)	Ele (m)
VLF END 1	45.30083096	-111.9275155	1904.617
VLF START 1	45.30299986	-111.9224584	1954.004
VLF START 2	45.30420674	-111.923336	1959.613
VLF START 3	45.30527107	-111.9245317	1961.702
VLF START 4	45.30639673	-111.9256127	1961.922
VLF START 5	45.30760283	-111.9264772	1968.605

Appendix C: Electrical Resistivity Data

											Sp-1 E-W	Sp-1 N-S	Sp-2 E-W	Sp-2 N-S
A (m)	B (m)	M (m)	N (m)	a (m)	center (m)	a (m)	A	B	M	N	App. Res	App. Res	App. Res	App.Res
0	30	10	20	10	15	10	1	4	2	3	79.8	10.2	49.2	471.2
10	40	20	30	10	25	10	2	5	3	4	52.2	12.1	35.7	424.3
20	50	30	40	10	35	10	3	6	4	5	103	12.3	25.6	258.3
30	60	40	50	10	45	10	4	7	5	6	56.2	12.3	13.5	150.8
40	70	50	60	10	55	10	5	8	6	7	44.1	12	18.6	157.2
50	80	60	70	10	65	10	6	9	7	8	22.6	12.3	25.6	166.3
60	90	70	80	10	75	10	7	10	8	9	16	12	26.3	154
70	100	80	90	10	85	10	8	11	9	10	16.2	11.3	24.8	199.3
80	110	90	100	10	95	10	9	12	10	11	30.1	15	19.5	161.8
90	120	100	110	10	105	10	10	13	11	12	14.4	17.2	15.9	135.2
100	130	110	120	10	115	10	11	14	12	13	28.6	79.2	40.8	148.5
110	140	120	130	10	125	10	12	15	13	14	14.4	136.6	118.2	135
120	150	130	140	10	135	10	13	16	14	15	13.4	167.4	132.8	170
130	160	140	150	10	145	10	14	17	15	16	13.5	179.4	154.7	247.1
140	170	150	160	10	155	10	15	18	16	17	14.8	181.6	145.3	266.1
150	180	160	170	10	165	10	16	19	17	18	17.6	156.6	84.1	413.9
160	190	170	180	10	175	10	17	20	18	19	50.1	192.1	76.5	476.6
170	200	180	190	10	185	10	18	21	19	20	25.6	206.1	58.5	360.2
0	60	20	40	20	30	20	1	7	3	5	17.8	10.6	14.8	317.7
10	70	30	50	20	40	20	2	8	4	6	13	10.6	14.2	199.1
20	80	40	60	20	50	20	3	9	5	7	18.6	10.4	13	151
30	90	50	70	20	60	20	4	10	6	8	17.2	11.4	14.4	120.9
40	100	60	80	20	70	20	5	11	7	9	14.6	11.4	13.6	100.8
50	110	70	90	20	80	20	6	12	8	10	13	10.6	11.5	126.2
60	120	80	100	20	90	20	7	13	9	11	13.6	12.6	12.4	134.9
70	130	90	110	20	100	20	8	14	10	12	10.6	16	15.4	108.5
80	140	100	120	20	110	20	9	15	11	13	10.2	46.4	22.6	120.9
90	150	110	130	20	120	20	10	16	12	14	14.4	97	59.8	180.8
100	160	120	140	20	130	20	11	17	13	15	14.8	100.2	71.7	196.9
110	170	130	150	20	140	20	12	18	14	16	11.8	107.4	88.9	227.2
120	180	140	160	20	150	20	13	19	15	17	11.6	111.2	86.5	209.9
130	190	150	170	20	160	20	14	20	16	18	18.2	146.4	99.9	160.6
140	200	160	180	20	170	20	15	21	17	19	41.8	165.6	90.5	246.3
0	90	30	60	30	45	30	1	10	4	7	13.2	10.8	11.5	132.6
10	100	40	70	30	55	30	2	11	5	8	11.1	11.1	12.6	92.7
20	110	50	80	30	65	30	3	12	6	9	12.3	10.8	13	79.5
30	120	60	90	30	75	30	4	13	7	10	11.1	10.8	13.1	71.9
40	130	70	100	30	85	30	5	14	8	11	11.4	11.7	12.3	59.5
50	140	80	110	30	95	30	6	15	9	12	9.9	13.2	12.2	73.3
60	150	90	120	30	105	30	7	16	10	13	10.8	30.3	14	98.9

70	160	100	130	30	115	30	8	17	11	14	11.1	54	31.77	131.6
80	170	110	140	30	125	30	9	18	12	15	12.3	76.8	53.68	153.8
90	180	120	150	30	135	30	10	19	13	16	11.7	73.5	73.81	161
100	190	130	160	30	145	30	11	20	14	17	13.5	59.1	80.44	120.2
110	200	140	170	30	155	30	12	21	15	18	15.9	55.8	68.65	86.1
0	120	40	80	40	60	40	1	13	5	9	11.6	10.4	12.8	51.3
10	130	50	90	40	70	40	2	14	6	10	10.4	10.4	13.2	39.1
20	140	60	100	40	80	40	3	15	7	11	10.4	10.8	12.8	52.9
30	150	70	110	40	90	40	4	16	8	12	9.6	11.6	11.7	53.4
40	160	80	120	40	100	40	5	17	9	13	10.4	19.6	11.5	63.3
50	170	90	130	40	110	40	6	18	10	14	11.2	38.4	23.6	79.5
60	180	100	140	40	120	40	7	19	11	15	11.2	46.8	41.2	88.6
70	190	110	150	40	130	40	8	20	12	16	12.8	44.8	60.8	89.3
80	200	120	160	40	140	40	9	21	13	17	13.6	38	71.7	47.9
0	150	50	100	50	75	50	1	16	6	11	11.5	10.5	11.8	43.7
10	160	60	110	50	85	50	2	17	7	12	10	11	11.7	43.8
20	170	70	120	50	95	50	3	18	8	13	10	16	11.5	46.2
30	180	80	130	50	105	50	4	19	9	14	10.5	24.5	19.8	48.1
40	190	90	140	50	115	50	5	20	10	15	12	28.5	34	40.6
50	200	100	150	50	125	50	6	21	11	16	12	28	49.9	31.4
0	180	60	120	60	90	60	1	19	7	13	10.8	13.2	11.4	30.1
10	190	70	130	60	100	60	2	20	8	14	11.4	16.8	17.8	28
20	200	80	140	60	110	60	3	21	9	15	11.4	19.2	28.8	22.3

Appendix D: VLF-EM Data

VLF	Line 1	
Distance	Real	Imaginary
0	-3.7	-4.8
5	-5.65	-5.2
10	-7.6	-2.7
18	-20.85	-7.65
25	-34.1	-12.6
30	28.6	-11.3
35	21.5	-8
40	18.9	-6.3
45	21.9	-5.3
50	17.2	-7.1
55	14.3	-4.9
60	15.5	-5.4
65	14.8	-2.6
70	14	-4.8
75	23	-6.4
83	6.95	0.25
90	-29.4	30.5
95	-24.9	25.6
100	-33.9	33.2
105	-25	30.6
143	-25.3	24.1
180	-25.6	17.6
185	-23.9	15.1
190	-32.1	20.2
195	-29.6	22.2
200	-9.4	15.1
205	-8.6	17.5
210	7.9	10.5
215	22.3	10.5
220	22.1	9
225	25	8.4
230	34	1.2
235	31.5	0.4
240	19.6	5.1
245	21.4	1.9
250	17.5	2.2
255	8.6	10.1
260	4.8	6.0

265	9.5	3.0
270	9.5	15.6
275	9.9	11.2
280	23.8	8.3
285	38.8	-4.8
290	7.7	9.5
295	22.4	-0.7
300	24.2	-2.2
305	3.2	7.7
310	34.8	-1.6
315	15.4	3.5
320	26.4	8.5
325	31.6	-1.3
330	12.9	0.4
335	22.1	-5.3
340	-0.4	10.2
345	-6.1	5.2
350	-12.5	3.1
355	7.5	-1.8
360	9.3	-3.7
365	-0.5	-2.1
370	-11.2	0.3
375	-0.7	2.0
380	-11.4	-1.7
385	-0.9	-6.5
390	-4.2	-0.8
395	-9.9	-0.7
400	-9.8	-0.4
405	-3.9	-2.8
410	-2.2	-6.0
415	0.4	-1.7
420	-3.5	-6.7
425	6.6	-14.0
430	19.2	-20.5
435	6.5	-12.6
440	21.7	-13.8
445	7.1	-14.3
450	8.7	-14.5
455	4.3	-10.0
460	15.0	-16.5
465	18.1	-20.4

470	20.7	-18.8
475	19.6	-17.9
480	9.8	-12.4
485	20.3	-24.3
490	15.8	-20.8
495	11.1	-11.6
500	7.5	-12.8

VLF-EM Line 2

Distance	Real	Imaginary
0	29.0	27.2
5	22.3	30.3
10	36.7	17.2
15	8.1	7.9
20	7.1	4.5
25	6.1	6.0
30	9.8	8.3
35	8.2	8.5
40	14.6	9.0
45	13.2	7.5
50	9.3	7.3
55	9.5	5.6
60	8.4	3.5
65	15.9	4.9
70	31.6	4.6
75	19.4	5.5
80	10.1	5.2
85	9.8	4.0
90	11.8	3.3
95	28.8	3.6
100	13.6	0.2
105	8.5	-0.7
110	22.9	-1.7
115	14.2	-0.9
120	11.2	-4.8
125	12.2	-4.1
130	6.1	-5.7
135	-0.7	-7.9
140	5.9	-6.6
145	3.4	-8.1
150	3.1	-8.0

155	11.0	-8.6
160	11.3	-11.9
165	6.4	-13.3
170	7.8	-15.3
175	6.0	-12.0
180	2.3	-11.9
185	5.3	-14.3
190	3.6	-14.7
195	9.2	-17.8
200	12.6	-20.4
205	11.7	-20.00
210	10.8	-17.67
215	9.5	-15.00
220	8.6	-13.01
225	7.5	-10.34
230	6.6	-7.67
242.5	5.7	-5.00
245	5.0	-4.42
265	4.1	-1.75
270	3.2	0.92
275	2.3	3.59
285	1.4	6.26
290	1.0	8.93
295	0.9	11.6
300	2.1	11.9
305	3.1	10.9
310	2.1	10.0
315	2.9	8.4
320	3.9	6.9
325	5.0	6.1
330	5.8	5.9
335	4.9	7.4
340	-0.9	6.0
345	1.7	4.0
350	5.3	3.8
355	0.6	1.3
360	4.6	-0.2
365	3.8	2.9
370	7.5	0.8
375	1.4	1.7
380	3.1	0.1

385	7.6	-1.2
390	2.1	-1.2
395	-1.1	-3.4
400	1.5	-4.2
405	4.6	-4.6
410	-0.3	-1.3
415	3.5	-5.0
420	0	-3.4
425	-0.1	-5.6
430	3.4	-7.6
435	2.3	-7.8
440	1.2	-6.8
445	-3.3	-7.6
450	0.9	-8.6
455	-3.7	-8.6

VLF-EM Line 3		
Distance	Real	Imaginary
0	-1.2	13.5
5	-6.2	14.3
10	-8.2	10.1
15	-9.6	19.1
20	6.6	17.4
25	9.9	19.7
30	13.3	18.9
35	12.0	18.5
40	10.7	17
45	16.4	12.2
50	21.4	16.9
55	13.8	14.9
60	24.1	20.2
65	17.5	14.7
70	3.8	11.2
75	18.9	19.9
80	21.1	21.5
85	18.9	14.9
90	18.1	9.3
95	18.0	5.1
100	11.8	-1.2
105	14.5	-2.0
110	11.8	-1.7

115	14.4	-3.2
120	16.8	-0.6
125	17.4	0.1
130	16.3	0.2
135	21.4	2.8
140	13.9	0.8
145	22.3	-0.4
150	26.8	2.1
155	27.6	1.2
160	21.9	0.6
165	25.4	6.5
170	29.8	9.3
175	33.4	11.5
180	29.4	9.7
185	32.2	8.7
190	36.8	9.8
195	28.0	8.2
200	22.7	6.3
205	20.0	4.6
210	20.0	5.2
215	17.5	5.7
220	10.9	4.4
225	15.1	8.5
230	9.9	8.8
235	18.0	7.1
240	16.5	9.6
245	22.4	13.2
250	23.5	12.6
255	25.7	13.6
260	23.0	14.9
265	25.7	10.5
270	21.5	10.4
275	15.6	7.6
280	13.6	3.9
285	9.8	4.8
290	9.0	5.6
295	13.1	4.2
300	10.0	2.5
305	10.0	1.5
310	8.9	-1.4
315	9.0	-1.2

320	7.9	-2.3
325	8.0	-3.9
330	13.0	-2.1
335	9.5	-1.8
340	12.2	-1.3
345	6.5	-1.8
350	11.4	-0.2
355	12.6	-5.5
360	5.7	-1.8
365	13.6	0.4
370	12.0	-1.6
375	6.9	-3.2
380	8.8	-4.4
385	11.7	-4.4
390	11.3	-5.1
395	15.1	-6.5
400	17.3	-7.8
405	17.7	-7.5
410	22.1	-5.9
415	22.3	-6.4
420	24.4	-3.4
425	34.3	-4.5
430	42.8	-3.5
435	56.7	-3.9
440	99.1	-7.8
445	N/A	N/A
450	-69.8	10.4
455	-43.4	0
460	-22.9	-2.7
465	-15.1	-4.2
470	-8.5	-3.3
475	-8.3	-7.3
480	-2.0	-4.6
485	-2.3	-5.0
490	6.3	-7.2
495	6.2	-7.6
500	6.7	-1.1

A Seismic Survey in Virginia City, Montana, to Investigate the Origin of Natural Springs

Prepared By:

Carson Coleman, Constance Fenske, Ngoc Ha, Sierra Luoma, Kaitlyn O'Connell, Jonathan Rice, Jess Scanlan, Kyle Schuerg, Scott Schmitt, Nathan Simons, Jon Szarkowski, Maren Tanberg, Tayler Todd

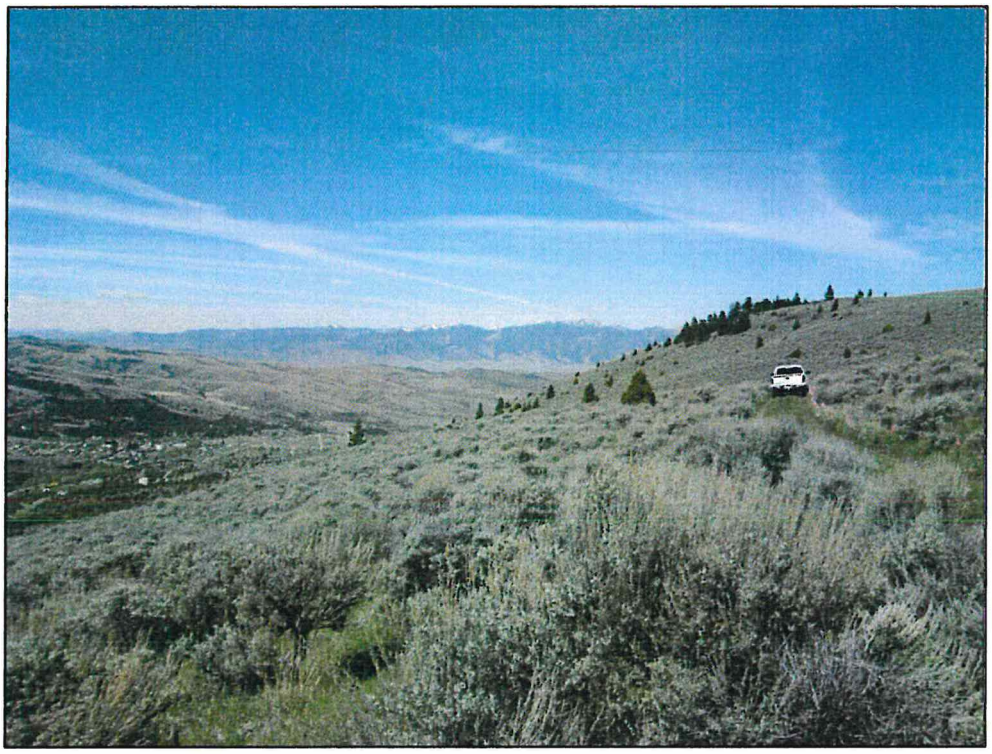

For:

Montana Bureau of Mines and Geology

Under the Supervision of:

Brad Rutherford and Dr. Marvin Speece

Department of Geophysical Engineering
Montana Tech of the University of Montana
Butte, MT 59701

May 22th — 27th, 2017

Executive Summary

A seismic surveys is a method used in determining subsurface geologic feature. We conducted as seismic survey in order to determine the subsurface structures in a landslide area located near Virginia City, Montana. The purpose of this survey was to determine the source of two local springs.

On May 23rd and 24th, 2017, students collected seismic reflection and refraction data near Virginia City. Data collection followed a dirt road to the north-east of Virginia City that crosses landslide material. The seismic survey used a 500 pound accelerated weight drop seismic source mounted on a trailer that was pulled by a truck. The source was dropped four times every two or four meters along the survey route. A streamer of 96 geophones trailed behind the trailer to measure the seismic signal. The signal was then recorded on a computer located in the truck.

From May 25th to May 27th, 2017, the collected field data were processed and analyzed. We interpreted the processed data and concluded that our data lacked sufficient reflections. The refraction data may indicate two listric normal faults and a detachment fault. We could not make definitive conclusions about the spring sources although spring recharge could be related to listric faults nearby.

Table of Contents

List of Figures

List of Tables

Introduction

On the week of May 22nd – 26th, 2017, the geology and geophysical summer course completed a seismic reflection and refraction survey outside Virginia City, Montana. We conducted this survey along a dirt road to the north-east of the city across an old landslide area. Our objective was to find the controlling structures of the nearby springs. Evidence suggests faults are present in this area, and these fault zones might act as conduits to supply recharge to the springs. We used seismic methods to attempt to locate these faults based on the wave's reaction in the subsurface.

Site Description

For this seismic survey, we looked at an area northeast of Virginia City. Virginia City is located in Madison County, Montana, roughly 100 kilometers (60 miles) southeast of Butte, Montana. Virginia City encompasses an area of 608 acres over Sections 22, 23, 24, 26, and 27 in Township 06 South, Row 03 West. Virginia City lies between two mountain ranges, the Tobacco Root Mountains and the Gravelly Range (Figure 1).

We completed the survey along a BLM road starting at 45.304116°N 111.906553°W and ending at 45.301468°N 111.925702°W (Figure 2). The site was designed to span our area of interest but technical difficulties prohibited us from collecting data over the entire pre-determined site area.

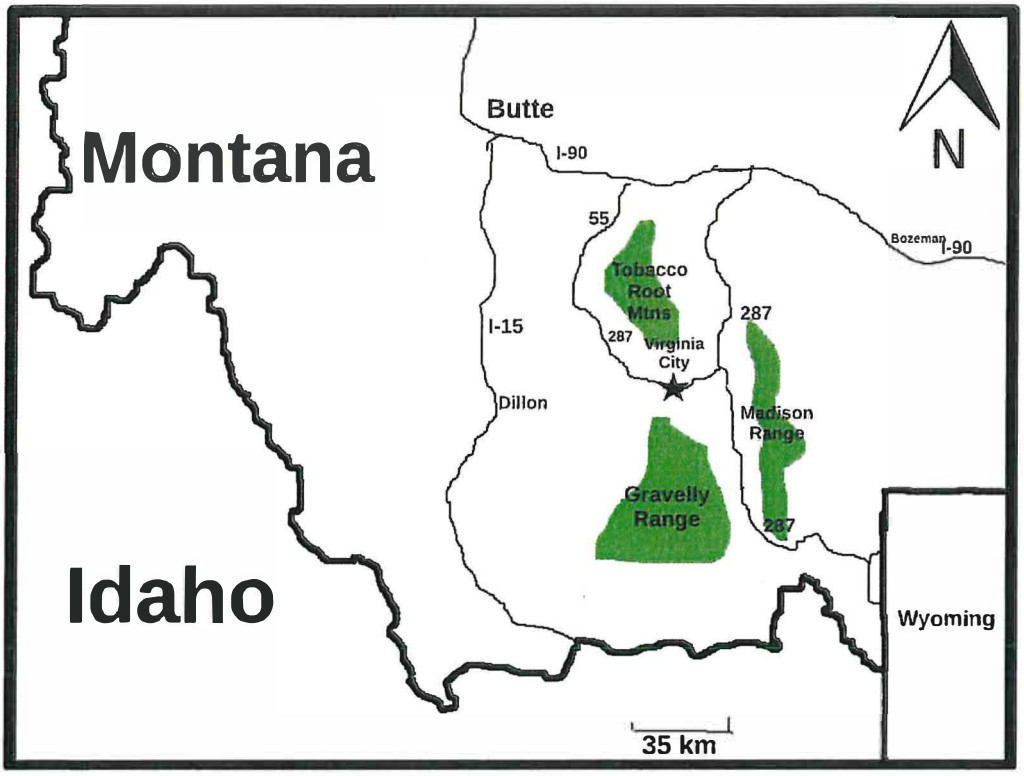

Figure 1. Regional map. Note mountain ranges surrounding Virginia City.

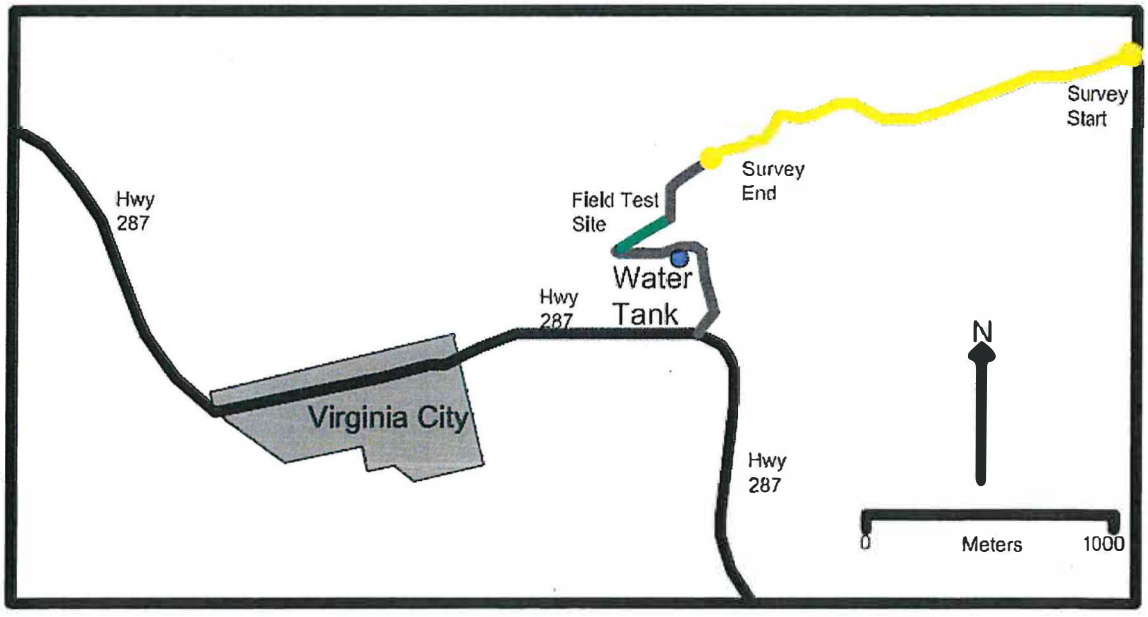

Figure 2. Seismic survey location. The yellow line indicates the path of the survey. The green line shows the location of a test survey done prior to the main survey.

Geologic Setting

The regional geology of Virginia City is dominated by Archean, metamorphic, crystalline basement rocks (Figure 3). These rocks are predominantly gneisses of varying composition from quartzo-feldspathic gneisses to hornblende-plagioclase gneisses and amphibolite. These rock are overlain by a thick sequence (≈ 550 meters) of Paleozoic clastic sediments. The appendix includes a stratigraphic column of Virginia City's regional geology as provided by Ruppel and Liu (2004). The area around Virginia City has been intruded by multiple igneous bodies, including granite pegmatites, mafic diabase dikes, and multiple iterations of basalt and ash flows.

The late protopaleozoic (1.6 Ga) granite pegmatite dikes extend in a northwest-trending belt west of the head of Alder Gulch (Figure 4). Mafic diabase dikes (1.4 Ga) intruded along the western extent of Virginia City along a similar trend. Basalt and ash flows in the northeast region of Virginia City intruded approximately 33 Ma. These basalts are underlain by volcanic ash and tuffs, separated by gravel beds (Ruppel and Liu 2004). Glaciation and erosion during the Quaternary period produced two units of sediments: the Pleistocene moraine and Holocene alluvium. The Pleistocene moraine consists of Tertiary basalt, Paleozoic limestone, and Archean basement rock. The Holocene alluvium consists of moderately well-rounded pebbles to boulders of Archean basement rocks. The matrix is a sand or silt. Due to dredge tailings, this unit is largely disturbed (Despotovic 2000).

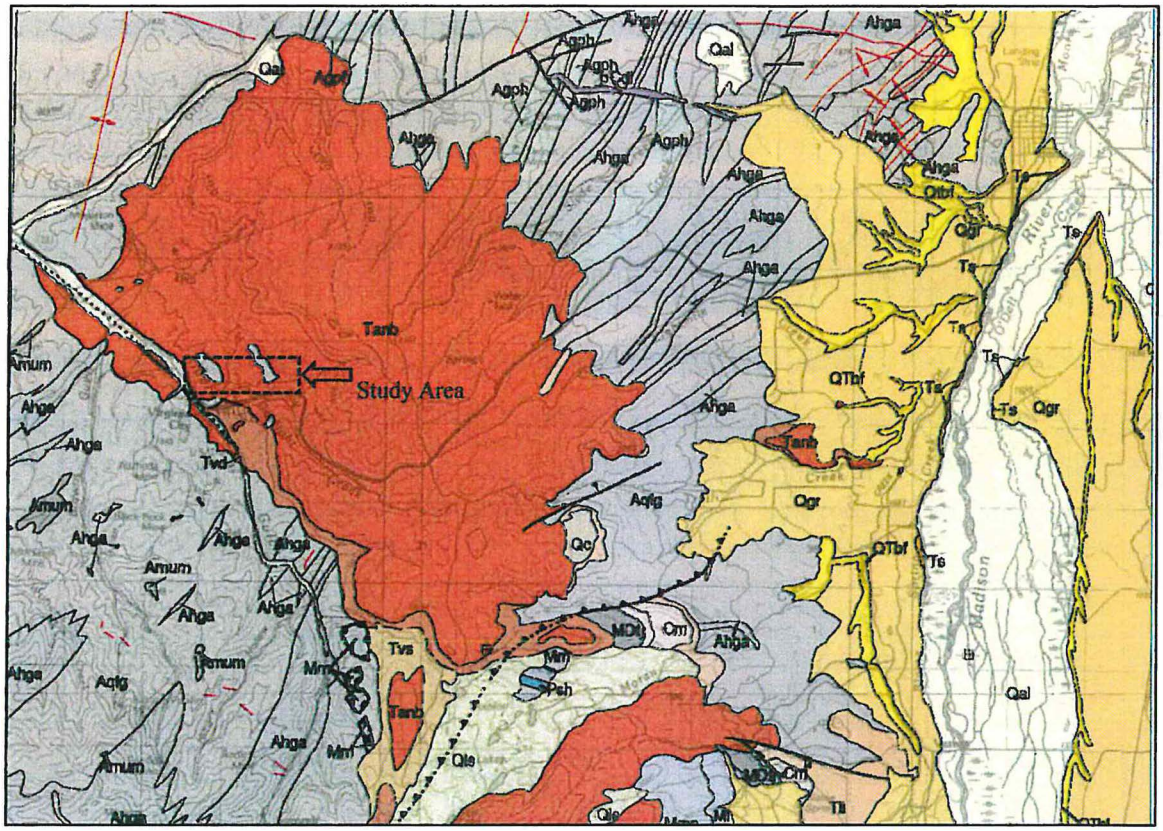

Figure 3. Geologic map containing our study area. A legend can be found in the appendices (Kellog and Williams 2006).

Regional Faults and Tectonics

The tectonics of the region trend to the northwest, along the Virginia City fault zone. Ruppel and Liu (2004) have observed that the older metamorphic rocks tend to be displaced by a left-lateral strike-slip fault. This fault could be the point where the lava field erupted. Evidence also suggests that left-lateral displacement is also observed across other fault zones. Figure 4 shows the faulting around the Virginia City area (Ruppel & Liu, 2004).

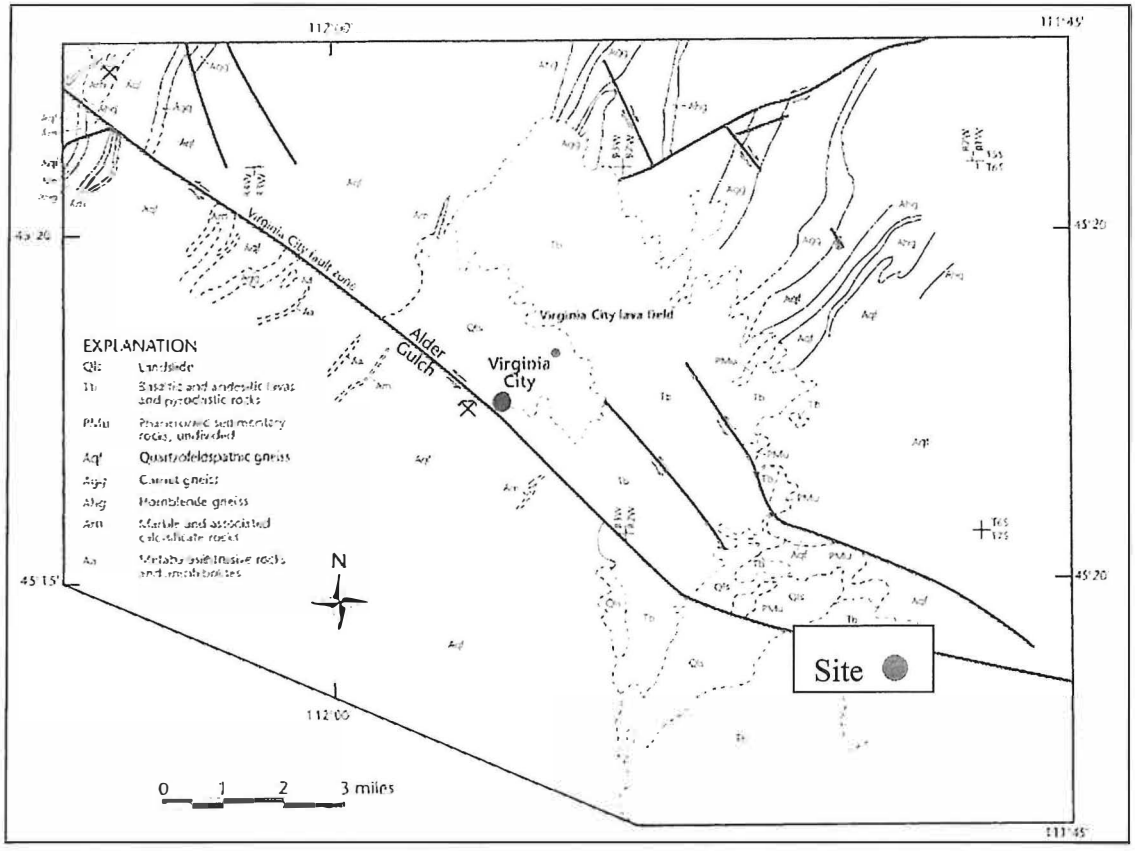

Figure 4. Apparent left-lateral displacements across the Virginia City fault zone. Geology modified from Vitaliano and Cordua, 1979; Weir, 1982; and Hadley, 1969. Geology partly remapped by Ruppel, 1985.

Recent electrical resistivity studies interpreted a normal fault (possibly oblique) at the site of two springs near the area of study. In addition, a listric fault and associated detachment faults were inferred using very low frequency electromagnetic methods. These faults were detected with low resistivity values, indicating that the faults in the area facilitate groundwater flow (Coleman, et al. 2017). Andrew Bobst (Pers. Com., 2017) speculates that these saturated faults allowed the two springs in the study area to surface. Figure 5 shows the likely location of these faults.

Figure 5. Google Earth topographic map. Interpreted faults are dashed in yellow. (Google Inc. 2015)

Seismic Theory

Seismic surveys use the principles of refracted and reflected waves to help determine subsurface lithology. In order to create seismic waves, an explosive charge or mechanical impacting device is used. A string of geophones is laid out in one direction from the seismic source. P- and S-waves radiate from the seismic source, interacting with the subsurface through a combination of reflection and refraction. P-waves travel is longitudinal, meaning that molecules move in the direction of wave propagation. S-waves use a material's shear properties to travel by moving molecules perpendicular to wave propagation. Waves that arrive back to the ground surface are picked up by geophones, which convert the waves' mechanical energy into an electrical signal. A computer records that electrical signal.

When processing seismic data with refraction methods, the first arriving energy (first-breaks) are the primary focus. Ideally, seismic velocity increases as the depth and rock density increases. The increase in seismic velocity causes the seismic energy to refract, or

bend, back toward the surface to create a diving wave. If a first-order discontinuity is encountered, such as one created by the water table, then a critically refracted head wave is created. These head waves can overtake the direct wave that travels along the ground surface because the head waves travel at the velocity of the underlying medium (Figure 6). Diving waves and head waves can be used to provide a subsurface image.

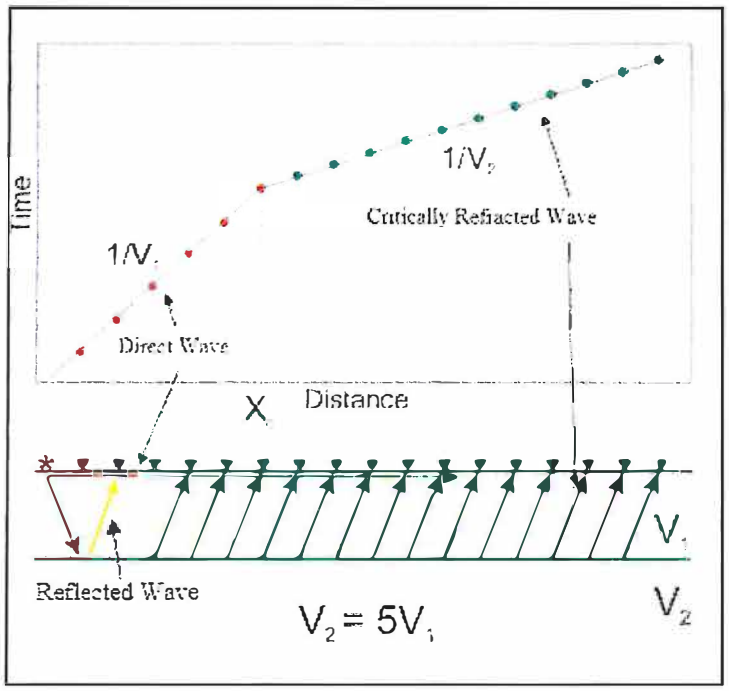

Figure 6. Schematic diagram showing direct wave, reflection, and critically refracted head wave (Geometrics 2017). The green arrows are the critically refracted waves (head waves), and the red arrow along the ground surface is the direct wave.

In addition to refractions, reflections can also provide a subsurface image. Reflections occur at all boundaries of contrasting seismic velocity and/or density. Figure 7 shows reflected waves passing through three layers; when velocity changes abruptly, waves are reflected back to the surface and recorded by geophones.

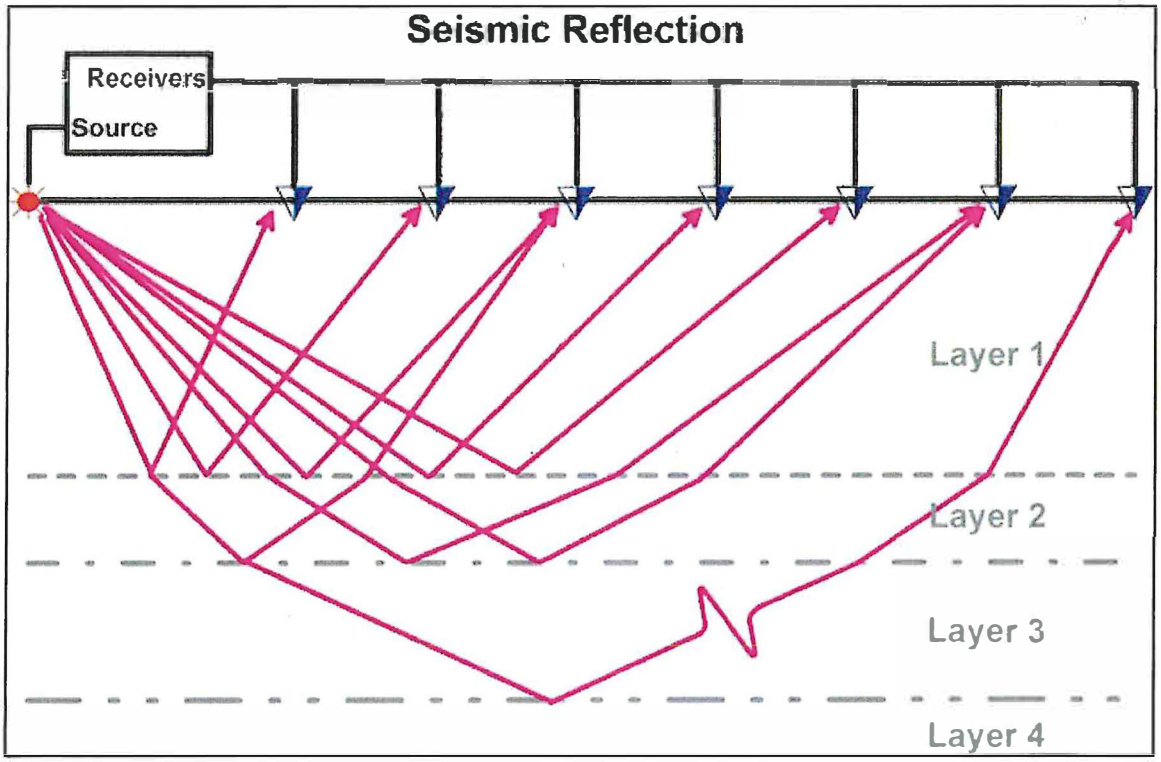

Figure 7. Seismic waves are reflected off the contacts between layers (Envioscan Inc. 2017).

After analyzing the raw geophone data, a geological interpretation is created based on observed layer velocities. Table 1 shows the P- and S-wave velocities of various rock types in our region (National Renewable Energy Laboratory, 2013).

Table 1. Comparative table of P and S wave velocities modified from National Renewable Energy Laboratory(2013).

Type of Formation	P-Wave Velocity (m/s)	S-Wave Velocity (m/s)	Density (g/cm^3)
Scree, vegetal soil	300-700	100-300	1.7-2.4
Dry sands	400-1200	100-500	1.5-1.7
Wet sands	1500-2000	400-600	1.9-2.1
Saturated shales and clays	1100-2500	200-800	2.0-2.4
Limestones	3500-6000	2000-3300	2.4-2.7
Granite	4500-6000	2500-3300	2.5-2.7
Basalt	5000-6000	2800-3400	2.7-3.1
Gneiss	4400-5200	2700-3200	2.5-2.7
Water	1450-1500	-	1.0

In this project, we used the diving-wave (DW) tomography method to construct near-surface velocity models. DW tomography requires the use of numerous shot points along a profile to maximize the number of wave paths in the subsurface. This method is more sensitive to near-surface lateral variations in velocity than a conventional refraction survey (Speece, et al. 2003). The inversion technique is Wavepath Eikonal Traveltime (WET) inversion. The algorithm for WET inversion is shown below:

1) Pick first-arrival travel times from the seismograms.
2) An initial slowness model is proposed and forward modeled by solving the Eikonal equation using a finite-difference method.

$$\left(\frac{\partial T}{\partial x}\right)^2 + \left(\frac{\partial T}{\partial z}\right)^2 = s(x,z)^2 \quad (1)$$

where T is travel time and s is slowness (inverse velocity)

3) Travel time residual is computed by subtracting the observed first-arrival travel times from finite-difference travel times.
4) Travel time residual is back-projected along the wavepath.
5) The slowness model is updated and these steps are iteratively repeated until a sufficiently small RMS error is achieved.

(Schuster and Quintus-Bosz 1993)

Field Methodology

Seismic Field Procedure

We employed a 96-channel gimbaled geophone landstreamer, with 2-m geophone spacing that decreased the time necessary to mobilize and move receiver spreads. A 227 kg (500 lb) accelerated weighted drop seismic source was used to create the seismic signal. The weight was assisted by a rubber band (Figure 8). The weight was raised by a hydraulic lift and then released to fall and strike a metal plate on the ground. The recording of each plate strike by the weight is called a shot record.

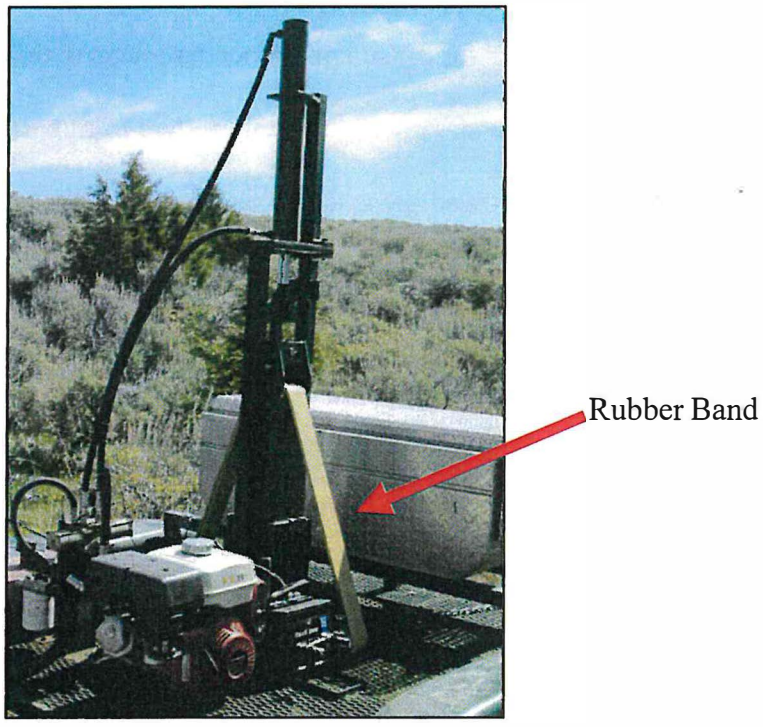

Figure 8. Weight drop with rubber band.

Figure 9 shows a seismic survey schematic. We recorded shots every station for first 304 m of the survey. Due to time constraints, we collected shots at every other station starting at 306 m.

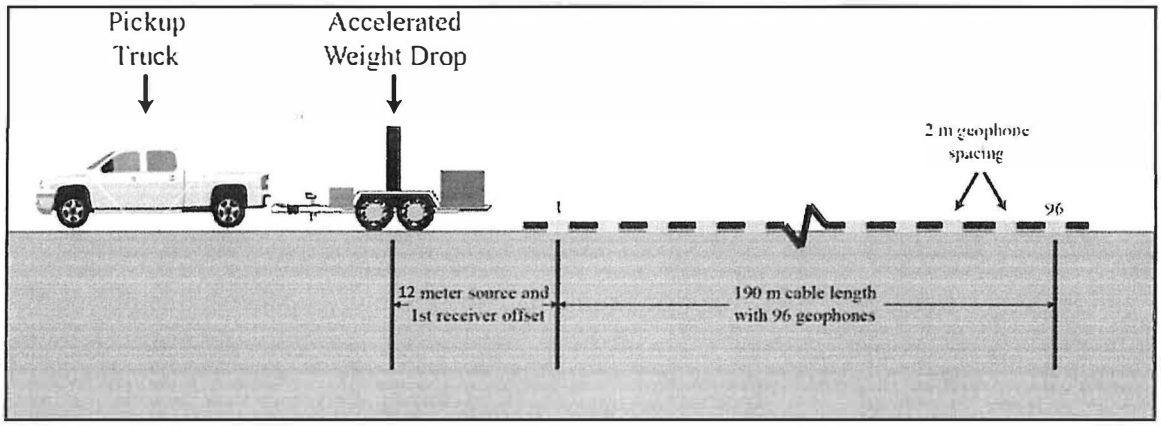

Figure 9. Seismic survey schematic (Ayers, et al. 2016).

The distance between the source and the first geophone was 12 meters. Table 2 details the field-recorded parameters for the seismic procedure. Due to the length of the landstreamer, students trailed along the streamer and set up rollers to move the streamer around curves in the road. Students followed the truck to spot the streamer and keep noise at a minimum along the survey area.

Table 2. Field parameters for the seismic survey.

Seismic Field Parameters	
Source	227 kg (500 lb) Weight Drop
Stations	856
Number of Geophones	96
Geophone Spacing	2 m
Source Offset	12 m
Shots per Station	4
Record Length	2 s
Sampling Interval	0.5 ms

After the weight struck the plate, seismic reflections and refractions were picked up by the geophones. The electrical signal was in turn recorded on a computer, located in the truck.

Three people were in the truck: a driver, a seismic observer who monitored waves and saved data files (Figure 10), and a note taker. The driver advanced the truck to each new source location. The data collector kept track of the locations of the source, first and last geophones, and field file number for the data collected at each station.

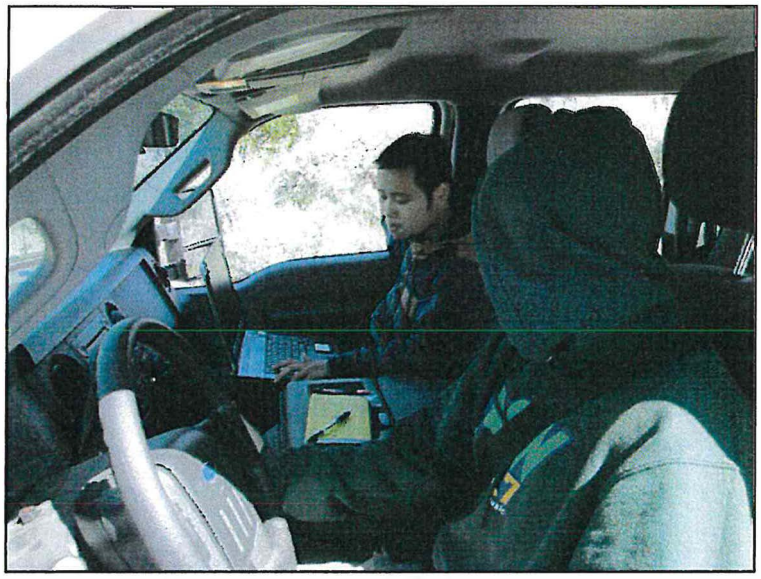

Figure 10. The driver and seismic observer.

GPS Survey

A Leica GPS (global positioning system) works by receiving signals from satellites and calculating the distance from the satellites to the receivers. Trilateration then determines the location of the GPS. The system must receive signals from at least four different satellites in order to pinpoint its location.

Our GPS survey used a Leica GPS to determine the latitude, longitude, and elevation of each station. The GPS survey defines the geometry to assist the creation of a cross section of the subsurface seismic survey.

We used real-time kinematic (RTK) to determine the position of each survey point. RTK involves a stationary reference receiver (base station) and one moving receiver (rover). The

base station receives signals from satellites and creates a correction factor. The base station then sends the correction factor via Bluetooth to the rover. The rover receives signals from the satellites and incorporates the correction factor to calculate the coordinates of the rover's position. Figure 11 shows one student using the rover in the field and Figure 2 shows the positions of the survey lines, determined by the GPS system.

Figure 11. The GPS rover.

Data Processing

Refraction Processing

We uploaded the raw data to Vista seismic processing software and used the GPS station coordinates to define the geometry of the survey. We performed a few initial processing steps including trace balancing and deconvolution to improve the coherency of the first breaks. Then we picked the first breaks.

After first break picking, we prepared an ASCII file containing first break data with information about locations and elevations of shots and receivers. We imported the ASCII

file to Rayfract diving wave inversion software, and we performed a WET inversion with 20 iterations to obtain a velocity profile of the subsurface.

Reflection Processing

Figure 12 shows the processing sequence for brute stacking, performed in Vista. We did not see coherent reflectors in the subsurface so the processing sequence was kept to a minimum number of steps to see if faint reflections could create an image.

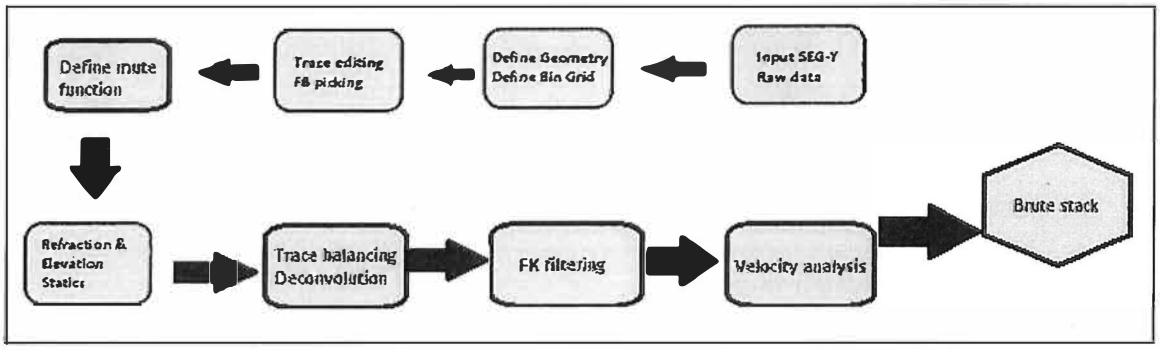

Figure 12. Processing sequence for brute stack.

Results

The refraction data (Figure 13) shows a low velocity area occurs at shot 251. This low velocity zone is along the projection of a fault scarp. We interpret the low velocity zone to be a listric normal fault. Another low velocity zone at shot 380 might indicate an additional listric fault. Figure 14 shows a highly speculative west-east profile of that includes the two faults.

Figure 16 shows our normal incident seismic reflection profile from this survey. Figure 16 shows a field test that we completed prior to our main seismic survey. These test data show strong reflections in the area under which the test survey was conducted

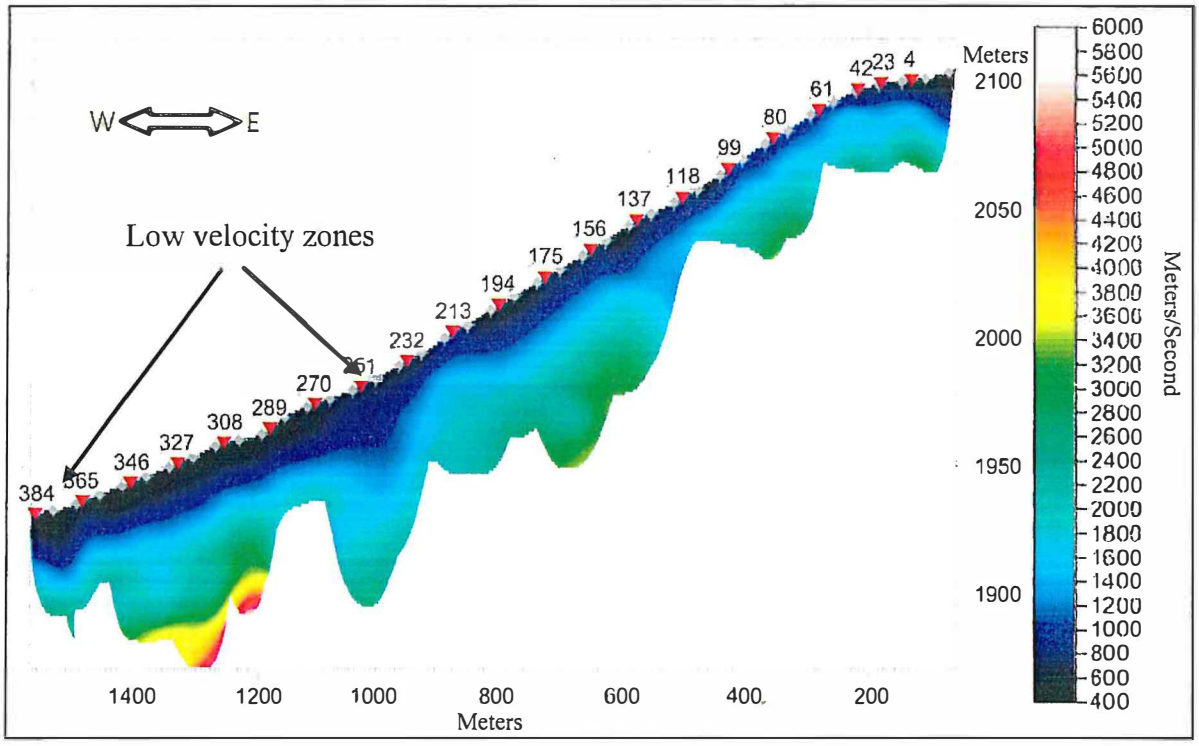

Figure 13. Diving wave tomography velocity model.

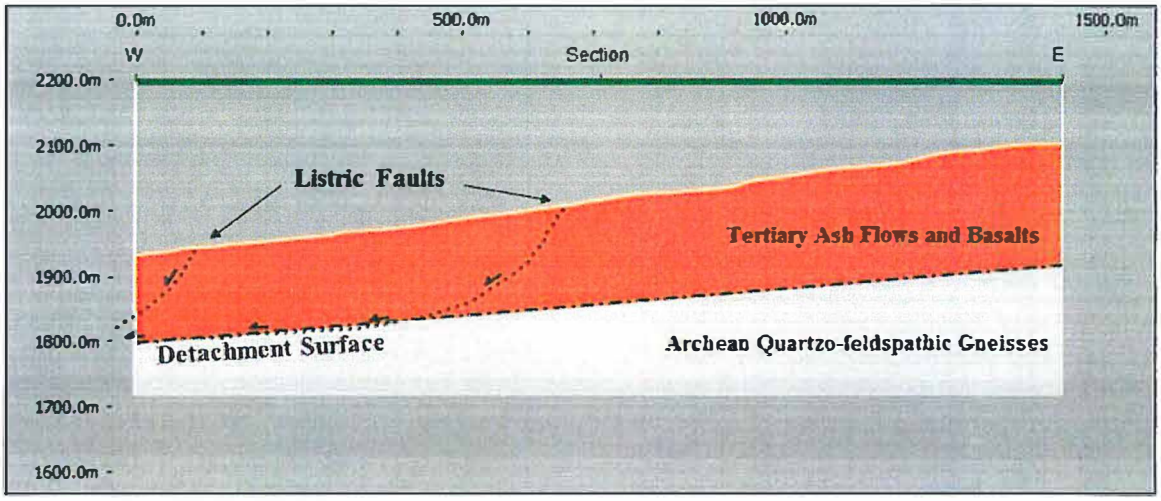

Figure 14. Cross section oriented east-west. Tertiary ash flows and basalts are shown in orange, and Archean Quartzo-feldspathic gneisses are shown in gray.

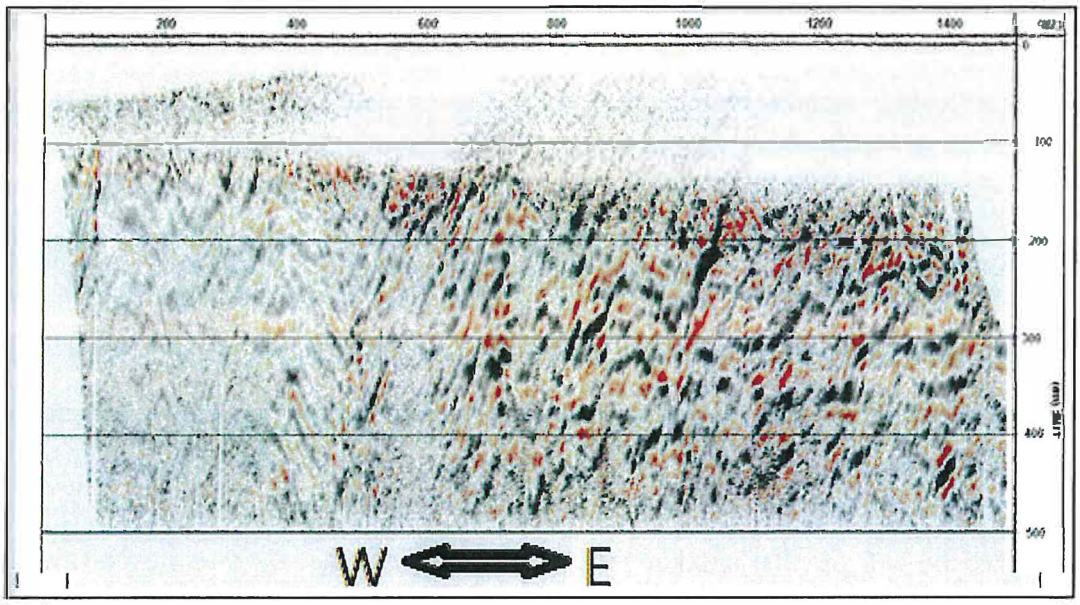

Figure 15. Normal incident reflection section. This profile shows mostly noise.

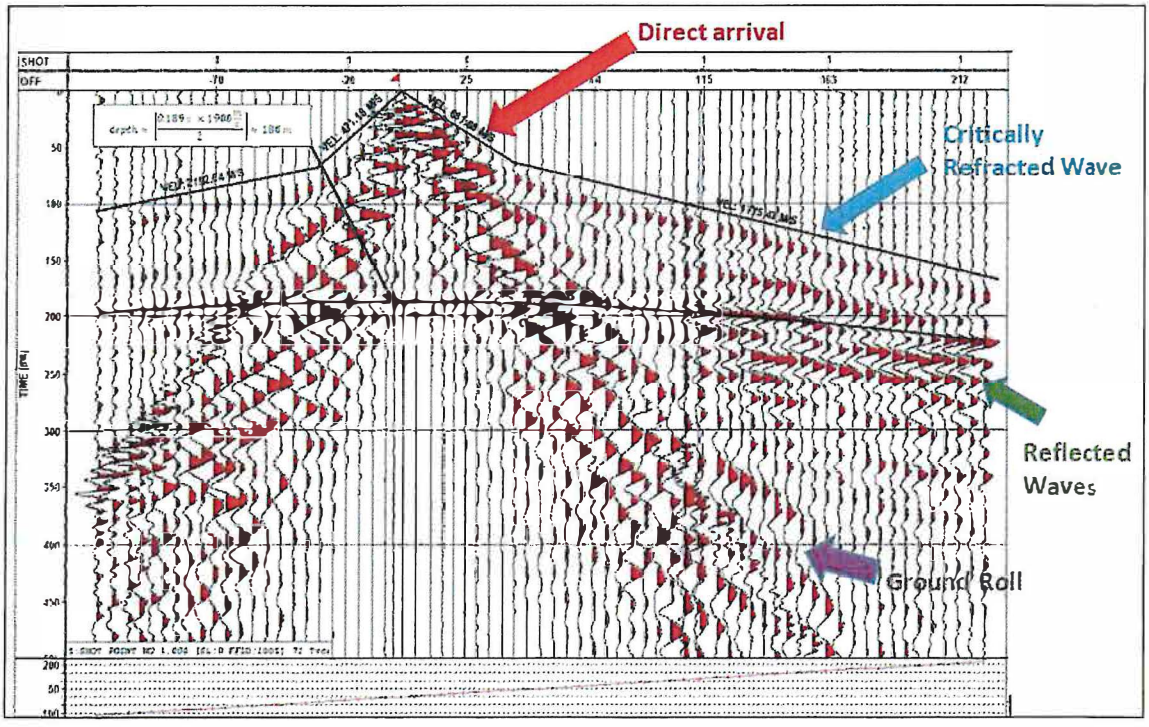

Figure 16. Field Test using 227 kg (500 lb) weight drop. See Figure 2 for location of this test survey.

(Figure 2). We estimate the depth to this reflector to be ~180 m. From the depth and high amplitude of this reflector, we speculate that this reflection occurs because of the hard and seismically fast basement. The basement rock might serve as the surface for a detachment that the listric faults sole into. Unfortunately, due to catastrophic cable failure

our seismic survey did not extend to the test site (Figure 2). As a consequence, our seismic reflection section (Figure 15) does not show a useful image because the survey did not progress far enough to obtain strong basement reflections.

The faults are regions where weathering and brecciation of the country rock occur. This processes create porosity and permeability along the fault surfaces, allowing groundwater to flow. While these two faults may facilitate groundwater flow, they do not appear to outcrop near the two springs. However, pressure ridges in surface topography beyond the area surveyed suggest that another set of listric faults to the southwest exist (Figure 5). These proposed faults would outcrop near one of the springs, and could explain groundwater recharge to the site.

Conclusions

Our target survey length was 2,266 meters; however, due to equipment failure we were only able to survey 1,766 meters. The refraction data shows two possible listric normal faults. A test seismic survey found a potential detachment fault surface at ~180 meters below ground. Unfortunately, reflections are lacking in our data from the main seismic survey and we could not build a detailed image of the subsurface. Groundwater might flow through fractured fault zones. Overall, we were unable to make any definitive conclusions about the sources of the groundwater springs.

References

Ayers, M., Beall, D., Callaghan, M., Clausen, C., Koerner, A., Krupla, B., McCormick, M., et al. 2016, Seismic Survey of the Bedrock in the Vicinity of Lolo Creek: Montana Tech, unpublished report.

Coleman, C., Fenske, C., Ha, N., Luoma, S., O'Connell, K., Rice, J., Scanlan, J., et al. 2017, 2D Electrical Resistivity Tomography and VLF-EM Survey in Virginia City, Montana: Montana Tech, unpublished report.

Despotovic, Pero, 2000, Geology and Geochemistry of Au-Ag-Mineralizations in the Virginia City Mining District (VCMD), Montana, U.S.A.: Technische Universität, Berlin.

Envioscan Inc, 2017, Seismic Shear Wave Studies: Accessed May 25, 2017, http://www.enviroscan.com/home/seismic-shear-wave-studies.

Geometrics, 2017, Seismic Refraction: Accessed May 25, 2017, http://www.geometrics.com/applications/frequency-asked-questions/seismic-refraction/.

Google Inc. 2015, Google Earth. December 15: Accessed May 27, 2017. http://Earth.google.com.

Kellog, Karl S, and Van S Williams. 2006. Geologic Map of Ennis 30' x 60' Quadrangle Madison and Gallatin Counties, Montana, and Park County, Wyoming: Montana Bureau of Mines and Geology.

National Renewable Energy Laboratory, 2013, Seismic Techniques. http://en.openei.org/wiki/Seismic_Techniques.

Ruppel, Edward T, and Yuguang Liu. 2004, The Gold Mines of the Virginia City Mining District, Madison County, Montana: Montana Bureau of Mines and Geology Bulletin 133.

Schuster, Gerard T., and Aksel Quintus-Bosz. 1993, Wavepath eikonal traveltime inversion: Theory: Geophysics, **58,** 1314-1323.

Speece, Marvin A., Carlyle R. Miller, Abdel-Khalek El-Werr, and Curtis A. Link, 2003, Land streamer aided, seismic diving wave tomography at an archaeological site, Saqqara, Egyp.: Technical Program Expanded Abstracts, SEG, 1255-1258.

Appendices

Appendix A: Stratigraphic Column

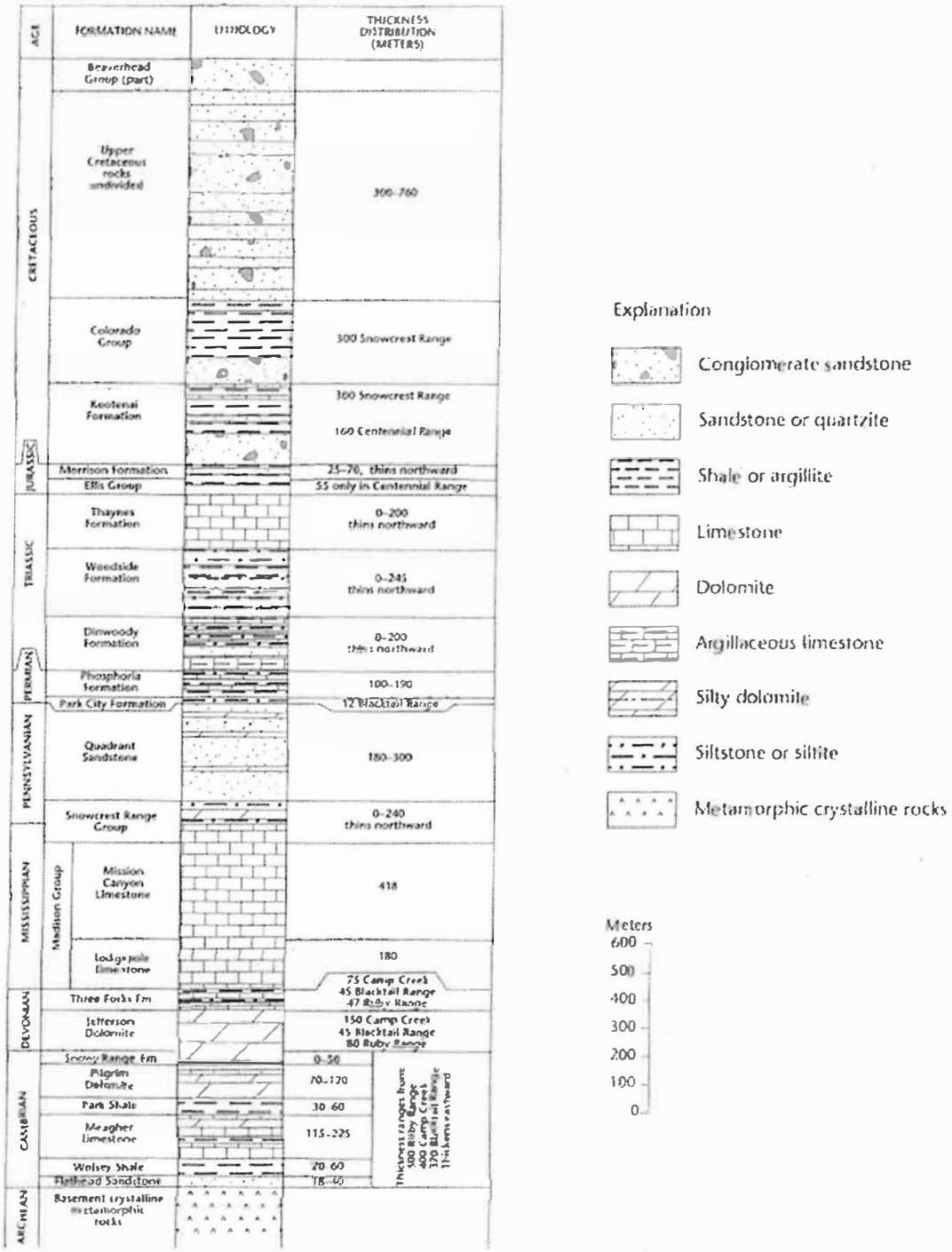

Appendix B: Legend for Geologic Map (Figure 3)

Appendix C: GPS Data

Station	Northing	Easting	Elevation [m]
1	428928.697	5017134.534	2117.422
2	428926.885	5017133.733	2117.349
3	428925.057	5017132.896	2117.267
4	428923.221	5017132.124	2117.225
5	428921.471	5017131.263	2117.058
6	428919.588	5017130.480	2116.922
7	428917.853	5017129.550	2116.778
8	428915.970	5017128.742	2116.590
9	428914.282	5017127.877	2116.490
10	428912.530	5017126.853	2116.324
11	428910.710	5017126.066	2116.182
12	428908.912	5017125.146	2116.009
13	428907.199	5017124.118	2115.879
14	428905.416	5017123.183	2115.748
15	428903.581	5017122.467	2115.652
16	428901.915	5017121.436	2115.479
17	428900.088	5017120.720	2115.372
18	428898.328	5017119.686	2115.159
19	428896.584	5017118.733	2114.977
20	428894.842	5017117.918	2114.839
21	428892.954	5017117.324	2114.788
22	428891.211	5017116.378	2114.550
23	428889.351	5017115.573	2114.382
24	428887.509	5017114.930	2114.268
25	428885.658	5017114.183	2114.085
26	428883.845	5017113.317	2113.903
27	428882.002	5017112.576	2113.711
28	428880.106	5017112.024	2113.618
29	428878.280	5017111.404	2113.450
30	428876.468	5017110.639	2113.286
31	428874.694	5017109.787	2113.045
32	428872.682	5017109.326	2112.961
33	428870.879	5017108.636	2112.802
34	428868.967	5017108.061	2112.642
35	428867.101	5017107.400	2112.460
36	428865.279	5017106.433	2112.242
37	428863.304	5017105.771	2112.094
38	428861.501	5017105.183	2111.925

39	428859.589	5017104.558	2111.879
40	428857.770	5017103.846	2111.670
41	428855.842	5017103.257	2111.581
42	428853.946	5017102.697	2111.446
43	428851.986	5017102.005	2111.273
44	428850.114	5017101.488	2111.198
45	428848.187	5017100.910	2111.067
46	428846.275	5017100.332	2110.981
47	428844.551	5017099.761	2110.843
48	428842.671	5017099.188	2110.716
49	428840.767	5017098.615	2110.498
50	428838.863	5017098.032	2110.311
51	428836.905	5017097.569	2110.085
52	428834.979	5017097.109	2109.897
53	428833.022	5017096.703	2109.546
54	428831.081	5017096.325	2109.300
55	428829.164	5017095.946	2109.050
56	428827.193	5017095.657	2108.821
57	428825.206	5017095.432	2108.541
58	428823.205	5017095.249	2108.271
59	428821.263	5017094.812	2107.879
60	428819.301	5017094.619	2107.573
61	428817.308	5017094.481	2107.317
62	428815.408	5017094.287	2106.998
63	428813.392	5017094.217	2106.676
64	428811.454	5017094.082	2106.381
65	428809.493	5017093.987	2106.066
66	428807.501	5017093.916	2105.860
67	428805.517	5017093.884	2105.517
68	428803.461	5017093.804	2105.194
69	428801.571	5017093.741	2104.978
70	428799.555	5017093.693	2104.713
71	428797.571	5017093.594	2104.517
72	428795.594	5017093.533	2104.260
73	428793.602	5017093.496	2104.092
74	428791.588	5017093.573	2103.938
75	428789.599	5017093.788	2103.779
76	428787.633	5017094.004	2103.636
77	428785.590	5017094.329	2103.521
78	428783.696	5017094.562	2103.380
79	428781.692	5017094.898	2103.249

80	428779.710	5017095.085	2103.048
81	428777.865	5017095.499	2102.940
82	428775.839	5017095.906	2102.894
83	428773.819	5017096.178	2102.605
84	428771.887	5017096.645	2102.637
85	428769.920	5017096.755	2102.307
86	428767.893	5017097.088	2102.209
87	428765.992	5017097.425	2102.067
88	428763.964	5017097.634	2101.828
89	428761.991	5017097.960	2101.758
90	428760.083	5017098.421	2101.654
91	428758.121	5017098.881	2101.655
92	428756.322	5017099.349	2101.519
93	428754.321	5017099.878	2101.573
94	428752.467	5017100.273	2101.422
95	428750.457	5017100.687	2101.433
96	428748.439	5017101.146	2101.411
97	428746.476	5017101.534	2101.268
98	428744.504	5017101.913	2101.183
99	428742.538	5017102.089	2101.088
100	428740.629	5017102.441	2101.042
101	428738.710	5017102.639	2100.943
102	428736.713	5017102.867	2100.869
103	428734.818	5017103.035	2100.793
104	428732.751	5017103.290	2100.744
105	428730.779	5017103.704	2100.731
106	428728.854	5017103.970	2100.694
107	428726.858	5017104.343	2100.593
108	428724.870	5017104.591	2100.589
109	428722.954	5017105.080	2100.576
110	428720.952	5017105.510	2100.564
111	428719.028	5017105.926	2100.425
112	428717.073	5017106.387	2100.393
113	428715.119	5017106.935	2100.380
114	428713.172	5017107.434	2100.345
115	428711.296	5017107.951	2100.311
116	428709.342	5017108.479	2100.281
117	428707.435	5017109.087	2100.300
118	428705.505	5017109.605	2100.256
119	428703.598	5017110.191	2100.220
120	428701.730	5017110.726	2100.185

121	428699.815	5017111.251	2100.163
122	428697.838	5017111.805	2100.155
123	428696.168	5017112.561	2100.186
124	428694.041	5017113.024	2100.124
125	428692.158	5017113.621	2100.063
126	428690.276	5017114.279	2100.000
127	428688.419	5017115.069	2099.968
128	428686.526	5017115.488	2099.829
129	428684.698	5017116.137	2099.696
130	428682.850	5017116.974	2099.654
131	428680.945	5017117.704	2099.488
132	428679.102	5017118.364	2099.376
133	428677.210	5017118.862	2099.155
134	428675.384	5017119.674	2099.091
135	428673.541	5017120.311	2098.912
136	428671.674	5017120.938	2098.789
137	428669.807	5017121.562	2098.638
138	428667.840	5017122.295	2098.520
139	428665.862	5017122.845	2098.343
140	428663.982	5017123.631	2098.301
141	428662.144	5017124.066	2098.115
142	428660.207	5017124.706	2097.992
143	428658.293	5017125.376	2097.833
144	428656.441	5017125.921	2097.737
145	428654.409	5017126.478	2097.551
146	428652.783	5017126.925	2097.427
147	428650.844	5017127.448	2097.348
148	428648.913	5017127.872	2097.170
149	428647.016	5017128.617	2097.162
150	428645.060	5017129.053	2096.987
151	428643.144	5017129.465	2096.839
152	428641.219	5017129.805	2096.666
153	428639.281	5017130.353	2096.560
154	428637.349	5017130.825	2096.328
155	428635.323	5017131.175	2096.044
156	428633.310	5017131.395	2095.806
157	428631.400	5017131.703	2095.629
158	428629.545	5017132.002	2095.424
159	428627.515	5017132.017	2095.104
160	428625.554	5017132.611	2094.916
161	428623.564	5017132.767	2094.662

162	428621.716	5017133.019	2094.486
163	428619.633	5017133.221	2094.132
164	428617.727	5017133.134	2093.745
165	428615.659	5017133.320	2093.574
166	428613.796	5017133.576	2093.485
167	428611.688	5017133.703	2093.175
168	428609.830	5017133.713	2092.962
169	428607.776	5017133.742	2092.635
170	428605.827	5017134.019	2092.491
171	428603.842	5017133.957	2092.163
172	428601.994	5017134.112	2091.935
173	428599.907	5017133.999	2091.588
174	428598.079	5017133.934	2091.324
175	428595.962	5017133.964	2091.070
176	428593.941	5017134.120	2090.933
177	428591.940	5017134.000	2090.599
178	428590.059	5017134.009	2090.363
179	428588.065	5017133.811	2090.066
180	428586.141	5017133.549	2089.745
181	428584.181	5017133.591	2089.489
182	428582.109	5017133.336	2089.111
183	428579.996	5017133.075	2088.785
184	428578.246	5017132.913	2088.574
185	428576.338	5017132.633	2088.268
186	428574.272	5017132.355	2088.041
187	428572.434	5017132.047	2087.858
188	428570.461	5017131.578	2087.570
189	428568.521	5017131.295	2087.409
190	428566.517	5017130.923	2086.986
191	428564.417	5017130.328	2086.741
192	428562.803	5017129.680	2086.475
193	428560.913	5017128.957	2086.127
194	428559.093	5017128.223	2085.775
195	428557.343	5017127.396	2085.383
196	428555.354	5017126.897	2085.226
197	428553.759	5017125.955	2084.780
198	428551.908	5017125.173	2084.428
199	428550.057	5017124.415	2084.172
200	428548.664	5017123.958	2083.977
201	428546.799	5017123.346	2083.787
202	428544.907	5017122.445	2083.324

203	428543.257	5017121.505	2083.108
204	428541.427	5017120.479	2082.677
205	428539.740	5017119.699	2082.392
206	428538.183	5017118.584	2081.961
207	428536.402	5017117.824	2081.749
208	428534.528	5017117.095	2081.480
209	428532.737	5017116.145	2081.109
210	428530.979	5017115.260	2080.836
211	428529.266	5017114.291	2080.637
212	428527.507	5017113.322	2080.319
213	428525.763	5017112.343	2080.014
214	428524.026	5017111.336	2079.739
215	428522.066	5017110.598	2079.514
216	428520.548	5017109.521	2079.189
217	428518.768	5017108.766	2079.000
218	428517.048	5017107.891	2078.663
219	428515.288	5017106.806	2078.389
220	428513.576	5017105.885	2078.163
221	428511.857	5017105.074	2077.941
222	428509.989	5017104.210	2077.680
223	428508.199	5017103.267	2077.377
224	428506.594	5017102.126	2077.046
225	428504.713	5017101.473	2076.815
226	428502.977	5017100.492	2076.568
227	428501.107	5017099.474	2076.198
228	428499.301	5017098.580	2075.898
229	428497.680	5017097.999	2075.709
230	428495.838	5017097.362	2075.374
231	428493.939	5017096.600	2075.075
232	428492.189	5017095.700	2074.685
233	428490.410	5017095.145	2074.443
234	428488.419	5017094.479	2074.176
235	428486.646	5017093.682	2073.796
236	428484.797	5017093.097	2073.564
237	428482.847	5017092.663	2073.327
238	428480.951	5017092.108	2072.957
239	428479.093	5017091.454	2072.574
240	428477.115	5017091.229	2072.401
241	428475.195	5017090.653	2071.898
242	428473.317	5017090.267	2071.624
243	428471.490	5017089.609	2071.027

244	428469.509	5017089.153	2070.741
245	428467.644	5017088.552	2070.388
246	428465.901	5017088.274	2070.200
247	428463.909	5017087.582	2069.772
248	428462.085	5017087.179	2069.529
249	428460.089	5017086.743	2069.179
250	428458.188	5017086.433	2068.930
251	428456.316	5017085.954	2068.544
252	428454.366	5017085.410	2068.123
253	428452.402	5017085.060	2067.893
254	428450.529	5017084.468	2067.493
255	428448.643	5017084.094	2067.197
256	428446.626	5017083.929	2066.980
257	428444.713	5017083.274	2066.648
258	428442.889	5017082.879	2066.254
259	428440.972	5017082.487	2065.892
260	428439.030	5017081.989	2065.561
261	428436.997	5017081.789	2065.303
262	428435.119	5017081.450	2065.016
263	428433.192	5017080.972	2064.612
264	428431.314	5017080.588	2064.276
265	428429.325	5017080.144	2063.941
266	428427.408	5017079.802	2063.635
267	428425.495	5017079.117	2063.278
268	428423.564	5017078.881	2063.066
269	428421.706	5017078.256	2062.779
270	428419.756	5017077.769	2062.451
271	428417.908	5017077.282	2062.138
272	428415.997	5017076.799	2061.934
273	428414.054	5017076.261	2061.638
274	428412.095	5017075.625	2061.398
275	428410.369	5017074.863	2061.026
276	428408.448	5017074.142	2060.631
277	428406.639	5017073.656	2060.341
278	428404.697	5017073.189	2059.949
279	428402.778	5017072.707	2059.686
280	428400.935	5017071.959	2059.323
281	428399.023	5017071.367	2059.060
282	428397.081	5017070.912	2058.753
283	428395.232	5017070.321	2058.508
284	428393.389	5017069.633	2058.157

285	428391.515	5017068.914	2057.953
286	428389.603	5017068.315	2057.866
287	428387.839	5017067.670	2057.526
288	428385.919	5017067.013	2057.286
289	428384.139	5017066.354	2057.070
290	428382.210	5017065.604	2056.725
291	428380.411	5017064.598	2056.273
292	428378.708	5017063.772	2055.974
293	428376.785	5017062.932	2055.700
294	428375.109	5017062.368	2055.504
295	428373.185	5017061.476	2055.251
296	428371.459	5017060.638	2055.057
297	428369.622	5017059.786	2054.820
298	428367.826	5017059.012	2054.601
299	428365.997	5017058.218	2054.290
300	428364.365	5017057.361	2054.029
301	428362.606	5017056.449	2053.800
302	428360.674	5017055.461	2053.555
303	428359.058	5017054.729	2053.403
304	428357.244	5017053.811	2053.069
305	428355.399	5017052.906	2052.747
306	428353.578	5017052.008	2052.435
307	428351.930	5017051.215	2052.152
308	428350.148	5017050.355	2051.930
309	428348.335	5017049.514	2051.792
310	428346.421	5017048.679	2051.578
311	428344.718	5017047.896	2051.385
312	428342.791	5017047.324	2051.012
313	428340.972	5017046.700	2050.789
314	428338.959	5017046.192	2050.608
315	428337.147	5017045.397	2050.425
316	428335.242	5017044.794	2050.274
317	428333.300	5017044.274	2050.111
318	428331.397	5017043.796	2049.935
319	428329.546	5017043.068	2049.640
320	428327.718	5017042.313	2049.436
321	428325.799	5017041.752	2049.254
322	428323.987	5017040.971	2048.993
323	428322.068	5017040.458	2048.785
324	428320.241	5017039.755	2048.607
325	428318.390	5017039.074	2048.376

326	428316.486	5017038.482	2048.143
327	428314.527	5017037.870	2047.948
328	428312.654	5017037.254	2047.775
329	428310.951	5017036.427	2047.499
330	428309.046	5017035.775	2047.305
331	428307.145	5017034.818	2046.908
332	428305.474	5017034.029	2046.667
333	428303.538	5017033.400	2046.415
334	428301.704	5017032.747	2046.168
335	428299.837	5017032.011	2045.885
336	428298.033	5017031.254	2045.645
337	428296.135	5017030.477	2045.380
338	428294.502	5017029.616	2045.074
339	428292.517	5017028.884	2044.785
340	428290.701	5017028.434	2044.568
341	428288.818	5017027.633	2044.237
342	428287.092	5017026.838	2043.809
343	428285.179	5017026.211	2043.495
344	428283.423	5017025.490	2043.267
345	428281.751	5017024.676	2042.885
346	428280.042	5017023.957	2042.634
347	428278.149	5017022.963	2042.255
348	428276.284	5017022.373	2042.027
349	428274.371	5017021.751	2041.803
350	428272.535	5017020.946	2041.473
351	428270.831	5017020.060	2041.083
352	428268.965	5017019.348	2040.799
353	428267.248	5017018.630	2040.506
354	428265.318	5017017.885	2040.230
355	428263.594	5017017.246	2039.904
356	428261.602	5017016.517	2039.599
357	428259.868	5017015.768	2039.291
358	428258.100	5017014.769	2038.884
359	428256.204	5017014.126	2038.634
360	428254.532	5017013.346	2038.304
361	428252.557	5017012.717	2037.980
362	428250.650	5017011.845	2037.581
363	428248.974	5017011.317	2037.313
364	428247.073	5017010.382	2036.967
365	428245.223	5017009.717	2036.748
366	428243.404	5017009.009	2036.393

367	428241.523	5017008.392	2036.134
368	428239.673	5017007.748	2035.846
369	428237.730	5017007.167	2035.520
370	428235.874	5017006.659	2035.254
371	428234.102	5017006.016	2034.900
372	428232.120	5017005.445	2034.621
373	428230.178	5017004.980	2034.391
374	428228.334	5017004.171	2034.003
375	428226.453	5017003.622	2033.701
376	428224.479	5017003.042	2033.454
377	428222.615	5017002.558	2033.106
378	428220.696	5017002.083	2032.785
379	428218.865	5017001.684	2032.596
380	428216.830	5017001.300	2032.196
381	428214.926	5017000.754	2031.945
382	428212.980	5017000.586	2031.720
383	428211.055	5017000.248	2031.399
384	428209.144	5016999.769	2031.076
385	428207.133	5016999.398	2030.797
386	428205.216	5016999.136	2030.561
387	428203.291	5016998.752	2030.353
388	428201.352	5016998.511	2030.124
389	428199.348	5016998.183	2029.867
390	428197.377	5016997.915	2029.634
391	428195.341	5016997.448	2029.299
392	428193.401	5016997.137	2028.991
393	428191.446	5016996.953	2028.746
394	428189.548	5016996.880	2028.520
395	428187.623	5016996.547	2028.132
396	428185.653	5016996.317	2027.777
397	428183.722	5016996.173	2027.528
398	428181.666	5016996.022	2027.277
399	428180.004	5016996.002	2027.078
400	428178.073	5016995.812	2026.797
401	428176.004	5016995.908	2026.521
402	428173.996	5016995.913	2026.252
403	428172.091	5016995.938	2026.013
404	428170.045	5016995.954	2025.748
405	428168.093	5016996.000	2025.488
406	428166.093	5016995.957	2025.221
407	428164.000	5016995.962	2024.887

408	428162.134	5016995.983	2024.674
409	428160.092	5016995.735	2024.317
410	428158.148	5016995.743	2023.991
411	428156.173	5016995.859	2023.706
412	428154.199	5016995.970	2023.449
413	428152.270	5016995.991	2023.184
414	428150.241	5016996.165	2022.939
415	428148.266	5016996.206	2022.634
416	428146.347	5016996.367	2022.336
417	428144.450	5016996.449	2022.066
418	428142.388	5016996.420	2021.720
419	428140.491	5016996.516	2021.430
420	428138.469	5016996.540	2021.109
421	428136.510	5016996.659	2020.878
422	428134.519	5016996.726	2020.567
423	428132.528	5016996.776	2020.292
424	428130.601	5016996.912	2019.972
425	428128.620	5016997.163	2019.687
426	428126.718	5016997.516	2019.439
427	428124.668	5016997.838	2019.156
428	428122.798	5016998.179	2018.949
429	428120.855	5016998.358	2018.708
430	428118.806	5016998.795	2018.449
431	428116.885	5016998.863	2018.173
432	428114.912	5016999.052	2017.863
433	428112.925	5016999.452	2017.586
434	428111.030	5016999.692	2017.291
435	428109.094	5016999.746	2016.962
436	428107.089	5016999.945	2016.667
437	428105.128	5016999.940	2016.398
438	428103.240	5017000.033	2016.124
439	428101.147	5017000.071	2015.809
440	428099.201	5016999.984	2015.489
441	428097.279	5016999.915	2015.226
442	428095.380	5016999.721	2014.961
443	428093.294	5016999.709	2014.667
444	428091.517	5016999.274	2014.425
445	428089.634	5016999.139	2014.131
446	428087.639	5016998.912	2013.838
447	428085.691	5016998.580	2013.536
448	428083.784	5016998.432	2013.282

449	428081.772	5016997.996	2012.981
450	428079.785	5016997.767	2012.717
451	428077.852	5016997.404	2012.493
452	428075.856	5016996.971	2012.222
453	428073.940	5016996.702	2011.977
454	428072.055	5016996.465	2011.748
455	428070.006	5016996.209	2011.430
456	428068.082	5016995.979	2011.152
457	428066.027	5016995.923	2010.915
458	428064.080	5016995.724	2010.679
459	428062.181	5016995.577	2010.403
460	428060.057	5016995.605	2010.131
461	428058.088	5016995.598	2009.819
462	428056.132	5016995.225	2009.395
463	428054.187	5016995.195	2009.097
464	428052.243	5016995.285	2008.850
465	428050.149	5016995.226	2008.631
466	428048.202	5016995.033	2008.249
467	428046.234	5016995.013	2007.955
468	428044.236	5016995.156	2007.596
469	428042.302	5016995.341	2007.289
470	428040.320	5016995.553	2006.992
471	428038.349	5016995.926	2006.655
472	428036.353	5016996.222	2006.283
473	428034.491	5016996.595	2005.946
474	428032.325	5016997.107	2005.602
475	428030.632	5016997.877	2005.467
476	428028.658	5016998.716	2005.260
477	428027.014	5016999.614	2005.156
478	428025.064	5017000.552	2004.937
479	428023.326	5017001.440	2004.629
480	428021.621	5017002.499	2004.429
481	428019.835	5017003.359	2004.153
482	428018.068	5017004.505	2003.975
483	428016.456	5017005.485	2003.639
484	428014.743	5017006.506	2003.304
485	428013.061	5017007.555	2003.078
486	428011.427	5017008.665	2002.845
487	428009.736	5017009.622	2002.501
488	428008.159	5017010.835	2002.210
489	428006.642	5017011.962	2001.914

490	428005.026	5017013.261	2001.520
491	428003.439	5017014.317	2001.176
492	428001.963	5017015.564	2000.928
493	428000.329	5017016.684	2000.561
	427998.672	5017017.772	2000.191
495	427997.134	5017019.087	1999.896
496	427995.642	5017020.287	1999.611
497	427994.096	5017021.521	1999.229
498	427992.415	5017022.581	1998.728
499	427990.939	5017023.786	1998.434
500	427989.345	5017024.969	1998.058
501	427987.437	5017026.166	1997.637
502	427986.140	5017027.231	1997.317
503	427984.600	5017028.337	1997.000
504	427983.047	5017029.660	1996.698
505	427981.358	5017030.712	1996.390
506	427979.701	5017031.909	1996.144
507	427978.160	5017032.954	1995.893
508	427976.505	5017034.210	1995.672
509	427974.926	5017035.324	1995.400
510	427973.230	5017036.545	1995.141
511	427971.603	5017037.515	1994.933
512	427970.095	5017038.720	1994.682
513	427968.352	5017039.909	1994.435
514	427966.830	5017041.149	1994.174
515	427965.196	5017042.234	1993.935
516	427963.672	5017043.441	1993.698
517	427962.046	5017044.515	1993.366
518	427960.484	5017045.727	1993.151
519	427958.826	5017046.801	1992.793
520	427957.040	5017047.684	1992.557
521	427955.317	5017048.492	1992.173
522	427953.428	5017049.254	1991.847
523	427951.648	5017049.959	1991.531
524	427949.871	5017050.870	1991.335
525	427948.007	5017051.701	1991.131
526	427946.131	5017052.234	1990.855
527	427944.358	5017052.862	1990.620
528	427942.367	5017053.589	1990.368
529	427940.626	5017054.257	1990.185
530	427938.743	5017054.827	1989.943

531	427936.851	5017055.340	1989.761
532	427934.864	5017055.676	1989.476
533	427933.000	5017055.880	1989.244
534	427931.080	5017056.018	1988.965
535	427929.121	5017056.067	1988.666
536	427927.129	5017056.041	1988.390
537	427925.163	5017055.574	1988.036
538	427923.164	5017055.619	1987.771
539	427921.232	5017055.974	1987.548
540	427919.245	5017055.735	1987.277
541	427917.304	5017055.321	1986.968
542	427915.362	5017054.906	1986.659
543	427913.424	5017054.715	1986.451
544	427911.381	5017054.338	1986.205
545	427909.724	5017054.107	1986.058
546	427907.960	5017053.465	1985.698
547	427905.877	5017053.039	1985.460
548	427904.077	5017052.605	1985.258
549	427902.048	5017052.060	1984.979
550	427900.192	5017051.620	1984.727
551	427898.256	5017050.986	1984.458
552	427896.541	5017050.443	1984.171
553	427894.497	5017050.031	1983.912
554	427892.639	5017049.361	1983.683
555	427890.795	5017048.567	1983.357
556	427888.976	5017047.842	1983.063
557	427887.187	5017047.032	1982.728
558	427885.468	5017046.254	1982.451
559	427883.639	5017045.368	1982.191
560	427881.794	5017044.420	1981.880
561	427880.108	5017043.700	1981.689
562	427878.161	5017042.826	1981.478
563	427876.472	5017041.858	1981.209
564	427874.612	5017041.059	1980.988
565	427872.839	5017040.305	1980.793
566	427871.019	5017039.467	1980.598
567	427869.276	5017038.620	1980.424
568	427867.470	5017037.732	1980.179
569	427865.598	5017037.151	1979.992
570	427863.776	5017036.210	1979.752
571	427861.932	5017035.458	1979.581

572	427860.096	5017034.656	1979.423
573	427858.284	5017033.918	1979.283
574	427856.448	5017033.091	1979.108
575	427854.597	5017032.313	1978.951
576	427852.722	5017031.525	1978.777
577	427850.880	5017030.923	1978.647
578	427849.036	5017030.134	1978.472
579	427847.261	5017029.203	1978.285
580	427845.463	5017028.296	1978.048
581	427843.596	5017027.490	1977.885
582	427841.909	5017026.711	1977.740
583	427840.064	5017025.809	1977.543
584	427838.275	5017024.995	1977.355
585	427836.469	5017024.118	1977.198
586	427834.680	5017023.334	1977.032
587	427832.929	5017022.412	1976.848
588	427831.131	5017021.481	1976.701
589	427829.467	5017020.676	1976.594
590	427827.575	5017019.755	1976.452
591	427825.723	5017018.983	1976.338
592	427824.041	5017017.939	1976.123
593	427822.328	5017016.922	1975.958
594	427820.608	5017016.012	1975.752
595	427818.857	5017015.104	1975.566
596	427817.268	5017013.960	1975.351
597	427815.547	5017012.898	1975.167
598	427813.850	5017011.931	1974.969
599	427812.254	5017010.838	1974.774
600	427810.766	5017009.664	1974.542
601	427809.037	5017008.633	1974.373
602	427807.411	5017007.672	1974.204
603	427805.689	5017006.579	1974.033
604	427803.866	5017005.566	1973.911
605	427802.216	5017004.581	1973.750
606	427800.581	5017003.502	1973.571
607	427798.907	5017002.487	1973.428
608	427797.099	5017001.398	1973.207
609	427795.496	5017000.437	1973.101
610	427793.643	5016999.527	1972.952
611	427792.024	5016998.447	1972.807
612	427790.178	5016997.508	1972.621

613	427788.373	5016996.641	1972.418
614	427786.637	5016995.743	1972.231
615	427784.865	5016995.007	1971.989
616	427782.856	5016994.193	1971.682
617	427781.000	5016993.724	1971.497
618	427779.020	5016993.318	1971.303
619	427777.031	5016992.851	1971.132
620	427775.120	5016992.384	1970.935
621	427773.149	5016992.129	1970.804
622	427771.363	5016991.642	1970.583
623	427769.336	5016991.274	1970.292
624	427767.340	5016990.905	1969.985
625	427765.392	5016990.548	1969.603
626	427763.468	5016990.295	1969.311
627	427761.615	5016990.112	1969.029
628	427759.588	5016989.748	1968.773
629	427757.711	5016989.448	1968.457
630	427755.741	5016989.259	1968.030
631	427753.751	5016988.796	1967.451
632	427751.867	5016988.531	1967.133
633	427749.905	5016988.409	1966.799
634	427747.982	5016988.271	1966.473
635	427745.850	5016988.276	1966.060
636	427743.961	5016988.379	1965.691
637	427741.986	5016988.441	1965.344
638	427740.059	5016988.586	1964.989
639	427738.187	5016988.811	1964.648
640	427736.183	5016989.052	1964.369
641	427734.195	5016989.385	1964.003
642	427732.090	5016989.720	1963.703
643	427730.241	5016989.888	1963.383
644	427728.331	5016990.141	1963.083
645	427726.500	5016990.486	1962.865
646	427724.583	5016990.808	1962.698
647	427722.649	5016991.064	1962.404
648	427720.622	5016991.413	1962.245
649	427718.659	5016991.813	1962.107
650	427716.663	5016992.136	1961.922
651	427714.796	5016992.775	1961.784
652	427712.906	5016993.403	1961.644
653	427710.936	5016993.948	1961.511

654	427708.991	5016994.585	1961.351
655	427707.142	5016995.376	1961.208
656	427705.444	5016996.355	1961.057
657	427703.821	5016997.790	1960.973
658	427702.391	5016998.915	1960.870
659	427700.832	5017000.326	1960.826
660	427699.492	5017001.763	1960.729
661	427698.080	5017003.154	1960.629
662	427696.685	5017004.590	1960.541
663	427695.418	5017006.169	1960.464
664	427694.063	5017007.677	1960.438
665	427692.612	5017009.005	1960.410
666	427690.955	5017010.184	1960.352
667	427689.074	5017010.952	1960.203
668	427687.263	5017011.658	1960.125
669	427685.341	5017012.241	1959.976
670	427683.345	5017012.553	1959.901
671	427681.361	5017012.528	1959.851
672	427679.402	5017012.655	1959.817
673	427677.355	5017012.583	1959.868
674	427675.473	5017011.922	1959.750
675	427673.646	5017011.173	1959.648
676	427671.818	5017010.380	1959.484
677	427669.960	5017009.729	1959.358
678	427668.191	5017008.681	1959.166
679	427666.680	5017007.480	1958.921
680	427664.972	5017006.189	1958.731
681	427663.849	5017004.734	1958.592
682	427662.648	5017003.218	1958.431
683	427661.431	5017001.705	1958.284
684	427660.298	5017000.023	1958.140
685	427659.274	5016998.247	1957.931
686	427658.321	5016996.465	1957.690
687	427657.175	5016994.983	1957.488
688	427656.028	5016993.404	1957.239
689	427655.106	5016991.656	1957.000
690	427654.255	5016989.910	1956.758
691	427653.434	5016988.090	1956.481
692	427652.653	5016986.291	1956.192
693	427652.020	5016984.400	1955.947
694	427651.180	5016982.258	1955.664

695	427650.793	5016980.656	1955.394
696	427650.199	5016978.768	1955.133
697	427649.582	5016976.943	1954.876
698	427648.957	5016975.069	1954.657
699	427648.434	5016973.255	1954.392
700	427647.880	5016971.439	1954.130
701	427647.302	5016969.509	1953.895
702	427646.723	5016967.576	1953.672
703	427646.409	5016965.474	1953.506
704	427645.449	5016963.830	1953.419
705	427644.479	5016962.019	1953.311
706	427643.519	5016960.355	1953.146
707	427642.456	5016958.567	1952.962
708	427641.356	5016956.993	1952.722
709	427640.012	5016955.319	1952.494
710	427638.787	5016953.833	1952.276
711	427637.437	5016952.333	1952.049
712	427636.110	5016950.799	1951.794
713	427634.714	5016949.383	1951.639
714	427633.247	5016947.981	1951.498
715	427631.970	5016946.695	1951.307
716	427630.557	5016945.232	1951.114
717	427629.113	5016943.737	1950.952
718	427627.772	5016942.341	1950.741
719	427626.243	5016940.985	1950.497
720	427624.699	5016939.608	1950.274
721	427623.171	5016938.379	1950.066
722	427621.667	5016937.151	1949.781
723	427619.992	5016936.004	1949.526
724	427618.301	5016934.903	1949.266
725	427616.620	5016933.886	1949.117
726	427614.773	5016932.866	1948.980
727	427613.084	5016931.874	1948.717
728	427611.238	5016930.931	1948.591
729	427609.466	5016930.259	1948.430
730	427607.537	5016929.507	1948.235
731	427605.756	5016928.810	1948.061
732	427603.984	5016928.072	1947.898
733	427602.054	5016927.325	1947.715
734	427600.171	5016926.569	1947.520
735	427598.297	5016925.850	1947.293

736	427596.501	5016925.159	1947.096
737	427594.659	5016924.478	1946.909
738	427592.761	5016923.808	1946.709
739	427590.909	5016922.983	1946.453
740	427588.973	5016922.342	1946.214
741	427587.084	5016921.733	1946.038
742	427585.183	5016921.364	1945.890
743	427583.264	5016920.899	1945.749
744	427581.276	5016920.503	1945.598
745	427579.389	5016920.120	1945.407
746	427577.427	5016919.973	1945.221
747	427575.401	5016919.662	1944.935
748	427573.403	5016919.804	1944.740
749	427571.460	5016919.964	1944.480
750	427569.218	5016919.973	1944.213
751	427567.263	5016920.431	1944.038
752	427565.355	5016920.903	1943.846
753	427563.455	5016921.396	1943.608
754	427561.603	5016921.876	1943.382
755	427559.625	5016922.410	1943.182
756	427557.788	5016922.929	1942.987
757	427555.897	5016923.468	1942.804
758	427553.934	5016923.939	1942.634
759	427551.910	5016924.529	1942.455
760	427550.080	5016924.894	1942.306
761	427548.141	5016925.466	1942.195
762	427546.211	5016925.986	1942.071
763	427544.342	5016926.483	1941.963
764	427542.433	5016926.818	1941.783
765	427540.425	5016927.419	1941.513
766	427538.416	5016927.942	1941.363
767	427536.611	5016928.487	1941.182
768	427534.705	5016929.151	1941.011
769	427532.816	5016929.911	1940.822
770	427530.943	5016930.698	1940.679
771	427529.087	5016931.569	1940.556
772	427527.373	5016932.529	1940.386
773	427525.603	5016933.375	1940.187
774	427523.907	5016934.510	1939.998
775	427522.193	5016935.472	1939.741
776	427520.558	5016936.482	1939.524

777	427518.845	5016937.600	1939.303
778	427517.250	5016938.600	1939.111
779	427515.599	5016939.614	1938.954
780	427513.784	5016940.683	1938.752
781	427512.054	5016941.636	1938.592
782	427510.199	5016942.587	1938.379
783	427508.460	5016943.389	1938.191
784	427506.807	5016944.254	1938.020
785	427504.892	5016944.781	1937.788
786	427503.041	5016945.375	1937.579
787	427501.227	5016945.848	1937.379
788	427499.194	5016946.349	1937.205
789	427497.356	5016946.728	1937.077
790	427495.462	5016946.995	1936.941
791	427493.386	5016947.182	1936.799
792	427491.396	5016947.323	1936.714
793	427489.363	5016947.157	1936.552
794	427487.447	5016946.936	1936.418
795	427485.643	5016946.163	1936.191
796	427483.657	5016945.996	1936.017
797	427481.677	5016945.633	1935.749
798	427479.829	5016945.141	1935.504
799	427478.032	5016944.375	1935.258
800	427476.361	5016943.544	1935.065
801	427474.787	5016942.390	1934.849
802	427473.189	5016941.130	1934.638
803	427471.723	5016939.839	1934.491
804	427470.170	5016938.447	1934.269
805	427468.814	5016937.067	1934.119
806	427467.877	5016935.414	1933.954
807	427467.142	5016933.556	1933.828
808	427466.549	5016931.682	1933.706
809	427466.117	5016929.648	1933.589
810	427465.767	5016927.789	1933.535
811	427465.712	5016925.714	1933.456
812	427465.581	5016923.860	1933.426
813	427465.534	5016921.834	1933.408
814	427465.557	5016919.741	1933.356
815	427465.621	5016917.783	1933.339
816	427465.784	5016915.628	1933.313
817	427466.123	5016913.727	1933.270

818	427466.470	5016911.830	1933.196
819	427466.784	5016909.871	1933.144
820	427466.996	5016907.861	1932.992
821	427467.280	5016905.952	1932.859
822	427467.391	5016903.957	1932.697
823	427467.570	5016901.813	1932.506
824	427467.383	5016899.885	1932.368
825	427467.383	5016897.799	1932.205
826	427467.400	5016895.846	1932.068
827	427467.125	5016893.771	1931.931
828	427466.421	5016891.858	1931.851
829	427465.717	5016889.953	1931.787
830	427464.989	5016888.068	1931.678
831	427464.115	5016886.359	1931.522
832	427463.208	5016884.496	1931.322
833	427462.022	5016882.959	1931.120
834	427460.624	5016881.435	1930.973
835	427459.066	5016880.234	1930.839
836	427457.475	5016879.002	1930.605
837	427455.909	5016877.769	1930.371
838	427454.326	5016876.490	1930.118
839	427452.713	5016875.332	1929.932
840	427451.093	5016874.241	1929.728
841	427449.481	5016873.136	1929.544
842	427447.828	5016871.921	1929.305
843	427446.177	5016870.843	1929.118
844	427444.471	5016869.760	1929.074
845	427442.702	5016868.691	1928.936
846	427441.107	5016867.711	1928.880
847	427439.469	5016866.459	1928.714
848	427437.756	5016865.377	1928.657
849	427436.083	5016864.518	1928.636
850	427434.337	5016863.386	1928.565
851	427432.741	5016862.298	1928.479
852	427431.028	5016861.264	1928.352
853	427429.298	5016860.214	1928.179
854	427427.686	5016859.080	1927.908
855	427425.941	5016858.080	1927.699
856	427424.090	5016857.356	1927.538
857	427422.425	5016856.394	1927.263
858	427420.541	5016855.553	1927.021

859	427418.822	5016854.728	1926.894
860	427417.085	5016853.681	1926.716
861	427415.449	5016852.569	1926.595
862	427413.778	5016851.785	1926.550
863	427412.090	5016850.917	1926.519
864	427410.405	5016849.629	1926.364
865	427408.723	5016848.577	1926.196
866	427406.994	5016847.536	1926.016
867	427405.374	5016846.506	1925.870
868	427403.538	5016845.677	1925.674
869	427401.878	5016844.504	1925.491
870	427400.180	5016843.452	1925.235
871	427398.404	5016842.475	1925.033
872	427396.700	5016841.514	1924.753
873	427394.933	5016840.623	1924.465
874	427393.298	5016839.552	1924.244
875	427391.615	5016838.499	1923.930
876	427389.848	5016837.530	1923.688
877	427388.119	5016836.524	1923.473
878	427386.607	5016835.230	1923.228
879	427384.817	5016834.372	1923.034
880	427382.902	5016833.599	1922.888
881	427381.276	5016832.600	1922.688
882	427379.401	5016831.881	1922.548
883	427377.572	5016830.966	1922.293
884	427375.661	5016830.535	1922.199
885	427373.779	5016829.828	1921.953
886	427371.889	5016829.103	1921.672
887	427370.093	5016828.430	1921.362
888	427368.380	5016827.385	1920.875
889	427366.484	5016826.868	1920.667
890	427364.734	5016826.069	1920.371
891	427363.038	5016825.166	1920.091
892	427361.193	5016824.241	1919.848
893	427359.449	5016823.288	1919.553
894	427357.752	5016822.334	1919.283
895	427356.015	5016821.297	1919.063
896	427354.310	5016820.360	1918.865
897	427352.604	5016819.274	1918.643
898	427351.001	5016818.230	1918.436
899	427349.240	5016817.172	1918.217

900	427347.582	5016816.164	1918.101
901	427345.869	5016815.194	1917.909
902	427344.209	5016814.073	1917.801
903	427342.712	5016812.744	1917.638
904	427341.254	5016811.458	1917.564
905	427339.710	5016810.153	1917.442
906	427338.384	5016808.649	1917.190
907	427337.158	5016807.035	1916.906
908	427335.862	5016805.486	1916.696
909	427334.824	5016803.935	1916.532
910	427333.607	5016802.372	1916.369
911	427332.428	5016800.758	1916.157
912	427331.359	5016799.159	1915.924
913	427330.188	5016797.568	1915.703
914	427328.971	5016796.050	1915.460
915	427327.658	5016794.435	1915.174
916	427326.450	5016793.020	1914.889
917	427324.936	5016791.631	1914.638
918	427323.291	5016790.384	1914.408
919	427321.663	5016789.273	1914.146
920	427320.097	5016788.131	1913.887
921	427318.198	5016787.276	1913.590
922	427316.408	5016786.436	1913.300
923	427314.448	5016785.787	1912.961
924	427312.575	5016785.144	1912.649
925	427310.682	5016784.883	1912.364
926	427308.685	5016784.406	1912.058
927	427306.760	5016784.120	1911.881
928	427304.748	5016783.672	1911.664
929	427302.798	5016783.252	1911.446
930	427300.837	5016783.190	1911.325
931	427298.897	5016782.852	1911.123
932	427296.958	5016782.685	1911.048
933	427295.010	5016782.389	1910.901
934	427293.038	5016782.065	1910.729
935	427291.142	5016781.546	1910.597
936	427289.280	5016781.159	1910.492
937	427287.607	5016780.260	1910.405
938	427286.026	5016779.183	1910.289
939	427284.444	5016777.933	1910.171
940	427282.978	5016776.666	1910.057

941	427281.651	5016775.144	1909.950
942	427280.692	5016773.517	1909.871
943	427279.847	5016771.680	1909.803
944	427279.152	5016769.857	1909.747
945	427278.628	5016767.929	1909.621
946	427278.362	5016765.959	1909.534
947	427278.158	5016763.927	1909.439
948	427278.105	5016761.984	1909.425
949	427278.026	5016759.940	1909.318
950	427278.350	5016758.091	1909.235
951	427278.271	5016755.970	1909.115
952	427277.997	5016753.972	1909.057
953	427277.927	5016751.985	1908.936
954	427277.786	5016749.980	1908.732
955	427277.630	5016747.982	1908.510
956	427277.529	5016746.024	1908.290
957	427276.803	5016744.278	1908.149
958	427276.263	5016742.294	1907.845
959	427275.820	5016740.575	1907.631
960	427275.193	5016738.623	1907.408
961	427274.654	5016736.721	1907.146
962	427274.130	5016734.798	1906.872
963	427273.536	5016732.909	1906.697
964	427273.105	5016730.905	1906.420
965	427272.660	5016729.036	1906.288
966	427272.300	5016727.026	1906.125
967	427271.956	5016725.100	1906.008
968	427271.603	5016723.065	1905.877
969	427271.244	5016721.174	1905.762
970	427271.010	5016719.216	1905.513
971	427271.003	5016717.249	1905.391
972	427271.019	5016715.258	1905.282
973	427270.965	5016713.232	1905.154
974	427270.942	5016711.260	1904.964
975	427270.856	5016709.263	1904.820
976	427270.834	5016707.320	1904.642
977	427270.936	5016705.267	1904.425
978	427270.805	5016703.394	1904.225
979	427270.876	5016701.407	1903.936
980	427271.002	5016699.454	1903.689
981	427271.073	5016697.386	1903.411

982	427271.168	5016695.470	1903.136
983	427271.279	5016693.520	1902.819
984	427271.319	5016691.509	1902.481
985	427271.312	5016689.570	1902.153
986	427271.596	5016687.640	1901.896
987	427271.683	5016685.672	1901.603
988	427271.660	5016683.730	1901.266
989	427271.888	5016681.692	1901.009
990	427271.960	5016679.766	1900.799
991	427272.078	5016677.750	1900.502
992	427272.392	5016675.794	1900.242
993	427272.588	5016673.706	1900.098
994	427272.659	5016671.743	1899.950
995	427272.794	5016669.848	1899.790
996	427273.171	5016667.838	1899.683
997	427273.470	5016665.896	1899.548
998	427273.840	5016663.954	1899.360
999	427274.036	5016661.940	1899.090
1000	427274.289	5016660.011	1898.786
1001	427274.266	5016658.078	1898.568
1002	427274.251	5016656.087	1898.344
1003	427274.534	5016654.054	1898.048
1004	427274.362	5016652.105	1897.740
1005	427273.996	5016650.227	1897.397
1006	427273.691	5016648.248	1897.084
1007	427272.785	5016646.563	1896.907
1008	427272.299	5016644.499	1896.594
1009	427271.269	5016642.888	1896.400
1010	427270.344	5016640.896	1896.024
1011	427268.808	5016639.621	1895.847
1012	427266.839	5016638.867	1895.856
1013	427265.134	5016637.923	1895.578
1014	427263.214	5016637.298	1895.366
1015	427261.362	5016636.498	1895.000
1016	427259.597	5016635.721	1894.675
1017	427257.776	5016634.907	1894.368
1018	427255.976	5016633.838	1894.051
1019	427254.451	5016632.809	1893.819
1020	427252.792	5016631.751	1893.562
1021	427251.187	5016630.642	1893.281
1022	427249.519	5016629.506	1893.041

1023	427247.883	5016628.390	1892.949
1024	427246.605	5016626.975	1892.673
1025	427244.952	5016625.764	1892.460
1026	427243.322	5016624.542	1892.319
1027	427241.857	5016623.288	1892.138
1028	427240.268	5016622.106	1891.908
1029	427238.678	5016620.915	1891.652
1030	427237.134	5016619.602	1891.404
1031	427235.537	5016618.469	1891.317
1032	427233.946	5016617.216	1891.136
1033	427232.427	5016616.022	1891.030
1034	427230.781	5016614.774	1890.911
1035	427229.145	5016613.620	1890.748
1036	427227.565	5016612.579	1890.626
1037	427225.882	5016611.499	1890.480
1038	427224.208	5016610.487	1890.330
1039	427222.424	5016609.486	1890.150
1040	427220.735	5016608.475	1889.991
1041	427218.975	5016607.553	1889.805
1042	427217.131	5016606.773	1889.646
1043	427215.257	5016606.068	1889.461
1044	427213.368	5016605.474	1889.310
1045	427211.434	5016605.047	1889.163
1046	427209.485	5016604.610	1888.927
1047	427207.635	5016604.032	1888.781
1048	427205.669	5016603.562	1888.568
1049	427203.687	5016603.019	1888.328
1050	427201.831	5016602.500	1888.155
1051	427199.974	5016601.943	1887.918
1052	427198.161	5016601.157	1887.800
1053	427196.223	5016600.399	1887.628
1054	427194.589	5016599.457	1887.416
1055	427192.767	5016598.477	1887.259
1056	427191.243	5016597.586	1887.083
1057	427189.545	5016596.532	1886.917
1058	427188.266	5016595.105	1886.716
1059	427187.344	5016593.360	1886.542
1060	427185.831	5016592.010	1886.319
1061	427183.884	5016591.173	1886.194
1062	427182.254	5016589.910	1886.046
1063	427180.611	5016588.832	1885.889

1064	427178.935	5016587.673	1885.745
1065	427177.168	5016586.756	1885.595
1066	427175.479	5016585.751	1885.407
1067	427173.789	5016584.726	1885.278
1068	427172.052	5016583.708	1885.109
1069	427170.231	5016582.884	1884.936
1070	427168.395	5016582.146	1884.777
1071	427166.505	5016581.411	1884.638
1072	427164.684	5016580.575	1884.537
1073	427162.863	5016579.763	1884.380
1074	427161.042	5016578.947	1884.258
1075	427159.361	5016577.967	1884.118
1076	427157.548	5016577.162	1883.996
1077	427155.727	5016576.290	1883.910
1078	427153.905	5016575.430	1883.757
1079	427152.256	5016574.541	1883.738
1080	427150.418	5016573.581	1883.623
1081	427148.612	5016572.683	1883.512
1082	427146.853	5016571.780	1883.401
1083	427145.147	5016570.739	1883.259
1084	427143.411	5016569.737	1883.157
1085	427141.736	5016568.681	1883.064
1086	427140.030	5016567.666	1882.971
1087	427138.324	5016566.595	1882.907
1088	427136.611	5016565.549	1882.810
1089	427134.897	5016564.486	1882.742
1090	427133.277	5016563.378	1882.674
1091	427131.563	5016562.372	1882.581
1092	427129.865	5016561.292	1882.507
1093	427128.136	5016560.282	1882.377
1094	427126.439	5016559.355	1882.290
1095	427124.641	5016558.397	1882.197
1096	427122.982	5016557.395	1882.118
1097	427121.222	5016556.420	1881.998
1098	427119.440	5016555.554	1881.938
1099	427117.595	5016554.637	1881.944
1100	427115.929	5016553.662	1881.777
1101	427114.269	5016552.511	1881.660
1102	427112.594	5016551.405	1881.631
1103	427110.956	5016550.140	1881.555
1104	427109.360	5016549.077	1881.447

1105	427107.646	5016548.001	1881.396
1106	427105.907	5016546.867	1881.268
1107	427104.303	5016545.772	1881.214
1108	427102.629	5016544.771	1881.040
1109	427101.158	5016543.706	1880.808
1110	427099.375	5016542.713	1880.694
1111	427097.698	5016541.516	1880.521
1112	427096.079	5016540.449	1880.391
1113	427094.365	5016539.416	1880.259
1114	427092.691	5016538.384	1880.172
1115	427091.062	5016537.234	1880.055
1116	427089.317	5016536.196	1880.082
1117	427087.657	5016535.032	1879.986
1118	427085.928	5016533.971	1879.938
1119	427084.331	5016532.844	1879.906
1120	427082.718	5016531.709	1879.867
1121	427081.121	5016530.601	1879.849
1122	427079.415	5016529.525	1879.817
1123	427077.710	5016528.536	1879.819
1124	427075.979	5016527.342	1879.755
1125	427074.303	5016526.229	1879.678
1126	427072.816	5016525.053	1879.621
1127	427071.172	5016523.930	1879.486
1128	427069.598	5016522.805	1879.432
1129	427067.929	5016521.570	1879.333
1130	427066.448	5016520.315	1879.265
1131	427065.363	5016518.705	1879.237
1132	427064.674	5016516.705	1879.248
1133	427064.254	5016515.021	1879.002

A Seismic Refraction Survey in Virginia City, Montana, to Investigate Streambed Hydrologic Conditions along Alder Creek

Prepared By:

Rachel Basnaw, Jacob Clarke, Emelina Doucette, John Fitzgerald, Jay Hillygus, Kenton Hoshino, Eva Hover, Brayden Hungrige, Richard Lee, Mariah Mosdal, Shane Namie, Joseph Natale, Kabree Nichols, Christopher Smith, Brent Sordo, Zane White, Andrew Wilson, Troy Wolff

For:

Montana Bureau of Mines and Geology

Under the Supervision of:

Dr. Marvin Speece

Department of Geophysical Engineering

Montana Tech of the University of Montana

Butte, MT 59701

May 7th-12th, 2018

Executive Summary

Seismic refraction surveys are a method of geophysical investigation employed to determine subsurface geology as a less expensive and quicker option than drilling or other, more traditional exploration methods. In this project, we used seismic refraction to determine the depth of the saturated layer and the depth to the basement rock based on velocity data of seismic waves collected on the outskirts of Virginia City, Montana. We performed this study for the Montana Bureau of Mines and Geology (MBMG), who will utilize it to determine the surface geometry, aiding in the evaluation of the potential development of a secondary clean water source for Virginia City.

On May 9, 2018, we traveled to Virginia City to collect seismic refraction and survey data. We laid out four different survey lines along the appointed areas specified by the MBMG. To gather the data for three survey lines, we used a 226.8 kg accelerated weight drop seismic source mounted on a trailer and pulled by a pickup. Each station required three drops of the weight to allow for stacking (summation) of the data to reduce noise. For one of the survey lines the pickup pulled weight drop was not an option due to inaccessibility of the location for the pickup and trailer. For this line, we used a manually swung twenty pound sledgehammer in which each station required nine drops.

Our 2-D velocity profiles produced from seismic refraction first arrivals show basement material, saturated alluvium sediments, and unsaturated alluvium sediments. The seismic velocity for unsaturated sediments is 400 m/s and for saturated sediments is 1720 m/s (corresponding to the seismic velocity of water). We determine the basement velocity to be 3550 m/s, which corresponds to a consolidated crystalline material. By inversion in Rayfract, the depth to basement ranges from 15 to 28 meters, depending on the survey line.

Table of Contents

List of Figures

List of Tables

Introduction

Geophysical seismic refraction surveys were completed in the area near Virginia City, Montana in association with an ongoing project by the Montana Bureau of Mines and Geology (MBMG). Virginia City has two natural springs located north-east of town that are used as the town's water sources. Home development is continuing to increase in this area, which may result in potential sewage contamination from the new development within the watershed area of these wells. The MBMG is currently investigating a future potential site for establishing a secondary water source and they require a thorough understanding of the saturated layers and depth to basement rock in the Alder Creek stream channel. The purpose of this project is to apply seismic refraction surveys to identify the thickness of the saturated and unsaturated sediment layers and the depth to bedrock.

Site Description

We conducted four seismic surveys within a mile of each other to the southwest and northwest of Virginia City (Figure 1). Figure 2 shows the location of our four survey lines in the Alder Creek drainage. The survey area consisted of two local county roads, the currently inactive railroad line that crosses Alder Creek, and one parking lot that is parallel to Alder Creek (Figure 2).

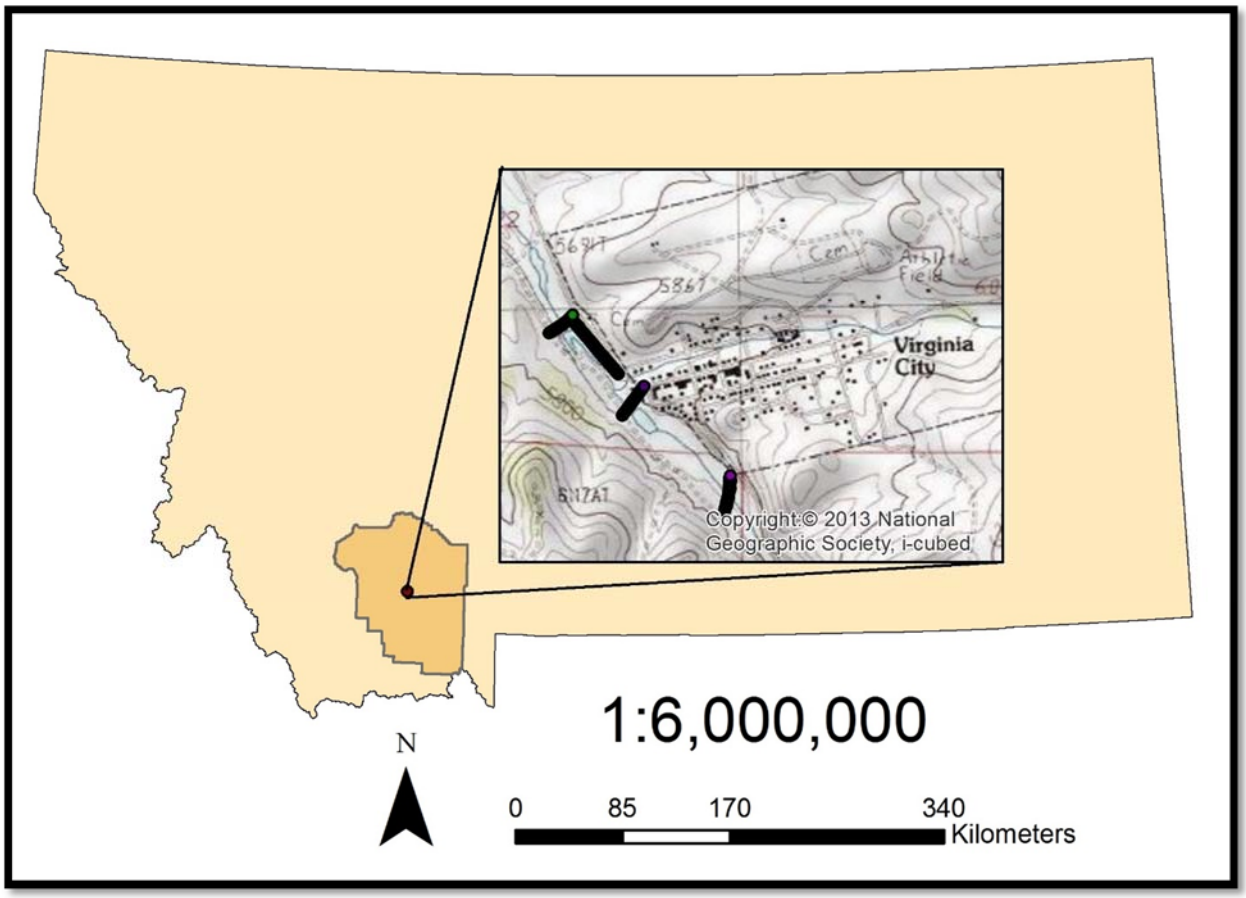

Figure 1. *Overview map showing Montana. Inset map shows the location of our survey, survey lines are shown in black. (modified from ESRI, 2018 and Montana State Library, 2018).*

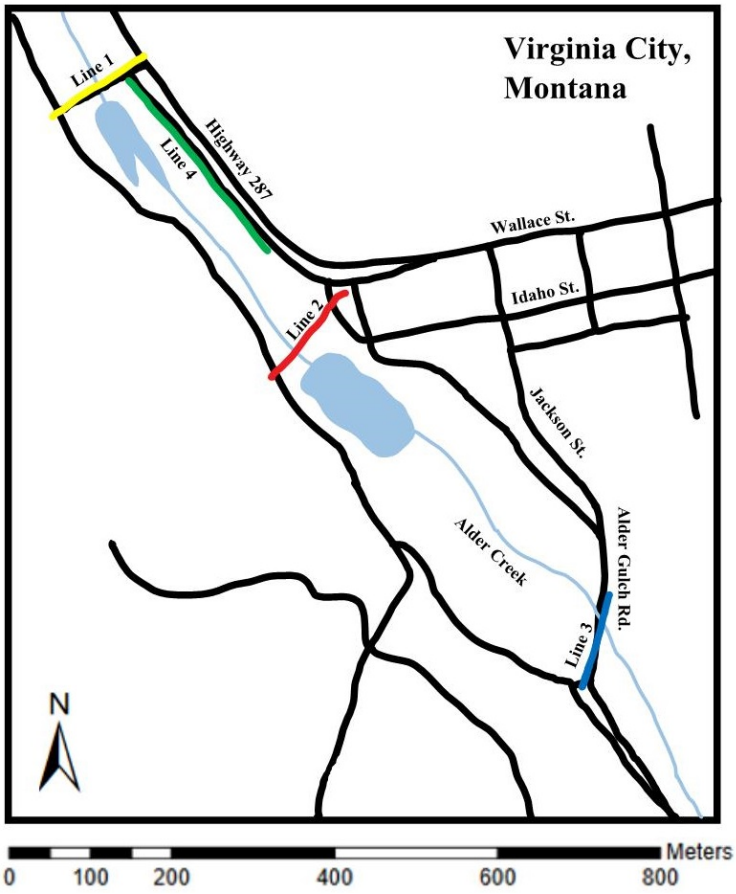

Figure 2*. Site map of Virginia City, Montana, showing the four survey lines and their relationship to each other, the roads and Alder Creek (map created by drawing over the top of Google Earth Pro Image, 2014).*

Geologic Setting

The geology surrounding Virginia City is characterized by an Archean gneiss basement overlain by Tertiary Volcanics with interbedded gravels. Two major faults pass through the area; the Virginia City fault trends to the northwest along Alder Gulch, and the Baldy Mountain Fault trends to the east-northeast, south of the study area (Ruppel and Liu, 2004).

The oldest stratigraphic units in the area are a series of Archean gneisses. Quartzofeldspathic gneiss is the dominant lithology. The gneisses are believed to be of mostly sedimentary origin with parts that are of igneous origin. These gneisses contain hornblende, andesine, quartz, and

garnet. A layer of volcanics is present over the northeastern end of Virginia City. Tuff overlies an unconformity and is covered by a basalt flow. This unit outcrops near the springs that supply Virginia City with clean water (Figure 3). The Virginia City fault is a left-lateral strike-slip fault trending northwest from Axolotl Lakes, located southeast from the study area (Vitaliano and Cordua, 1979). The fault cuts the Archean basement along the trace (Ruppel and Liu, 2004).

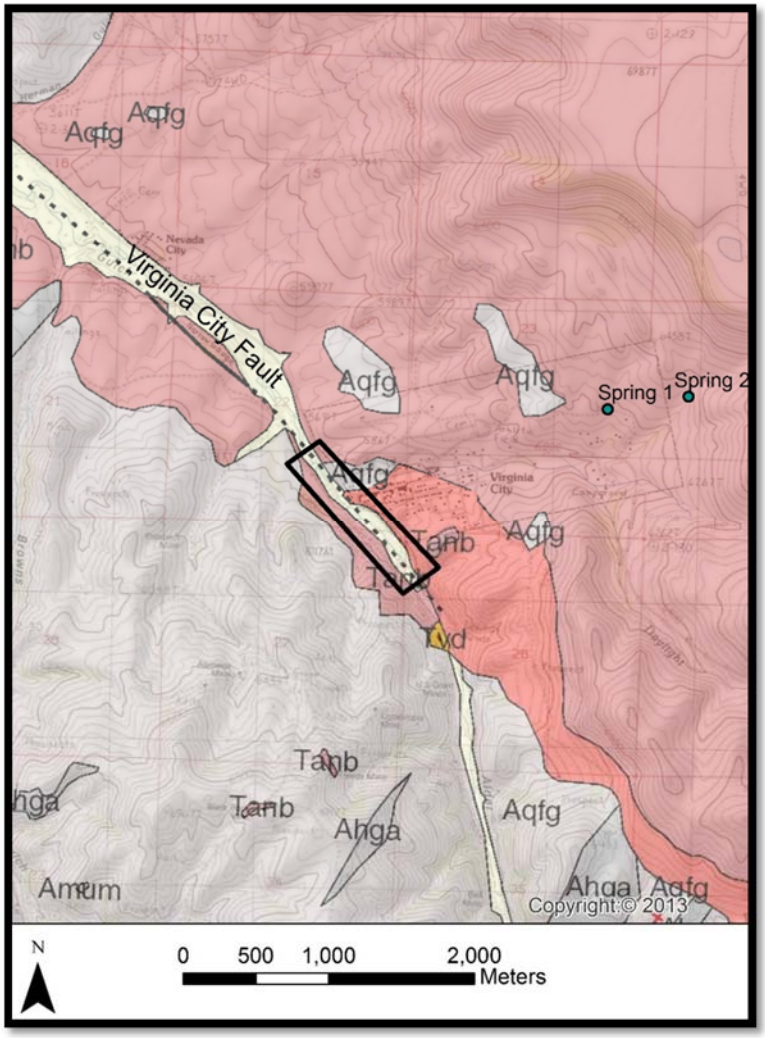

Figure 3*. Geological Map of the study area (boxed). Agfg is the quartzofeldspathic gneiss, Tanb is andesite and basalts flows, Ahga is hornblende-plagiocase gneiss and amphibolite, Amum is meta-ultramafic rocks (modified from Kellog and Williams, 2006, National Geographic, 2013).*

Seismic Refraction Theory

The seismic refraction method, due to its versatility, is one of the most commonly used geophysical methods in subsurface investigation. This method is utilized to provide detailed information on the thicknesses of subsurface layers by distinguishing between the different seismic velocities each layer. Overburden and basement rocks may be classified to some degree in order to differentiate, for example, between highly fractured rock and more competent rock. The technique is also widely used to assess the rippability of bedrock.

Seismic waves change their trajectory when they travel from one material into another of differing density in accordance with Snell's Law, also known as the Law of Refraction. If the seismic wave velocity increases when entering the underlying rock layer, the waves will refract upward. If the seismic wave passes across a boundary to a lower velocity layer, the wave will be refracted downward, nearer to a vertical trajectory, and the velocity will decrease. Because velocity tends to increase with depth the wave paths bend upward at each material boundary until they reach a critical angle at which the waves traverse horizontally along the boundary until returning to an upward trajectory and returning to the surface in the same pattern as the wave descended. Figure 4 shows a three-layer refraction model appropriate for our survey.

The amount the ray refracts at a material boundary is defined by Snell's Law (EQN 1) (Sabra, 1981). According to this law, the change in direction depends on the ratio of the wave velocities of the two different rocks.

$$\frac{sin\theta_2}{sin\theta_1} = \frac{v_2}{v_1}, \qquad \text{EQN 1}$$

Where θ_1, θ_2, V_1, and V_2 are defined in Figure 5.

When waves reach a boundary between different rock types, a portion of the energy is transmitted across the boundary. The transmitted wave travels in a different direction which is dictated by the ratio of velocities of the two rock types (Figure 5). Geophones positioned at the surface detect the return of the waves.

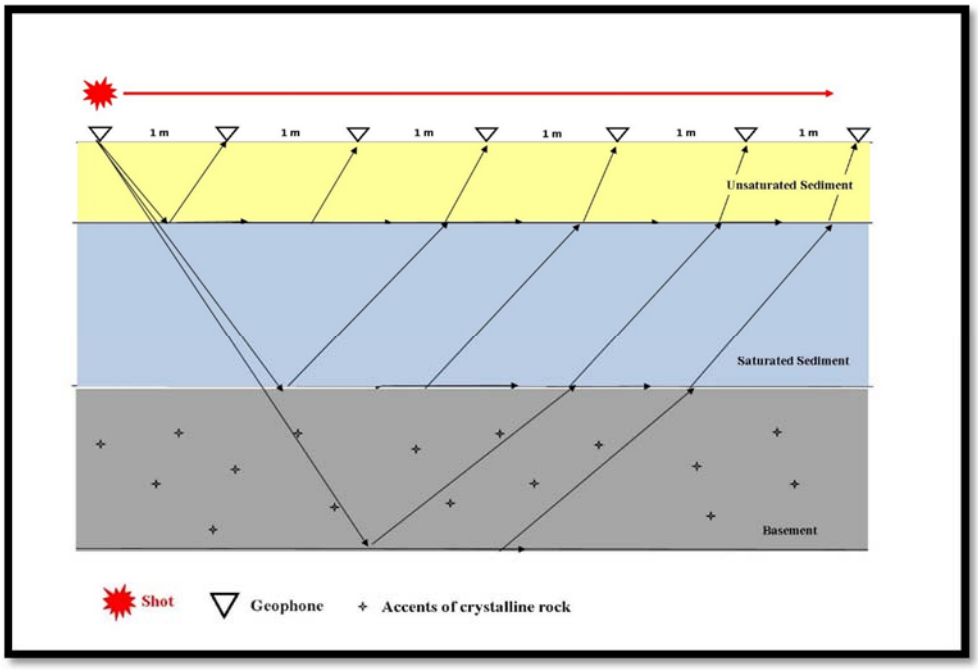

Figure 4. *Illustration of refraction of the three layer model. The first layer is the unsaturated colluvium where the first interface represents the water table, layer two the saturated colluvium, and layer three represents the gneiss bedrock.*

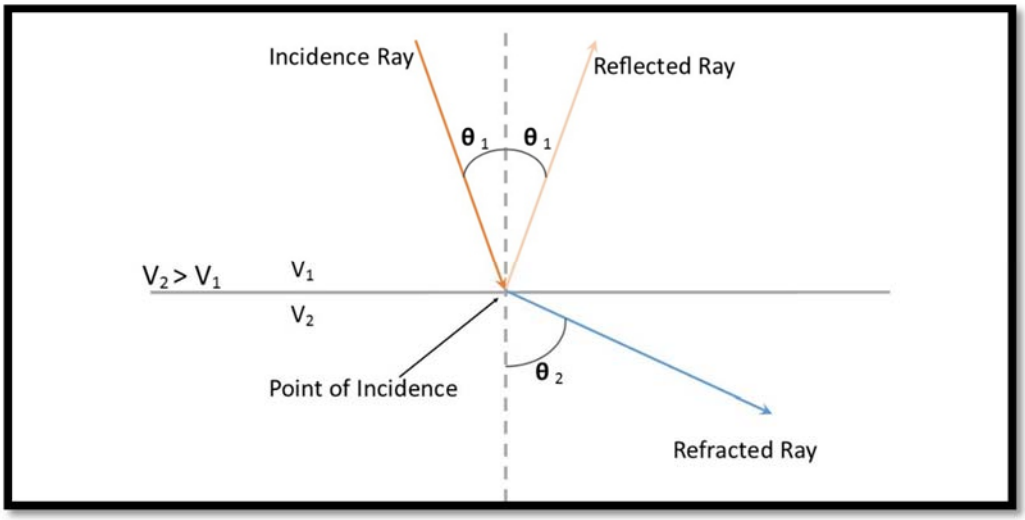

Figure 5. *Diagram showing the path of a ray as it reaches the boundary of a slower velocity material, above the boundary, and a faster velocity material, below the boundary. The ray can be seen to bend away from the vertical as it moves to the faster velocity. If the situation was reversed (i.e. the faster velocity material was above the boundary) the ray would bend closer to the vertical and would be pointing almost straight down (Sabra, 1981).*

GPS Survey

Before we collected the GPS coordinates, each seismic line was measured and flagged. The Virginia City seismic lines 1-3 were across the creek and the fourth seismic line was parallel with the creek valley (Figure 2). We surveyed every geophone on the seismic line using a Leica GS-15 Rover on a leveling rod (Figure 6). This equipment records coordinates on NAD 1983 Montana State Plane. Before we surveyed each geophone location, the instrument had to collect at least ten iterations.

A base station was setup when this survey began. After multiple troubleshooting efforts, the base station was not used when it would not correct the Leica rover position. The resulting 3DCQ (three dimensional error) for each survey point, without base station corrections, ranged between 2.74 m to 6.71 m.

Figure 6. *GPS survey using the Leica GPS system.*

Seismic Survey

The seismic investigation at four sites near Virginia City, Montana involved collecting seismic profiles using the fixed geophone locations. We established profile lines using pin-flags labeled with station numbers. Then, we collected spatial locations for each station using a Leica GPS system. Seismic survey parameters for the four profiles such as the number of geophones per profile and their spacing are listed in Table 1.

Table 1. Seismic Survey Parameters

Seismic Survey Parameters				
Profile Number	1	2	3	4
Source	226.8 kg (500 lb) Weight Drop	9.07 kg (20 lb) Sledge Hammer	226.8 kg (500 lb) Weight Drop	226.8 kg (500 lb) Weight Drop
Number of Geophones	113	144	134	134
Geophone Spacing (m)	1	1	1	2
Shot Spacing (m)	2	2	2	4
Last Geophone Shot	103	135	127	127
Perpendicular Source Offset (m)	2	0.5	2	2
Stacks per Station	3	9	3	3

Profile 1, 3, and 4 all use the same 226.8 kg (500 lb) weight drop, which is mounted to a trailer (Figure 7), to generate a source signal for imaging the subsurface. Profile 2 is in an area that was inaccessible by our truck; instead, a 9.07 kg (20 lb) sledge hammer (Figure 8) was used for generating a source signal. Poor data collection is observed in profile 2 where the profile crosses Alder Creek, and no geophones could be placed on the bridge across the creek. The source signals generated from these hammer drops would then trigger the seismograph to begin recording (Figure 9). After collecting measurements, we processed the GPS elevations and seismic refraction data and were then able to interpret the results from our survey.

Figure 7. *Large weight drop used on this survey.*

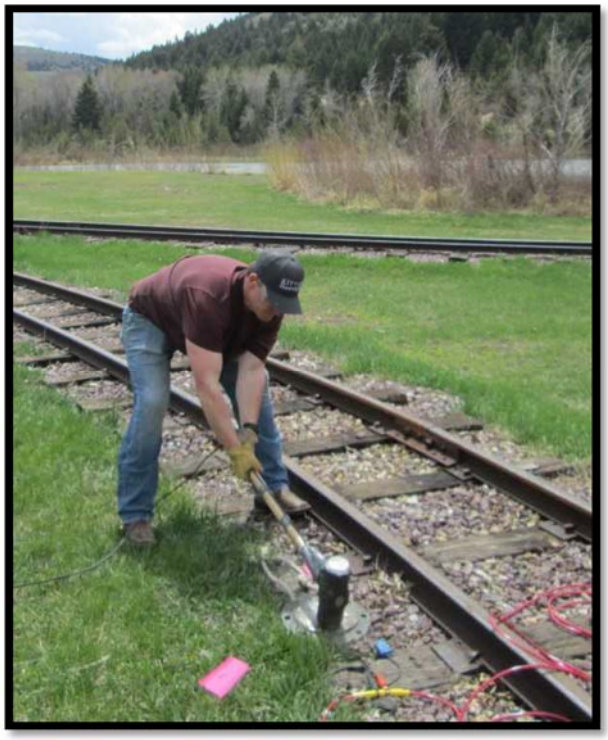

Figure 8*. The 9.07 kg (20 lb) sledgehammer used on this survey.*

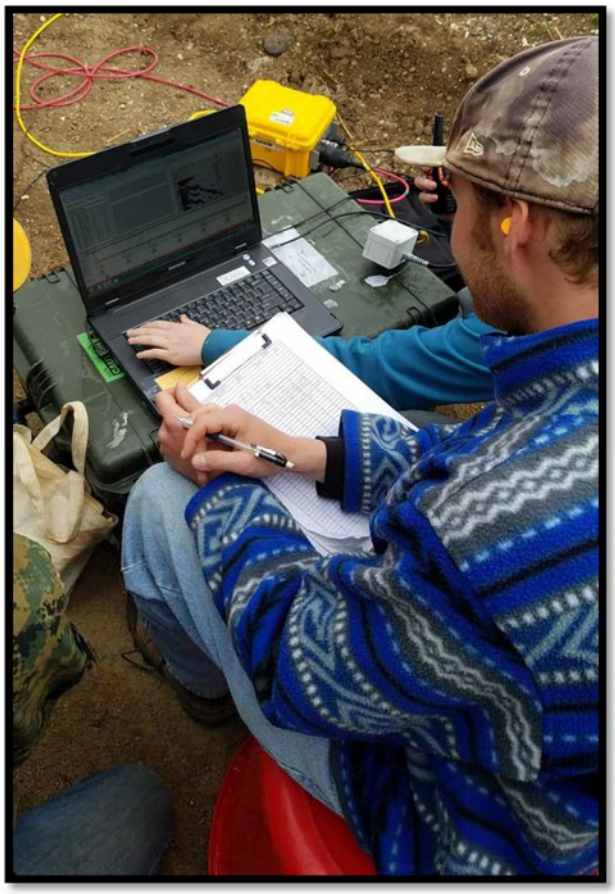

Figure 9*. Seismic data collected in the field and recorded on a laptop computer.*

Data Processing

The data reduction procedure involved correcting relative GPS data and processing our seismic refraction data using two software packages: Vista 2D-3D Seismic Processing 2013 and Rayfract version 3.22. We corrected GPS spatial locations in ArcGIS from NAD 1983 Montana State Plane coordinate system to UTM 12N, with northing and easting coordinates. We then, applied an exponential smoothing filter to GPS elevation values. Table 2 describes the broad overview of the seismic processing steps.

Figure 10 shows the first breaks that we picked using VISTA, a 64-bit processing software copyrighted by Schlumberger to construct the geometry that we imported into Rayfract. We

estimated subsurface velocities of the direct arrival, saturated fill, and basement from the slopes of these first break picks.

Table 2. Data Processing Techniques

Data Processing Steps	
VISTA 2D-3D Seismic Processing 2013	Applied an exponential smoothing filter to GPS elevation data
	Uploaded geometry for each seismic profiles to integrate elevations with first arrival times
	Picked first-breaks for refractions
Rayfract 3.22	Defined header information, which integrates station spacing and file ID's for each line
	Imported ASCII first break picks and elevations
	Updated elevation information for shots and receivers
	Preformed smoothing inversion with 20 iterations to obtain a 1-D initial velocity gradient model and 2-D WET (Wavepath Eikonal Traveltime) tomography. This accounts for uncertainty in first break picks and eliminates noise from traces; WET tomography also interpolates any missing traces.
	Combined 1-D velocity gradient and 2-D WET tomography to produce a 2-D velocity gradient model (Rayfract, 2006).

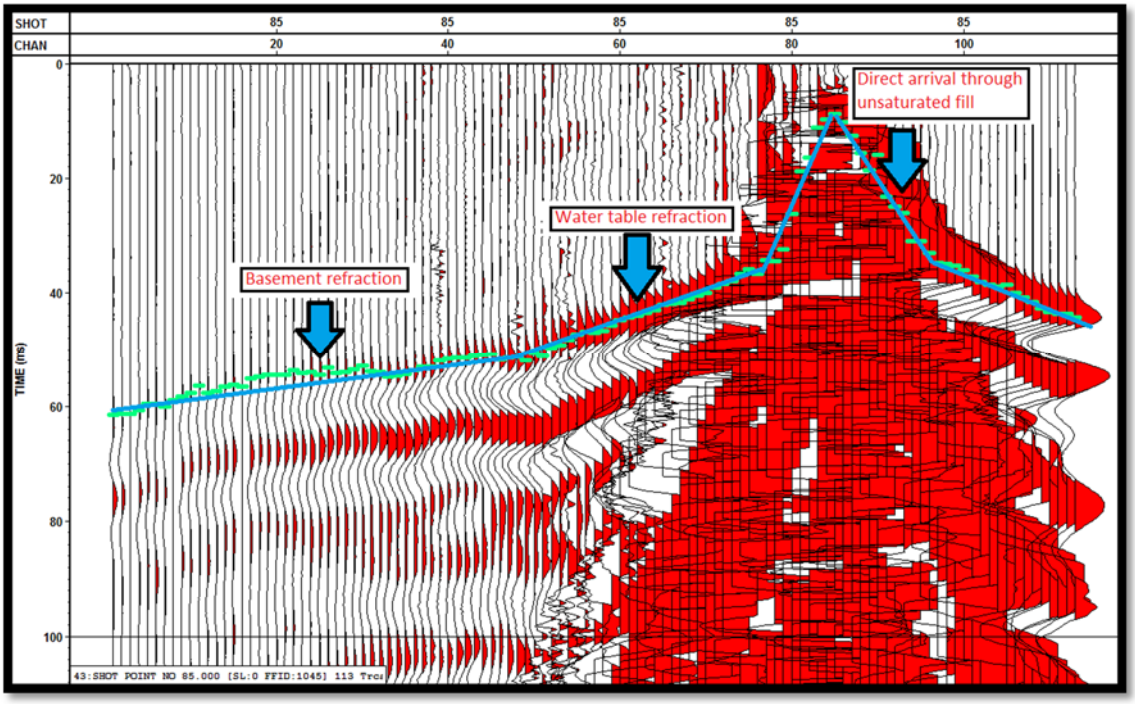

Figure 10*. Shot gather 31 of line 1 showing first break picks (green) and interpreted wave arrivals for velocity estimation (blue). We estimated subsurface velocities of the direct arrival, saturated fill and basement from the slopes of these first break picks.*

Results

After processing, we used 20 iterations of WET inversion using Rayfract 3.22 software. Rayfract produces three different models: a 1D-Gradient smooth initial velocity model, a 2-D-Wavepath Eikonal Traveltime (WET) tomography model, and a 2D-Gradient velocity model. Appendix A shows all of the 1D-Gradient velocity models. Appendix B displays the 2D-WET calculated rays through the subsurface. The 1-D Gradient smooth initial velocity model is used as the starting model to the WET inversion to get the 2-D Gradient velocity model. We chose to use the 2D-Gradient velocity model for interpretation because it outlines seismic velocities that correlate to the thickness of alluvium and depth to basement. Our interpretation of velocities for unsaturated alluvium sediments is 400 m/s, saturated sediments is 1720 m/s, and the basement is 3550 m/s. These are average velocities determined from the slope of first breaks on shot gathers for example Figure 10. Figures 11-14 display the results of our inversion processing; the upper blue line distinguishes the water table, and the lower black line represents the basement depth. Based on these figures, the depth to basement varies across each profile. For the northwest lines 1, 2, and 4, the basement depth ranges from 15 m to 26 m, and we suspect the basement is gneiss. Line 1 and 2 run perpendicular to each other, and show corresponding basement depths of 20 m at their intersection. For the southwest line 3, the basement depth ranges from 20 m to 28 m. Several bad source shots resulted from merging first break picks in VISTA and geometry in ASCII format to Rayfract. The problem may be in the geometry file or in the first break file. We

attempted to correct both the first breaks and the geometry multiple times with no resolution. The RMS error for all the profiles is below 3.5%.

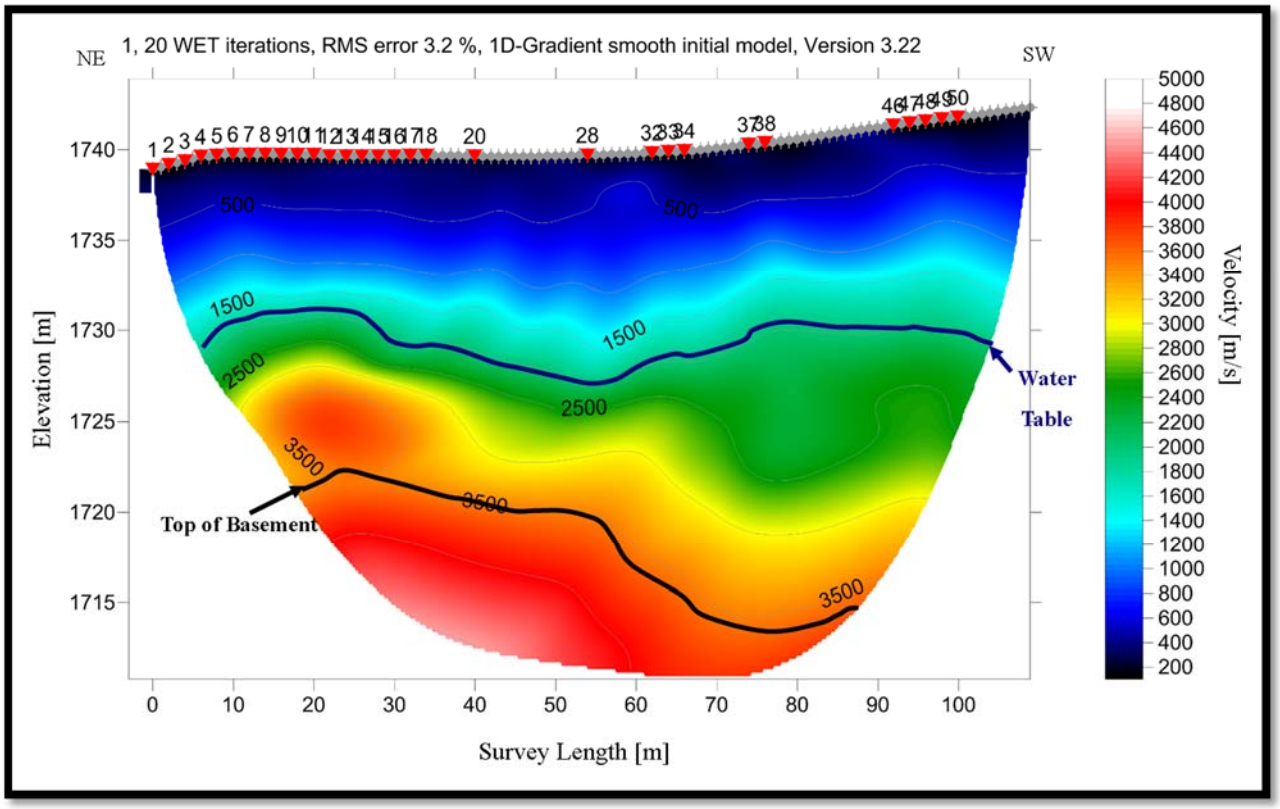

Figure 11. *Displayed above is the 2-D velocity model of survey line 1 using 20 iterations of Wavepath Eikonal Traveltime (WET) inversion. Based on the interpretation of the above velocity model, the thickness of the unsaturated unconsolidated layer is the upper line, the lower line is to bedrock .*

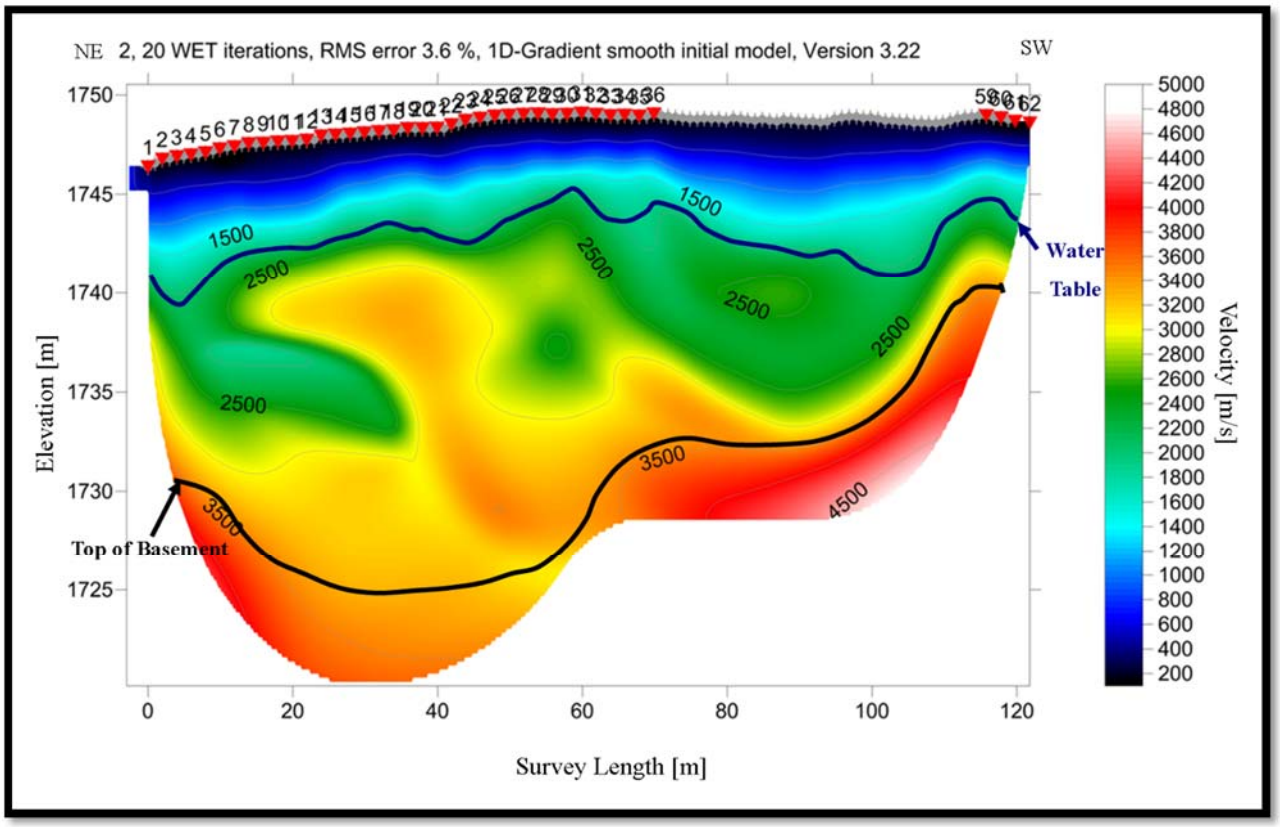

***Figure 12**. Displayed above is the 2-D velocity model of survey line 2 using 20 iterations of Wavepath Eikonal Traveltime (WET) inversion.*

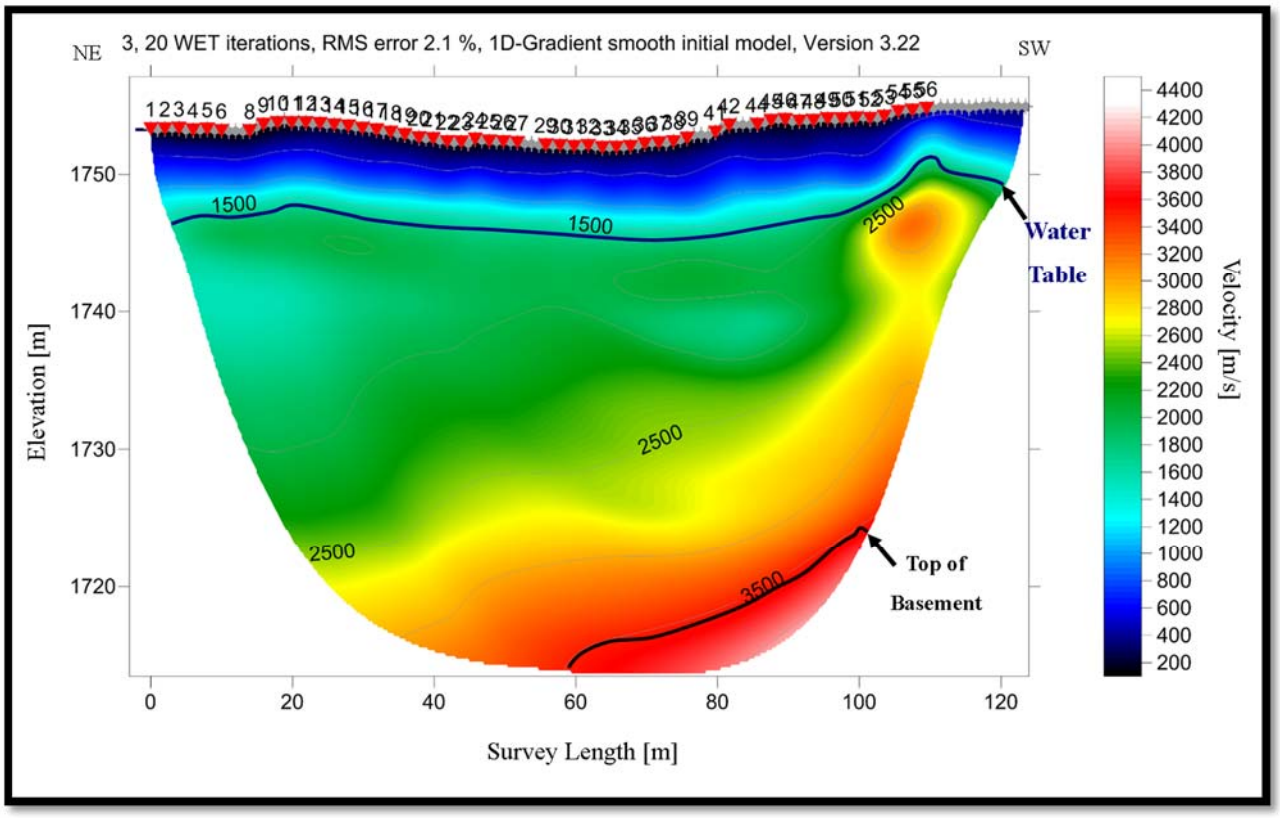

Figure 13*. Displayed above is the 2-D velocity model of survey line 3 using 20 iterations of Wavepath Eikonal Traveltime (WET) inversion. Based on the interpretation of the above velocity model, the thickness of the unsaturated unconsolidated layer is the upper line, the lower line is to bedrock .*

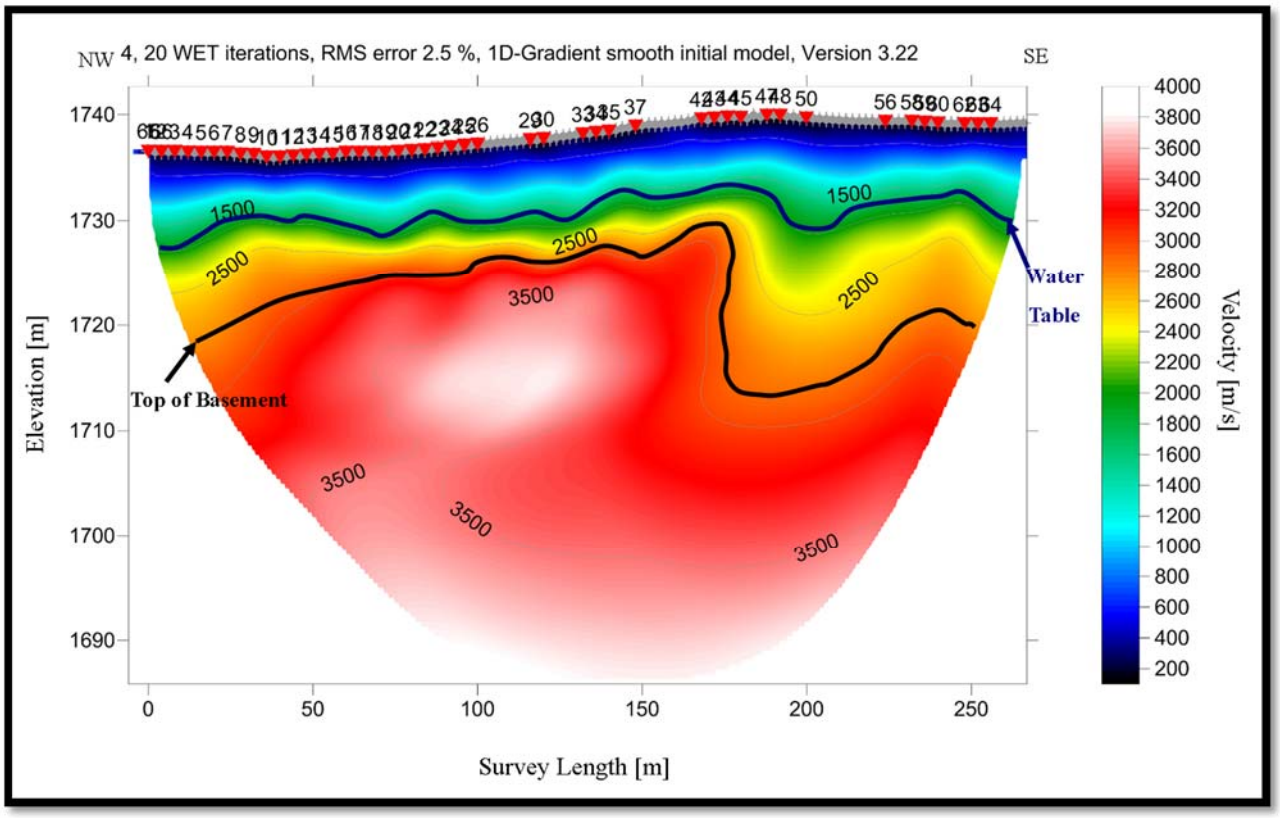

Figure 14. *Displayed above is the 2-D velocity model of survey line 4 using 20 iterations of Wavepath Eikonal Traveltime (WET) inversion. Based on the interpretation of the above velocity model, the thickness of the unsaturated unconsolidated layer is the upper line, the lower line is to bedrock.*

Conclusions

The seismic refraction method provides detailed information regarding thickness of subsurface layers by distinguishing between the different velocities of each layer. The geology for this area is an Archean gneiss basement overlain by Tertiary Volcanics with interbedded gravels. The purpose of our project was to determine the basement depth, and alluvium thickness, for the unconfined aquifer near Virginia City, Montana. Our 2-D velocity profiles produced from seismic refraction first arrivals show basement material, saturated alluvium sediments, and unsaturated alluvium sediments. The seismic velocity for unsaturated sediments is 400 m/s and for saturated sediments is 1720 m/s (corresponding to the seismic velocity of water). We determine the basement velocity to be 3550 m/s, which corresponds to a consolidated crystalline material. By inversion in Rayfract, the depth to basement ranges from 15 to 28 meters, depending on the survey line.

References

Daniel, Faith, and Richard B. Berg, 1981, Radiometric Dates of Rocks in Montana, Bulletin 114. Butte, MT: Montana Bureau of Mines and Geology.

Despotovic, Pero, Geology and Geochemistry of Au-Ag-Mineralizations in the Virginia City Mining District (VCMD), Montana, U.S.A, Master's thesis, Technical University of Berlin, 2000.

ESRI. *USA Topo Map* [basemap]. Scale not given. National Geographic Society, 2018

Google Earth Pro, 2014, July 19, Virginia City, Montana, Eye alt 8613 feet, Google Images 2018.

Kellog, Karl S. and Van S. Williams, *Geologic Map of the Ennis 30'x60' Quadrangle, Madison and Gallatin Counties, Montana and Park County, Wyoming* [map], 1:100,000, MBMG Open File 529, Butte, MT.: MBMG, 2006.

Krogh, Thomas E., Sandra L. Kamo, Thomas B. Handley, David F. Hess, Peter S. Dahl, and Robert E. Johnson. 2011. *Geochronology and geochemistry of Precambrian gneisses, metabasites, and pegmatite from the Tobacco Root Mountains, northwestern Wyoming craton, Montana*. Vol. 48, Ottawa, ON: NRC Research Press.

Montana State Library. *Cadastral: State Boundary* [map], 1:6,000,000, Montana State Library, Helena, MT, 2018.

Rayfract Manual, 2006, Rayfract Tutorial Manual: Intelligent Resources.

Ruppel, Edward T., and Yuguang, Liu. 2004, *The Gold Mines of the Virginia City Mining District, Madison County, Montana,* Bulletin 113, Butte, MT: Montana Bureau of Mines and Geology.

Sabra, A. I., 1981, Theories of Light from Descartes to Newton: Cambridge University Press.

Vitaliano, Charles J., and William S Cordua, *Geologic Map of Southern Tobacco Root Mountains, Madison County, Montana* [map]. 1:62,500. Map and Chart Series. Boulder, CO.: GSA, 1979.

Appendices

Appendix A. 1-D Gradient Profiles

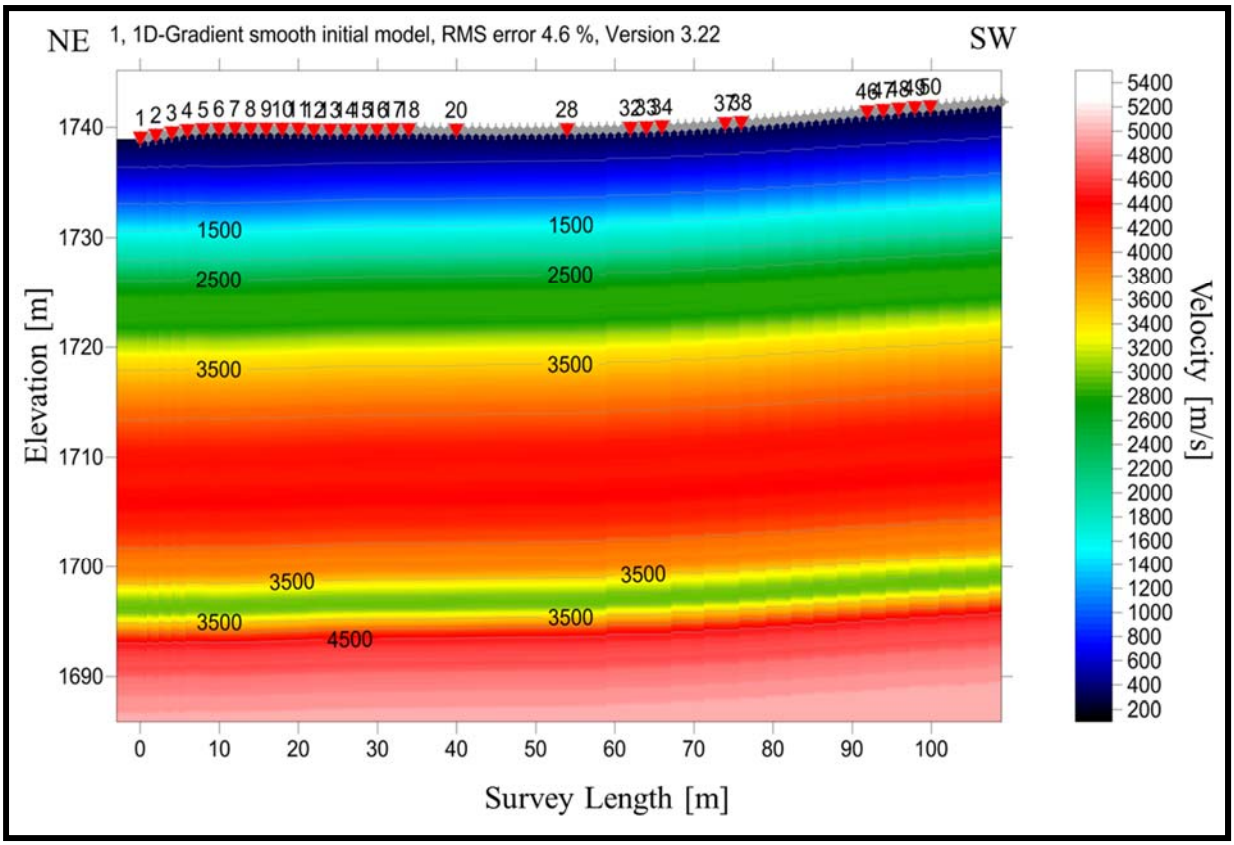

Figure A.1*. 1-D gradient used as initial model for WET inversion of line 1.*

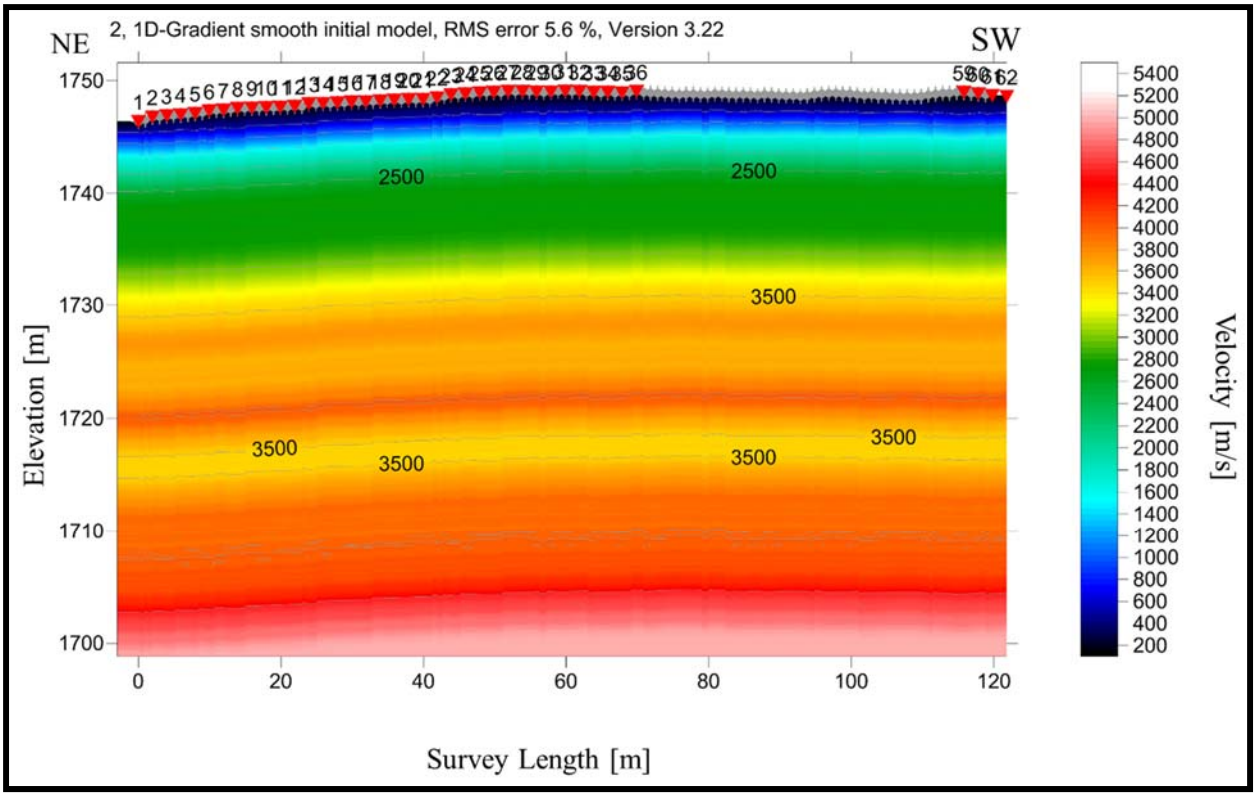

Figure A.2*. 1-D gradient used as initial model for WET inversion of line 2.*

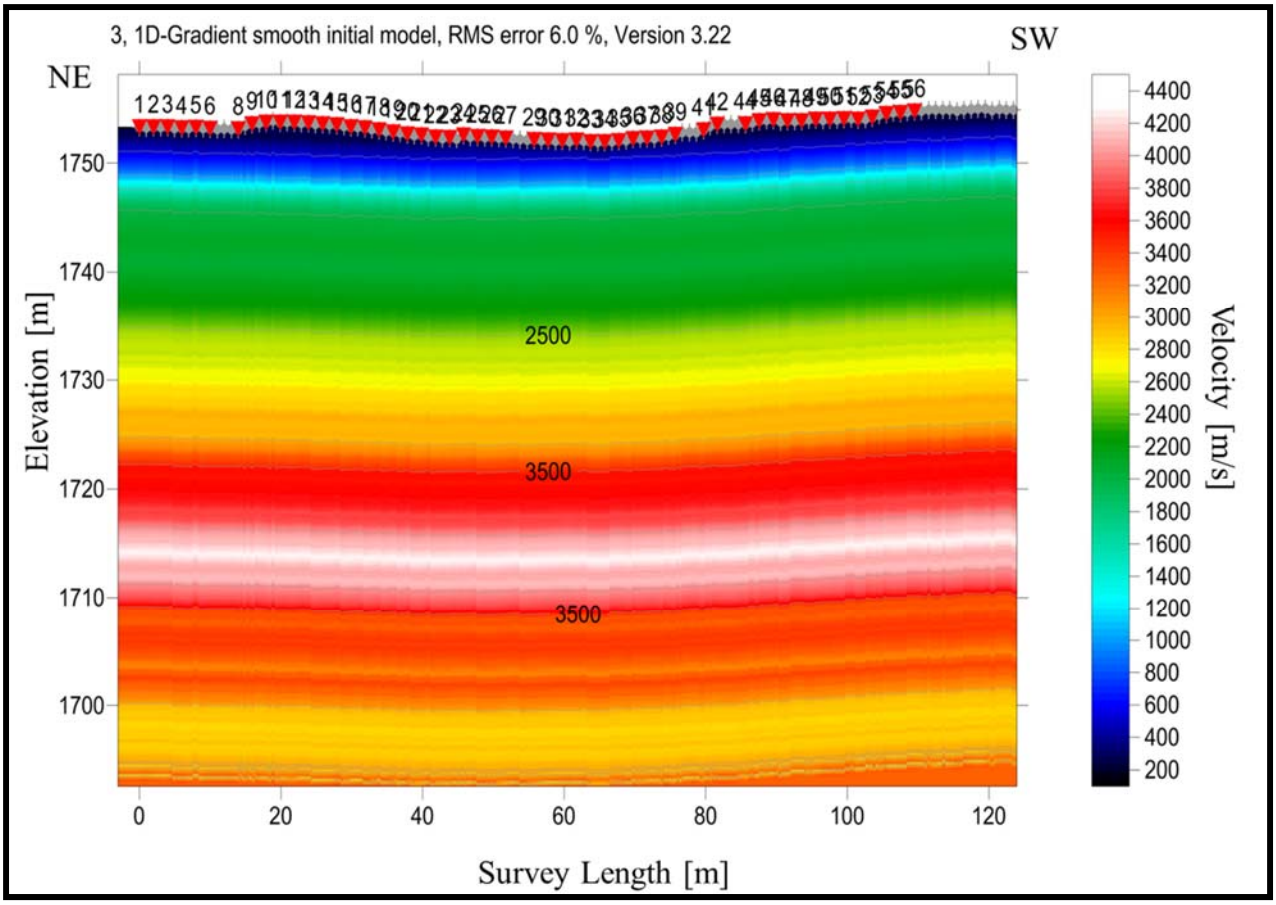

Figure A.3*. 1-D gradient used as initial model for WET inversion of line 3.*

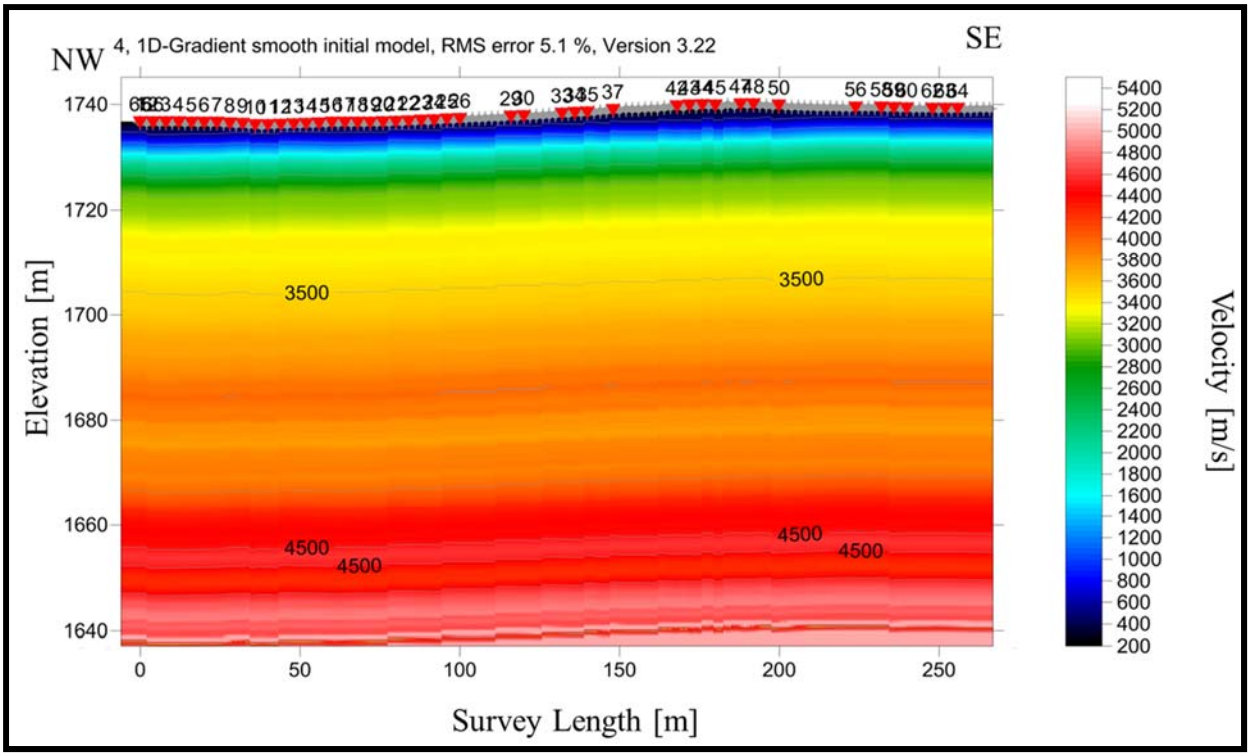

Figure A.4*. 1-D gradient used as initial model for WET inversion of line 4.*

Appendix B. Predicted Ray Paths

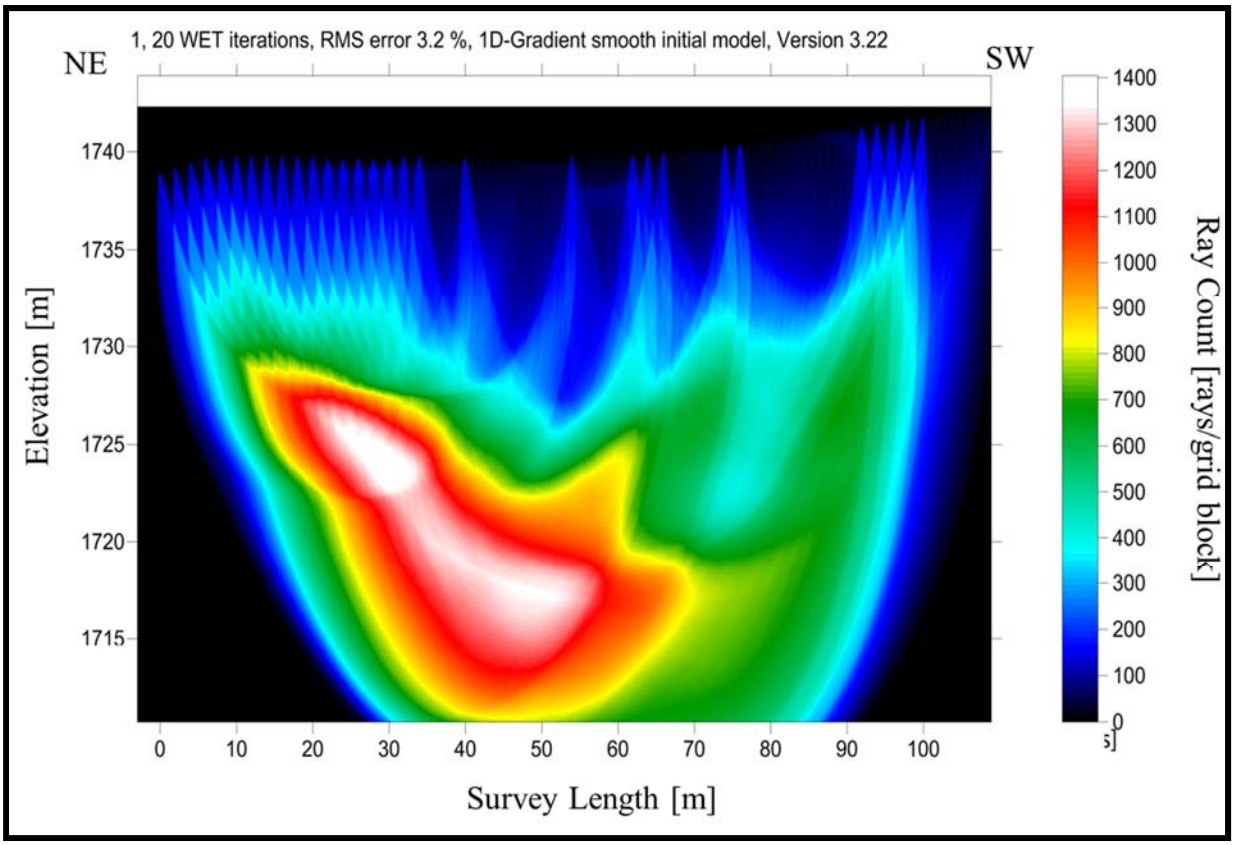

Figure B.1. *Predicted ray paths through the subsurface of profile 1.*

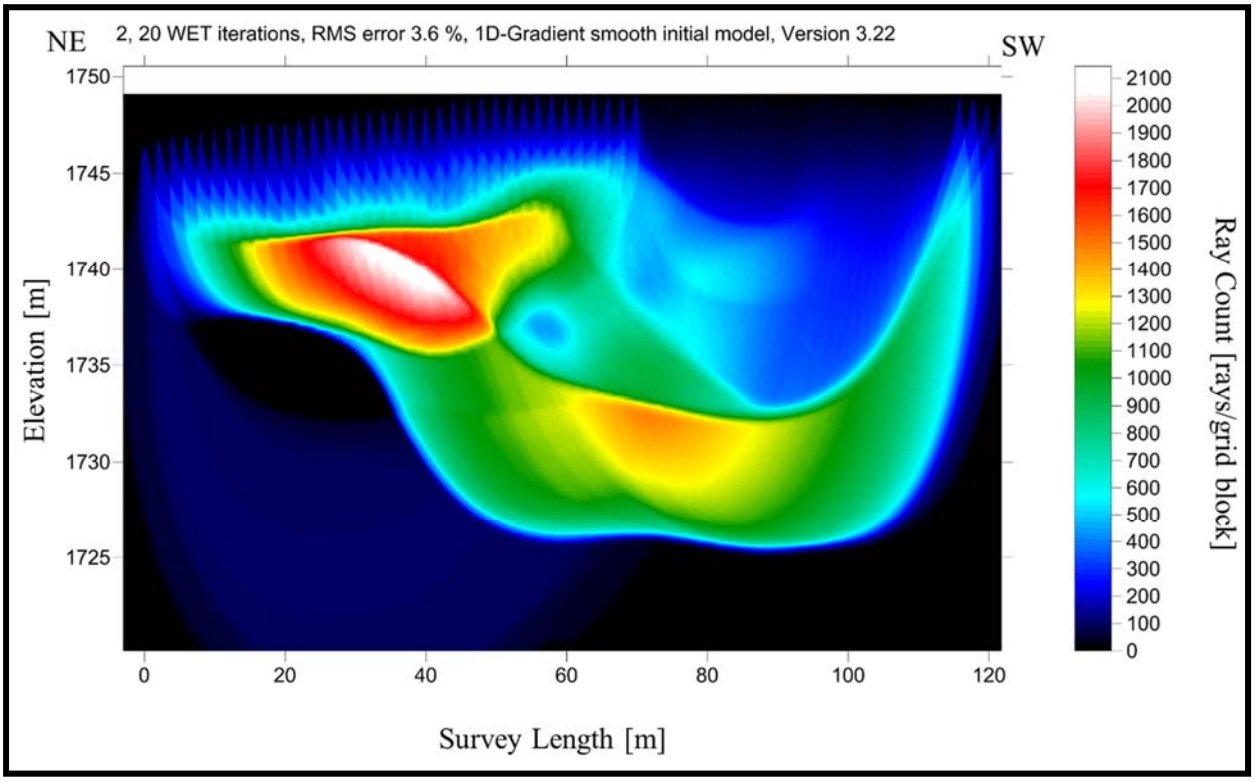

Figure B.2. *Predicted ray paths through the subsurface of profile 2.*

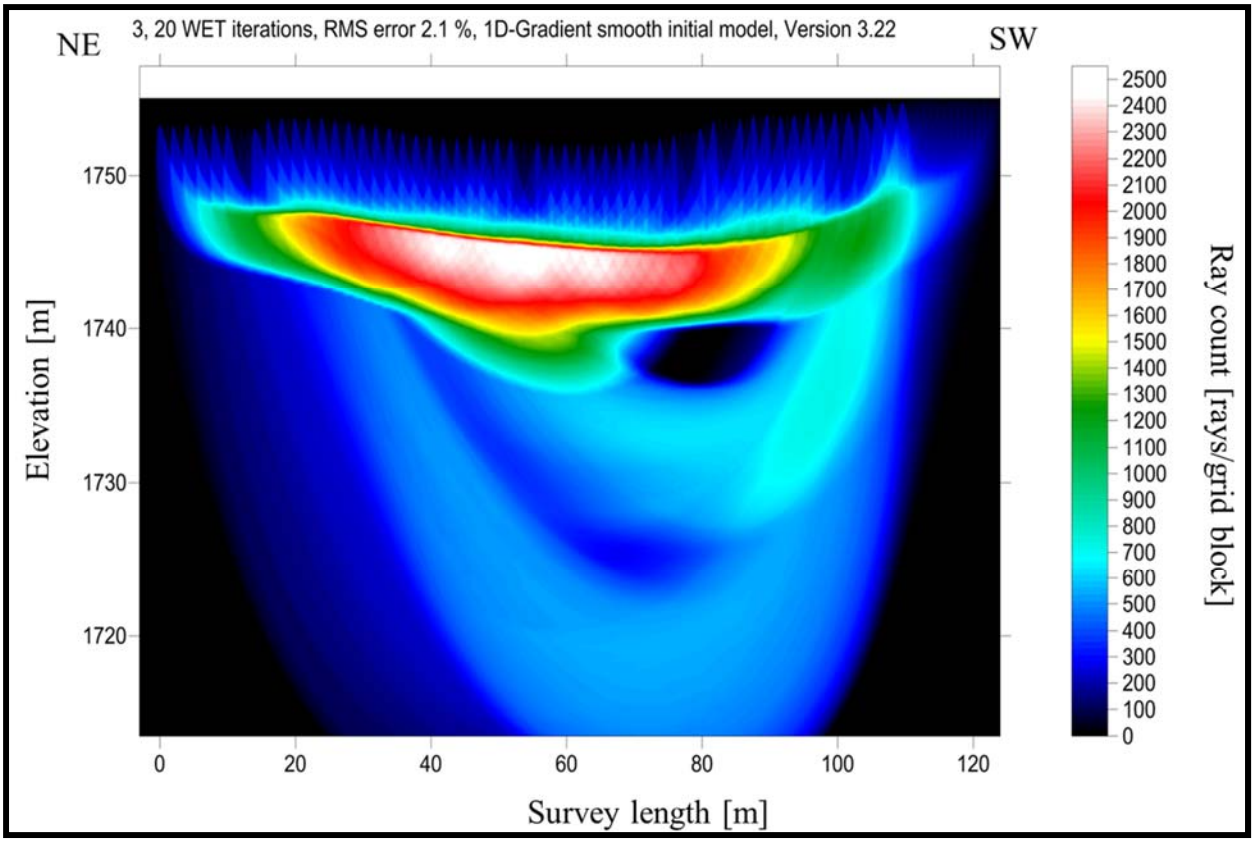

Figure B.3. *Predicted ray paths through the subsurface of profile 3.*

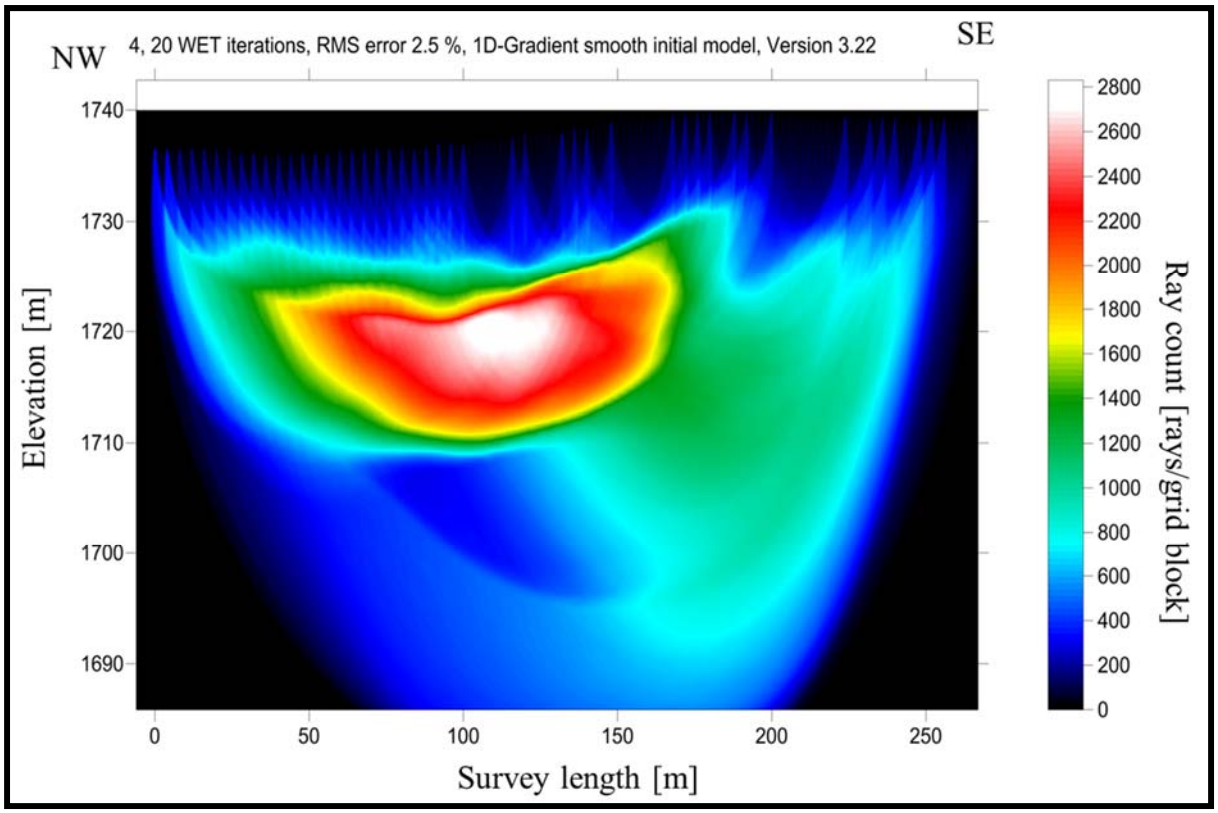

Figure B.4. *Predicted ray paths through the subsurface of profile 4.*

Appendix C. Line 1 GPS Coordinates

Each record includes 113 stations.

Station #	Latitude	Longitude	Elevation (m.)
1	45.29510832	-111.9524243	1741.495526
2	45.29510353	-111.9524325	1741.431214
3	45.29509931	-111.9524425	1741.374521
4	45.29509282	-111.9524523	1741.362024
5	45.29508581	-111.9524593	1741.902434
6	45.29508045	-111.9524692	1741.681454
7	45.29506873	-111.9524746	1740.178181
8	45.29506332	-111.9524837	1740.337286
9	45.29506026	-111.9524961	1741.198346
10	45.2950479	-111.9524994	1739.605157
11	45.29504304	-111.9525099	1739.854178
12	45.2950384	-111.9525197	1739.880086
13	45.29503229	-111.9525298	1739.655449
14	45.2950257	-111.9525387	1739.712142
15	45.29501964	-111.9525477	1739.625578
16	45.29501355	-111.9525572	1739.59327
17	45.29500745	-111.9525663	1739.606071
18	45.2950011	-111.952576	1739.63015
19	45.29499583	-111.9525873	1739.392711
20	45.29498687	-111.9525947	1739.93617
21	45.29498399	-111.9526059	1739.47074
22	45.29498064	-111.9526166	1738.69289
23	45.29497123	-111.9526241	1739.496648
24	45.29496268	-111.9526342	1739.714275
25	45.29495819	-111.9526423	1739.70757
26	45.2949515	-111.9526512	1739.687453
27	45.2949463	-111.9526601	1739.706655
28	45.29494037	-111.9526693	1739.713056
29	45.29493268	-111.952679	1739.754814
30	45.29492839	-111.9526889	1739.749937
31	45.29492228	-111.9526977	1739.79779
32	45.2949159	-111.9527073	1739.849911
33	45.29491374	-111.9527124	1739.742622
34	45.2949041	-111.9527256	1739.696597
35	45.29489932	-111.9527354	1739.700864
36	45.29489319	-111.9527446	1739.585345
37	45.29488662	-111.9527541	1739.621616
38	45.2948817	-111.9527634	1739.528347

39	45.29487553	-111.952773	1739.528957
40	45.29487182	-111.9527815	1739.504573
41	45.29486653	-111.9527908	1739.490857
42	45.29486108	-111.9528	1739.580468
43	45.29485237	-111.9528129	1739.589917
44	45.29484698	-111.9528231	1739.592355
45	45.2948415	-111.9528334	1739.674651
46	45.29483626	-111.9528436	1739.635942
47	45.29483079	-111.9528537	1739.680747
48	45.29482538	-111.9528639	1739.753899
49	45.29482005	-111.9528744	1739.822174
50	45.29481435	-111.9528847	1739.84412
51	45.294809	-111.9528954	1739.833452
52	45.29480335	-111.9529055	1739.925502
53	45.29479795	-111.9529152	1739.881001
54	45.29479216	-111.9529265	1739.888621
55	45.2947872	-111.9529367	1739.89685
56	45.29478219	-111.9529478	1739.99591
57	45.2947766	-111.952959	1740.024257
58	45.29477172	-111.9529684	1740.002311
59	45.29476632	-111.9529788	1740.095275
60	45.2947618	-111.9529893	1740.150749
61	45.29475657	-111.9529999	1740.24097
62	45.29475169	-111.9530107	1740.307111
63	45.29474961	-111.9530196	1740.26383
64	45.2947459	-111.953029	1740.307416
65	45.29473979	-111.953042	1740.387883
66	45.29473517	-111.9530509	1740.43909
67	45.29473096	-111.9530596	1740.482371
68	45.29472241	-111.9530742	1740.698779
69	45.29471778	-111.953085	1740.790829
70	45.29471271	-111.9530958	1740.957859
71	45.29470787	-111.9531064	1741.080389
72	45.29470354	-111.9531166	1741.145311
73	45.29469754	-111.9531267	1741.002055
74	45.2946919	-111.9531377	1740.996569
75	45.29468836	-111.9531481	1741.105078
76	45.29468258	-111.9531586	1741.255039
77	45.29467724	-111.9531693	1741.340993
78	45.29467211	-111.9531795	1741.484858
79	45.29466698	-111.9531901	1741.597025

80	45.29466179	-111.9532013	1741.643659
81	45.29465723	-111.9532118	1741.765579
82	45.29465239	-111.9532223	1741.83995
83	45.29464749	-111.9532335	1741.950898
84	45.29464251	-111.953244	1742.097506
85	45.29463784	-111.9532543	1742.165477
86	45.29463326	-111.9532647	1742.191385
87	45.29462852	-111.9532755	1742.228875
88	45.29462372	-111.9532855	1742.308733
89	45.29461897	-111.9532973	1742.357196
90	45.29461428	-111.9533085	1742.392553
91	45.29460957	-111.9533196	1742.485212
92	45.29460463	-111.9533306	1742.430043
93	45.29460041	-111.9533404	1742.501671
94	45.29459524	-111.953353	1742.482774
95	45.29459099	-111.9533637	1742.568727
96	45.29458692	-111.9533752	1742.738806
97	45.29458175	-111.9533865	1742.914066
98	45.29457703	-111.9533955	1742.547086
99	45.29457261	-111.9534055	1742.652242
100	45.29456787	-111.9534164	1742.674188
101	45.29456437	-111.9534269	1742.89212
102	45.29456028	-111.9534398	1742.964662
103	45.29455693	-111.9534515	1742.997886
104	45.29454875	-111.9534662	1743.167354
105	45.29454461	-111.9534775	1743.227705
106	45.29454025	-111.9534895	1743.275254
107	45.29453484	-111.9535	1743.311525
108	45.29453034	-111.953511	1743.376142
109	45.29452501	-111.9535213	1743.336518
110	45.29452032	-111.9535319	1743.267634
111	45.29451519	-111.9535424	1743.314268
112	45.29451052	-111.9535536	1743.322802
113	45.29450592	-111.9535648	1743.399917

Appendix D. Line 2 GPS Coordinates

Each record includes 135 stations.

Station #	Latitude	Longitude	Elevation (m.)
1	45.292728	-111.94905	1750.1927
2	45.292664	-111.94912	1750.7313
3	45.292015	-111.94981	1747.48
4	45.292005	-111.94981	1748.3395
5	45.292	-111.94982	1747.8494
6	45.291992	-111.94983	1747.8756
7	45.291983	-111.94983	1748.2648
8	45.291973	-111.94985	1748.0567
9	45.291963	-111.94985	1748.9256
10	45.291956	-111.94986	1749.2228
11	45.291951	-111.94987	1748.6577
12	45.291946	-111.94988	1747.8658
13	45.292659	-111.94913	1749.9934
14	45.291939	-111.94989	1747.8802
15	45.291931	-111.9499	1747.9783
16	45.291924	-111.9499	1747.9811
17	45.291917	-111.94991	1748.0533
18	45.29191	-111.94992	1748.0463
19	45.291902	-111.94993	1747.9777
20	45.291896	-111.94993	1748.0323
21	45.291889	-111.94994	1748.0999
22	45.29188	-111.94995	1748.1795
23	45.291873	-111.94996	1748.199
24	45.292648	-111.94913	1752.0087
25	45.291866	-111.94997	1748.2185
26	45.291859	-111.94997	1748.2484
27	45.29185	-111.94998	1748.3465
28	45.291844	-111.94999	1748.5041
29	45.291837	-111.94999	1748.7257
30	45.291829	-111.95	1748.7074
31	45.291823	-111.95001	1748.7117
32	45.291816	-111.95002	1748.6919
33	45.291809	-111.95002	1748.641
34	45.291801	-111.95003	1748.5276
35	45.292644	-111.94915	1750.2369
36	45.291793	-111.95004	1748.4078

37	45.291786	-111.95005	1748.3694
38	45.291779	-111.95005	1748.4486
39	45.291772	-111.95006	1748.4456
40	45.291764	-111.95007	1748.4063
41	45.291757	-111.95008	1748.3758
42	45.292635	-111.94915	1751.7484
43	45.29263	-111.94916	1750.9154
44	45.292622	-111.94917	1750.7334
45	45.292616	-111.94918	1749.7989
46	45.292609	-111.94918	1749.7422
47	45.2926	-111.94919	1749.5767
48	45.292723	-111.94906	1750.2213
49	45.292595	-111.9492	1749.5194
50	45.292584	-111.94921	1749.182
51	45.292577	-111.94922	1749.1945
52	45.292573	-111.94922	1749.7026
53	45.292564	-111.94923	1749.3624
54	45.292557	-111.94924	1749.0911
55	45.29255	-111.94925	1748.7449
56	45.292542	-111.94925	1748.5751
57	45.292534	-111.94926	1748.3151
58	45.292526	-111.94926	1749.936
59	45.292716	-111.94907	1750.2119
60	45.292519	-111.94927	1749.3609
61	45.292513	-111.94928	1748.3642
62	45.292505	-111.94929	1748.3608
63	45.292499	-111.9493	1748.5535
64	45.292492	-111.94931	1748.341
65	45.292484	-111.94932	1748.1591
66	45.292476	-111.94932	1749.8531
67	45.292466	-111.94933	1748.135
68	45.292464	-111.94933	1749.0369
69	45.29246	-111.94934	1749.5273
70	45.292709	-111.94908	1750.2418
71	45.292449	-111.94935	1748.1895
72	45.292442	-111.94936	1747.6223
73	45.292434	-111.94937	1748.1277
74	45.292427	-111.94937	1748.3185
75	45.292419	-111.94938	1748.0838

76	45.292411	-111.94939	1748.4849
77	45.292404	-111.94939	1749.2612
78	45.292396	-111.9494	1748.765
79	45.29239	-111.94941	1748.2813
80	45.292383	-111.94942	1748.1341
81	45.292702	-111.94908	1750.3762
82	45.292376	-111.94943	1748.1072
83	45.292369	-111.94944	1747.9862
84	45.292362	-111.94944	1748.0314
85	45.292362	-111.94945	1749.5819
86	45.292347	-111.94946	1747.8905
87	45.29234	-111.94947	1747.968
88	45.292343	-111.94947	1750.286
89	45.292327	-111.94948	1748.2548
90	45.292319	-111.94949	1747.9384
91	45.292311	-111.9495	1747.8902
92	45.292697	-111.9491	1748.9363
93	45.292303	-111.94951	1747.7994
94	45.292294	-111.94951	1749.1542
95	45.292288	-111.9495	1751.368
96	45.292281	-111.94952	1750.147
97	45.292273	-111.94953	1749.6319
98	45.292267	-111.94954	1749.0503
99	45.292255	-111.94955	1747.7558
100	45.292257	-111.94955	1749.1393
101	45.292241	-111.94957	1747.4099
102	45.292234	-111.94957	1747.2672
103	45.292689	-111.9491	1748.8866
104	45.29223	-111.94958	1747.6897
105	45.292227	-111.94959	1748.4514
106	45.292216	-111.9496	1747.7528
107	45.292211	-111.9496	1748.3618
108	45.292204	-111.94961	1748.4084
109	45.292198	-111.94962	1748.6224
110	45.292187	-111.94962	1749.0905
111	45.292178	-111.94963	1750.7188
112	45.292173	-111.94964	1750.8767
113	45.292163	-111.94964	1749.7705
114	45.292681	-111.94911	1749.3923

115	45.292148	-111.94964	1750.1351
116	45.29215	-111.94966	1748.5702
117	45.292144	-111.94967	1747.7528
118	45.292138	-111.94968	1747.939
119	45.29213	-111.94969	1747.6671
120	45.29212	-111.94969	1747.483
121	45.292114	-111.9497	1747.5418
122	45.292107	-111.94971	1747.5906
123	45.292101	-111.94972	1748.1231
124	45.292095	-111.94973	1747.7506
125	45.292672	-111.94911	1750.7194
126	45.292081	-111.94972	1748.8049
127	45.292072	-111.94973	1748.7184
128	45.292066	-111.94974	1748.715
129	45.292062	-111.94975	1747.7479
130	45.292052	-111.94975	1747.8939
2131	45.292051	-111.94977	1746.9877
2132	45.292041	-111.94978	1747.9174
2133	45.292034	-111.94978	1748.3365
2134	45.292031	-111.9498	1747.3215
2135	45.292019	-111.94979	1748.9628

Appendix E. Line 3 GPS Coordinates

Each record includes 134 station.

Station #	Latitude	Longitude	Elevation (m.)
1	45.28976	-111.94494	1753.2998
2	45.289756	-111.94495	1752.6168
3	45.289744	-111.94495	1753.9789
4	45.289736	-111.94495	1753.4684
5	45.289726	-111.94496	1753.2898
6	45.289723	-111.94496	1750.8367
7	45.289704	-111.94495	1753.4784
8	45.289698	-111.94495	1753.4827
9	45.289693	-111.94494	1754.1594
10	45.289687	-111.94495	1752.1492
11	45.289674	-111.94496	1752.3485
12	45.289672	-111.94495	1752.6927
13	45.289653	-111.94495	1753.2937
14	45.289636	-111.94496	1752.1401
15	45.289636	-111.94495	1753.8613
16	45.28961	-111.94494	1759.1139
17	45.289596	-111.94495	1756.969
18	45.289604	-111.94497	1755.3725
19	45.289592	-111.94495	1754.4974
20	45.289577	-111.94493	1757.1857
21	45.289593	-111.94497	1750.3177
22	45.289574	-111.94495	1754.2206
23	45.289567	-111.94497	1753.4446
24	45.289554	-111.94496	1752.2184
25	45.289541	-111.94497	1754.0804
26	45.289534	-111.94496	1752.2854
27	45.289528	-111.94496	1752.9856
28	45.28952	-111.94497	1752.9901
29	45.289504	-111.94497	1752.1324
30	45.289491	-111.94498	1752.2955
31	45.289489	-111.94497	1751.5454
32	45.289474	-111.94496	1752.8975
33	45.289471	-111.94497	1751.1827
34	45.289462	-111.94497	1751.9852
35	45.289452	-111.94497	1751.1616
36	45.289446	-111.94497	1750.8572

37	45.289446	-111.94498	1751.3963
38	45.289437	-111.94498	1751.1757
39	45.289423	-111.94498	1750.1686
40	45.289418	-111.94498	1751.3625
41	45.289402	-111.94498	1752.4619
42	45.289395	-111.94499	1749.8611
43	45.289384	-111.94498	1750.7176
44	45.289375	-111.94499	1751.4369
45	45.289363	-111.94497	1752.5235
46	45.289355	-111.94499	1750.9117
47	45.289329	-111.94496	1758.1571
48	45.289342	-111.94499	1750.4448
49	45.289331	-111.945	1751.7228
50	45.289311	-111.94498	1751.3509
51	45.289308	-111.945	1752.6183
52	45.289302	-111.945	1751.482
53	45.289293	-111.945	1752.0504
54	45.289291	-111.945	1750.403
55	45.289277	-111.94501	1751.8886
56	45.289271	-111.945	1750.713
57	45.289262	-111.94499	1752.2129
58	45.289243	-111.94501	1751.325
59	45.289238	-111.945	1751.7158
60	45.289236	-111.94502	1751.6234
61	45.289225	-111.945	1751.7347
62	45.28922	-111.94501	1751.7502
63	45.289202	-111.945	1753.1041
64	45.289199	-111.94501	1751.1824
65	45.289187	-111.94502	1750.3509
66	45.289173	-111.94502	1752.151
67	45.289166	-111.94502	1752.219
68	45.289157	-111.94502	1752.7503
69	45.28915	-111.94502	1752.2528
70	45.289142	-111.94502	1753.0057
71	45.289143	-111.94502	1754.9296
72	45.289125	-111.94503	1753.6903
73	45.289111	-111.94503	1751.9383
74	45.28911	-111.94503	1752.3458
75	45.289114	-111.94503	1754.1584

76	45.289093	-111.94503	1755.1405
77	45.289076	-111.94503	1754.6473
78	45.289056	-111.94504	1757.2247
79	45.289064	-111.94505	1753.1553
80	45.289056	-111.94505	1752.5988
81	45.28903	-111.94503	1756.7011
82	45.28901	-111.94505	1760.2072
83	45.288999	-111.94506	1756.3542
84	45.289019	-111.94508	1754.3267
85	45.289008	-111.94506	1754.0877
86	45.289001	-111.94507	1753.6421
87	45.288996	-111.94508	1753.4544
88	45.288988	-111.94508	1755.99
89	45.288976	-111.94506	1757.0705
90	45.28898	-111.94508	1755.52
91	45.288973	-111.94508	1753.4562
92	45.288956	-111.94508	1751.5509
93	45.288969	-111.94508	1754.2996
94	45.288945	-111.94509	1754.4873
95	45.288918	-111.9451	1753.6083
96	45.288926	-111.9451	1757.1699
97	45.288916	-111.94508	1753.4352
98	45.288901	-111.9451	1752.8978
99	45.288891	-111.9451	1755.2966
100	45.288883	-111.94511	1753.764
101	45.288875	-111.94512	1755.3167
102	45.288872	-111.9451	1755.1582
103	45.288848	-111.94511	1752.3574
104	45.288841	-111.94511	1754.5986
105	45.288838	-111.94511	1756.5837
106	45.288806	-111.94509	1758.5659
107	45.288805	-111.94511	1757.0955
108	45.288798	-111.94511	1756.7636
109	45.288794	-111.94513	1754.3026
110	45.288784	-111.94513	1755.8577
111	45.288778	-111.94514	1756.011
112	45.288776	-111.94514	1755.2643
113	45.288762	-111.94515	1757.3616
114	45.288755	-111.94514	1754.1502

115	45.288743	-111.94516	1755.6172
116	45.288732	-111.94516	1754.5736
117	45.288726	-111.94516	1753.056
118	45.288712	-111.94517	1756.9373
119	45.288711	-111.94517	1755.595
120	45.2887	-111.94517	1756.2329
121	45.288698	-111.94518	1754.3505
122	45.288697	-111.94518	1752.9264
123	45.288686	-111.94519	1756.1637
124	45.288674	-111.94519	1754.5449
125	45.288669	-111.94519	1754.4861
126	45.288658	-111.94519	1754.9079
127	45.28865	-111.94519	1754.7184
128	45.28864	-111.94519	1754.4946
129	45.28863	-111.94519	1754.4904
130	45.288622	-111.9452	1754.9848
131	45.288614	-111.94521	1755.1561
132	45.288605	-111.94521	1755.3094
133	45.288596	-111.94521	1755.4724
134	45.288587	-111.94521	1755.456

Appendix F. Line 4 GPS Coordinates

Each record includes 134 stations.

Shot Record #	Latitude	Longitude	Elevation (m.)
1	45.29495102	-111.9524562	1736.43859
2	45.29493805	-111.9524378	1736.211209
3	45.29492155	-111.9524237	1736.555633
4	45.29490858	-111.9524061	1736.383726
5	45.2948948	-111.9523902	1736.393784
6	45.29488181	-111.9523729	1736.287104
7	45.29486989	-111.9523525	1735.800948
8	45.29485449	-111.9523387	1736.312402
9	45.29484078	-111.9523219	1736.241079
10	45.29482677	-111.9523055	1736.33191
11	45.29481411	-111.9522905	1736.341054
12	45.29479856	-111.9522732	1736.588551
13	45.29478935	-111.9522493	1734.848448
14	45.29477592	-111.9522318	1734.717994
15	45.29476148	-111.9522177	1735.149895
16	45.29474395	-111.952213	1736.821418
17	45.29473656	-111.9521752	1733.65607
18	45.29472288	-111.9521592	1733.714897
19	45.29470548	-111.9521509	1734.963053
20	45.29468652	-111.9521485	1737.206381
21	45.29467621	-111.9521325	1737.16889
22	45.29465936	-111.9521127	1736.97961
23	45.29464544	-111.9520927	1736.591904
24	45.29462872	-111.9520793	1737.209429
25	45.29461839	-111.9520611	1736.65134
26	45.29460361	-111.952046	1736.911944
27	45.29458875	-111.9520287	1736.8647
28	45.2945751	-111.9520118	1736.781794
29	45.29455833	-111.9519984	1737.488016
30	45.29454294	-111.9519828	1738.092739
31	45.29453476	-111.9519617	1736.796425
32	45.29452303	-111.9519431	1736.43798
33	45.29451057	-111.9519263	1736.40049
34	45.29449734	-111.95191	1736.50595
35	45.29448373	-111.9518937	1736.802521
36	45.29446723	-111.9518732	1736.541612
37	45.29445502	-111.95186	1737.018929
38	45.29444033	-111.9518425	1737.064954

39	45.2944276	-111.9518265	1737.267341
40	45.2944132	-111.9518107	1737.350856
41	45.294402	-111.9517931	1737.629443
42	45.29438552	-111.9517786	1737.792206
43	45.29437199	-111.9517615	1737.897667
44	45.29435783	-111.9517432	1737.993984
45	45.29434527	-111.951727	1737.981792
46	45.29433037	-111.9517116	1738.035437
47	45.29431815	-111.9516935	1738.055554
48	45.29430355	-111.9516777	1738.13785
49	45.29429018	-111.9516608	1738.260379
50	45.29427607	-111.9516444	1738.278362
51	45.29426297	-111.9516272	1738.302137
52	45.29424749	-111.9516098	1738.317377
53	45.29423823	-111.9515972	1738.362182
54	45.29422649	-111.951584	1738.339932
55	45.29421218	-111.9515686	1738.516716
56	45.29419733	-111.9515486	1738.332007
57	45.29418389	-111.9515339	1738.637722
58	45.29416976	-111.9515182	1738.719103
59	45.2941554	-111.9515019	1738.785854
60	45.2941418	-111.9514858	1738.905031
61	45.29414166	-111.9514796	1738.916004
62	45.29412923	-111.9514679	1739.306758
63	45.29411612	-111.9514505	1739.368327
64	45.29410128	-111.9514344	1739.309501
65	45.29408839	-111.9514177	1739.456414
66	45.29407457	-111.9514016	1739.516155
67	45.29406082	-111.9513854	1739.582602
68	45.29404948	-111.9513734	1739.685624
69	45.29403941	-111.95136	1739.657582
70	45.29402345	-111.9513429	1739.237568
71	45.29400078	-111.9513135	1740.873125
72	45.293991	-111.9512988	1741.642135
73	45.29397324	-111.9512806	1740.701522
74	45.29395963	-111.9512638	1740.762178
75	45.29394581	-111.9512467	1740.719506
76	45.29393191	-111.9512305	1740.690245
77	45.29391344	-111.9512097	1739.62314
78	45.29390443	-111.9511955	1739.825222
79	45.29389046	-111.951178	1739.886792

80	45.29387696	-111.951163	1740.243408
81	45.29386357	-111.9511472	1740.59149
82	45.29384926	-111.9511319	1741.008456
83	45.29383572	-111.951118	1742.369693
84	45.29382178	-111.9510995	1740.966089
85	45.2938089	-111.9510772	1738.107979
86	45.29379386	-111.9510685	1742.786659
87	45.29378049	-111.9510462	1738.817249
88	45.29376583	-111.9510311	1742.03929
89	45.29375359	-111.9510145	1740.656717
90	45.29374007	-111.9509954	1738.522507
91	45.29372628	-111.9509797	1738.813896
92	45.2937112	-111.9509705	1744.321632
93	45.29369866	-111.9509443	1737.341407
94	45.29368372	-111.9509342	1742.162429
95	45.29366708	-111.9509115	1741.166647
96	45.29365641	-111.9508972	1738.788902
97	45.29364255	-111.9508794	1738.570666
98	45.29362904	-111.9508623	1738.621567
99	45.29361591	-111.9508463	1738.712093
100	45.29360152	-111.9508299	1738.826088
101	45.29358807	-111.9508141	1738.753241
102	45.29357356	-111.9507968	1738.620348
103	45.2935596	-111.9507812	1738.780368
104	45.2935463	-111.9507648	1738.767566
105	45.29353273	-111.9507484	1738.788598
106	45.29351813	-111.9507312	1738.759032
107	45.29350507	-111.9507147	1738.853215
108	45.29349173	-111.9506986	1738.941912
109	45.29347783	-111.9506831	1739.24275
110	45.29346394	-111.9506674	1739.127535
111	45.29345053	-111.9506496	1739.240616
112	45.29343645	-111.9506335	1739.514326
113	45.29342293	-111.9506171	1739.54694
114	45.29340943	-111.9506021	1739.458853
115	45.29339583	-111.9505855	1739.377166
116	45.29338212	-111.9505698	1738.825174
117	45.2933698	-111.9505542	1738.40394
118	45.29335665	-111.9505364	1738.393272
119	45.29334219	-111.9505206	1738.53348
120	45.2933291	-111.950503	1738.622482

121	45.29331627	-111.9504857	1738.772443
122	45.29330122	-111.95047	1738.924234
123	45.29328665	-111.950453	1738.908079
124	45.29327408	-111.950437	1738.781282
125	45.29326002	-111.9504197	1738.877904
126	45.29324693	-111.950402	1739.100103
127	45.29323232	-111.9503867	1739.100103
128	45.29321865	-111.95037	1739.201906
129	45.29320508	-111.9503541	1739.248846
130	45.2931913	-111.9503369	1739.272925
131	45.293178	-111.9503214	1739.489638
132	45.29316575	-111.9503053	1739.66185
133	45.293152	-111.9502875	1739.762738
134	45.29313882	-111.9502711	1739.846863

Appendix G. Line 1 Observer Notes

Montana Tech Observer Notes Date: 5/7/2018- 5/13/2018
State: MT County: Madison
Remarks: Line 1
Receivers: 1,2,3,…113
Shots: 1,2,3….52
Last shot 103
Receiver Interval 1.0 m.
Shot Interval 2.0 m., 3 stacks,
Lateral Offset: 2.0 m.
Notes: 120 channel system used, only 113 channels live.

SP#	FFID	Station#	1st	113th	Notes
1	1000	1	1	113	Good
2	1001	3	1	113	Bad record
2	1002	3	1	113	Good
3	1003	5	1	113	Good
4	1004	7	1	113	Good
5	1005	9	1	113	Good
6	1006	11	1	113	Good
7	1007	13	1	113	Good
8	1008	15	1	113	Good
9	1009	17	1	113	Good
10	1010	19	1	113	Good
11	1011	21	1	113	Good
12	1012	23	1	113	Good
13	1013	25	1	113	Good
14	1014	27	1	113	Good
15	1015	29	1	113	Good
16	1016	31	1	113	Good
17	1017	33	1	113	Good
18	1018	35	1	113	Good
19	1019	37	1	113	Bad record
19	1020	37	1	113	Good
20	1021	39	1	113	Good
21	1022	41	1	113	Good
22	1023	43	1	113	Good
23	1024	45	1	113	Good
24	1025	47	1	113	Good
25	1026	49	1	113	Good
26	1027	51	1	113	Good
27	1028	53	1	113	Bad record

27	1029	53	1	113	Good
28	1030	55	1	113	Good
29	1031	57	1	113	Good
30	1032	59	1	113	Good
31	1033	61	1	113	Good
32	1034	63	1	113	Good
33	1035	65	1	113	Good
34	1036	67	1	113	Good
35	1037	69	1	113	Good
36	1038	71	1	113	Good
37	1039	73	1	113	Good
38	1040	75	1	113	Good
39	1041	77	1	113	Good
40	1042	79	1	113	Good
41	1043	81	1	113	Good
42	1044	83	1	113	Good
43	1045	85	1	113	Good
44	1046	87	1	113	Good
45	1047	89	1	113	Good
46	1048	91	1	113	Good
47	1049	93	1	113	Good
48	1050	95	1	113	Good
49	1051	97	1	113	Good
50	1052	99	1	113	Good
51	1053	101	1	113	Good
52	1054	103	1	113	Last shot

Appendix H. Line 2 Observer Notes

Montana Tech Observer Notes Date: 5/7/2018- 5/13/2018
State: MT County: Madison
Remarks: Line 2
Receivers: 1,2,3,…135
Shots 1,2,3,…64
Last shot 135,
Shot Interval 1.0 m.
Channel Interval 2.0 m., 9 stacks,
Lateral Offset: 0.5 m.
Note: This line crossed a bridge, indicated by the sequence of bad records. 144 channel system used, only 135 channels live.

SP#	FFID	Station #	1st	135th	Notes
1	1000	1	1	135	Bad record
1	1001	3	1	135	Bad record
2	1002	5	1	135	Bad record
3	1003	7	1	135	Bad record
4	1004				Bad record
	1001				Bad record
	1001				Bad record
	1002				Bad record
	1002				Bad record
	1002				Bad record
	1003				Bad record
	1003				Bad record
	1004				Bad record
	1004				Bad record
	1004				Bad record
	1005				Bad record
	1005				Bad record
	1005				Bad record
	1006				Bad record
	1006				Bad record
	1006				Bad record
	1007				Bad record
1	1007	1	1	135	Good
	1008	1	1	135	Bad record
2	1009	3	1	135	Good
3	1010	5	1	135	Good
3	1011	5	1	135	Bad record
4	1012	7	1	135	Good

5	1013	9	1	135	Good
6	1014	11	1	135	Good
7	1015	13	1	135	Good
8	1016	15	1	135	Good
9	1017	17	1	135	Good
10	1018	19	1	135	Good
11	1019	21	1	135	Good
12	1020	23	1	135	Good
13	1021	25	1	135	Good
14	1022	27	1	135	Good
15	1023	29	1	135	Good
16	1024	31	1	135	Good
17	1025	33	1	135	Good
18	1026	35	1	135	Good
19	1027	37	1	135	Good
20	1028	39	1	135	Good
21	1029	41	1	135	Good
22	1030	43	1	135	Good
23	1031	45	1	135	Good
24	1032	47	1	135	Good
25	1033	49	1	135	Good
26	1034	51	1	135	Good
27	1035	53	1	135	Good
	1036	55	1	135	Bad record
28	1037	55	1	135	Good
29	1038	57	1	135	Good
30	1039	59	1	135	Good
31	1040	61	1	135	Good
32	1041	63	1	135	Good
33	1042	65	1	135	Good
34	1043	67	1	135	Good
35	1044	69	1	135	Good
36	1045	71	1	135	Good
37	1046	81	1	135	Good
38	1047	83	1	135	Good
39	1048	85	1	135	Good
40	1049	87	1	135	Good
41	1050	89	1	135	Good
42	1051	91	1	135	Good
43	1052	93	1	135	Good
44	1053	95	1	135	Good

45	1054	97	1	135	Good
46	1055	99	1	135	Good
47	1056	101	1	135	Good
48	1057	103	1	135	Good
49	1058	105	1	135	Good
50	1059	107	1	135	Good
51	1060	109	1	135	Good
52	1061	111	1	135	Good
53	1062	113	1	135	Good
54	1063	115	1	135	Good
55	1064	117	1	135	Good
56	1065	119	1	135	Good
57	1066	121	1	135	Good
58	1067	123	1	135	Good
59	1068	125	1	135	Good
60	1069	127	1	135	Good
61	1070	129	1	135	Good
62	1071	131	1	135	Good
63	1072	133	1	135	Good
64	1073	135	1	135	Good

Appendix I. Line 3 Observer Notes

Montana Tech Observer Notes Date: 5/7/2018- 5/13/2018
State: MT County: Madison
Remarks: Line 3
Receivers: 1,2,3,…134
Shots: 1,2,3,…64
Last shot: 134,
Shot Interval: 1.0 m.
Channel Interval 2.0 m., 3 stacks,
Lateral Offset: 2.0 m.
Notes: 114 channel system used, only 1334 channels live

SP #	FFID	Station #	1st	134th	Notes
1	1000	1	1	134	Good
2	1001	3	1	134	Good
3	1002	5	1	134	Good
4	1003	7	1	134	Good
5	1004	9	1	134	Good
6	1005	11	1	134	Good
7	1006	13	1	134	Good
8	1007	15	1	134	Good
9	1008	17	1	134	Good
10	1009	19	1	134	Good
11	1010	21	1	134	Good
12	1011	23	1	134	Good
13	1012	25	1	134	Good
14	1013	27	1	134	Good
15	1014	29	1	134	Good
16	1015	31	1	134	Good
17	1016	33	1	134	Good
18	1017	35	1	134	Good
19	1018	37	1	134	Good
20	1019	39	1	134	Good
21	1020	41	1	134	Good
22	1021	43	1	134	Good
23	1022	45	1	134	Good
24	1023	47	1	134	Good
25	1024	49	1	134	Good
26	1025	51	1	134	Good
27	1026	53	1	134	Good
28	1027	55	1	134	Good
29	1028	57	1	134	Good

30	1029	59	1	134	Good
31	1030	61	1	134	Good
32	1031	63	1	134	Good
33	1032	65	1	134	Good
34	1033	67	1	134	Good
35	1034	69	1	134	Good
36	1035	71	1	134	Good
37	1036	73	1	134	Good
38	1037	75	1	134	Good
39	1038	77	1	134	Good
40	1039	79	1	134	Good
41	1040	81	1	134	Good
42	1041	83	1	134	Good
43	1042	85	1	134	Good
44	1043	87	1	134	Good
45	1044	89	1	134	Good
46	1045	91	1	134	Good
47	1046	93	1	134	Good
48	1047	95	1	134	Good
49	1048	97	1	134	Good
50	1049	99	1	134	Good
51	1050	101	1	134	Good
52	1051	103	1	134	Good
53	1052	105	1	134	Good
54	1053	107	1	134	Good
55	1054	109	1	134	Good
56	1055	111	1	134	Good
57	1056	113	1	134	Duplicate Shot
57	1057	113	1	134	Good
58	1058	115	1	134	Good
59	1059	117	1	134	Good
60	1060	119	1	134	Good
61	1061	121	1	134	Good
62	1062	123	1	134	Good
63	1063	125	1	134	Good
64	1064	127	1	134	Last shot

Appendix J. Line 4 Observer Notes

Montana Tech Observer Notes Date: 5/7/2018- 5/13/2018
State: MT County: Madison
Remarks: Line 4
Receivers: 1,2,3,…134
Shots: 1,2,3,…52
Last shot 127
Shot Interval 2.0 m.
Channel Interval 2.0 m., 3 stacks,
Lateral Offset: 2.0 m.
Notes: 144 channels used, only 134 channels live.

SP #	FFID	Station #	1st	134th	Notes
1	1000	1	1	134	Good
2	1001	3	1	134	Good
3	1002	5	1	134	Good
4	1003	7	1	134	Good
5	1004	9	1	134	Good
6	1005	11	1	134	Good
7	1006	13	1	134	Good
8	1007	15	1	134	Good
9	1008	17	1	134	Good
10	1009	19	1	134	Good
11	1010	21	1	134	Good
12	1011	23	1	134	Good
13	1012	25	1	134	Good
14	1013	27	1	134	Good
15	1014	29	1	134	Good
16	1015	31	1	134	Good
17	1016	33	1	134	Good
18	1017	35	1	134	Good
19	1018	37	1	134	Good
20	1019	39	1	134	Good
21	1020	41	1	134	Good
22	1021	43	1	134	Good
23	1022	45	1	134	Good
24	1023	47	1	134	Good
25	1024	49	1	134	Bad record
25	1025	49	1	134	Good
26	1026	51	1	134	Good
27	1027	53	1	134	Bad record
27	1028	53	1	134	Good

28	1029	55	1	134	Good
29	1030	57	1	134	Good
30	1031	59	1	134	Good
31	1032	61	1	134	Good
32	1033	63	1	134	Good
33	1034	65	1	134	Good
34	1035	67	1	134	Good
35	1036	69	1	134	Good
36	1037	71	1	134	Good
37	1038	73	1	134	Good
38	1039	75	1	134	Good
39	1040	77	1	134	Good
40	1041	79	1	134	Good
41	1042	81	1	134	Good
42	1043	83	1	134	Good
43	1044	85	1	134	Good
44	1045	87	1	134	Good
45	1046	89	1	134	Good
46	1047	91	1	134	Good
47	1048	93	1	134	Good
48	1049	95	1	134	Good
49	1050	97	1	134	Good
50	1051	99	1	134	Good
51	1052	101	1	134	Good
52	1053	103	1	134	Good
53	1054	105	1	134	Good
54	1055	107	1	134	Good
55	1056	109	1	134	Good
56	1057	111	1	134	Good
57	1058	113	1	134	Good
58	1059	115	1	134	Good
59	1060	117	1	134	Good
60	1061	119	1	134	Good
61	1062	121	1	134	Good
62	1063	123	1	134	Good
63	1064	125	1	134	Good
64	1065	127	1	134	Good
65	1066	129	1	134	Good
66	1067	131	1	134	Good